Structure elucidation of antiplasmodial sesquiterpene lactones from *Vernonia staehelinoides* and *Oncosiphon piluliferum*

by

Pamisha Pillay

Submitted in partial fulfillment of the requirements for the degree

MASTER OF SCIENCE

in the Faculty of Natural & Agricultural Sciences

University of Pretoria

Pretoria

Supervisor : Prof R. Vleggaar

December 2005

Declaration

I, the undersigned, hereby declare that the work contained in this dissertation is my own original work and that I have not previously, in its entirety or in part, submitted it at any university for a degree.

Signature: ……. **Date**: ……..

P. Pillay

SUMMARY

Malaria continues to be a major cause of mortality and morbidity especially in Sub-Saharan Africa. The emergence and spread of drug resistant parasites has highlighted the need for new chemically diverse, effective drugs. Historically, one of the major sources of antimalarial agents and novel template compounds has been higher order plants. The widespread use of medicinal plants for the treatment of malaria in South Africa represents a diverse resource of potential antimalarial drugs.

Two South African plants, *Vernonia staehelinoides* and *Oncosiphon piluliferum*, were identified as potential sources of new antimalarial drugs through a national multidisciplinary-consortium project aimed at scientifically validating South African medicinal plants for the treatment of malaria. The *in vitro* antiplasmodial activity of extracts of these plants warranted further investigation to identify the biologically active components. Bio-assay guided fractionation based on *in vitro* antiplasmodial activity against the D10 *P. falciparum* strain was used to identify the compounds responsible for the observed activity. Compounds were purified using silica gel column chromatography. The structures of the isolated compounds were elucidated using spectroscopic techniques.

Bioassay-guided fractionation of the organic extracts of *V. staehelinoides* leaves identified a pair of structurally-related hirsutinolides with significant *in vitro* antiplasmodial activity. The compounds were found to be cytotoxic at similar concentrations but proved to be interesting scaffolds for potential structure-activity relationship studies.

Three germacranolides and two eudesmanolides were identified through bioassay-guided fractionation of the organic *O. piluliferum* extract. Selected derivatizations were conducted in order to fully characterize the compounds. The absolute configuration of the major active germacranolide was determined using Mosher's method. The effect of the reduction of the α-methylene group of the major active

germacranolide on antiplasmodial activity and cytotoxicity was also investigated. The 5 compounds and the reduction product were found to possess varying degrees of *in vitro* antiplasmodial activity and cytotoxicity. None was sufficiently active or selective to be a viable drug candidate but the potential for further structure-activity relationship studies exists.

ACKNOWLEDGEMENTS

I would like to express my gratitude to my supervisor, Prof. R. Vleggaar, for his invaluable supervision and insight throughout the duration of this work. In addition, I wish to thank my CSIR colleagues Dr Vinesh Maharaj, Dr Gerda Fouche and Dr Louis Ackerman for their guidance.

I gratefully acknowledge the Department of Science and Technology for the Innovation fund Grant (Project 31313) and am also grateful to the Innovation Fund Project Administrators and the CSIR for permission to present this work for degree purposes.

Special mention must be made of members of the Antimalarial consortium who personally contributed to this research: Prof Peter Folb (MRC), Dr Niresh Bhagwandhin (MRC), Prof Pete Smith (UCT), Dr Cailean Clarkson (UCT), Dr Neil Crouch (SANBI), Jean Meyer (SANBI) and Dr Kelly Chibale (UCT).

Heartfelt thanks to my family and friends for their love and support. To my brothers, thank you for your inspiration and encouragement. I dedicate this thesis to my mum and dad who have made great sacrifices to ensure we were able to pursue our dreams.

Om Saraswati Namah

ABBREVIATIONS/FORMULAE COMMONLY USED

SANBI	South African National Biodiversity Institute
MRC	Medical Research Council
CSIR	Council for Scientific and Industrial Research
UCT	University of Cape Town
WHO	World Health Organisation
Ac	acetyl
Acetyl-CoA	acetyl coenzyme A
APAD	3-acetylpyridine adenine dinucleotide
$CDCl_3$	deuterated chloroform
C_6D_6	deuterated benzene
CHO	Chinese Hamster Ovarian
DMAP	4-(dimethylamino)pyridine
DMAPP	dimethylallyl pyrophosphate
DMF	dimethylformamide
DMSO	dimethyl sulphoxide
FPP	farnesyl pyrophosphate
GGPP	geranylgeranyl pyrophosphate
GAP	glyceraldehyde 3-phoshate
GPP	geranyl pyrophosphate
H_2O	water
HMG-CoA	3-hydroxy-3-methylglutaryl coenzyme A
HEPES	*N*-[2-hydroxyethyl]-piperazine-*N*'-[2-ethanesulphonic acid]
IPP	isopentenyl pyrophosphate
MVA	mevalonic acid
MTT	3-(4,5-dimethylthiazol-2-yl)-2,5-diphenyltetrazolium bromide
MeOH	methanol
MTPA	α-methoxy-α-trifluoromethylphenyl acetic acid

$NaBH_4$	sodium borohydride
$NaHCO_3$	sodium hydrogen carbonate
Na_2SO_4	sodium sulphate
NAD	nicotinamide adenine dinucleotide
NADP	nicotinamide adenine dinucleotide phosphate
NADPH	reduced form of nicotinamide adenine dinucleotide phosphate
NBT	nitroblue tetrazolium
Me	methyl
MeOH	methanol
pLDH	parasite lactate dehydrogenase
PES	phenazine ethosulphate
PBS	phosphate buffered saline
PRBC	packed red blood cells
RPMI	Roswell Park Memorial Institute medium
RBC	red blood cells
SH	thiol or sulfanil
TRIS	tris(hydroxymethyl)aminomethane

A	absorbance
br	broad resonance
COSY	correlated spectroscopy
c	concentration
d	doublet
dd	doublet of doublets
ddd	doublet of doublets of doublets
dddd	doublet of doublets of doublets of doublets
ddq	doublet of doublets of quartets
ddt	doublet of doublets of triplets
DEPT	distortionless enhancement by polarisation transfer
dq	doublet of quartets
dt	doublet of triplets

EI- MS	electron ionization- mass spectrometry
^{1}H NMR	proton (^{1}H) nuclear magnetic resonance spectroscopy
^{13}C NMR	carbon-13 nuclear magnetic resonance spectroscopy
HR EI-MS	high resolution electron ionization- mass spectrometry
HMBC	heteronuclear multiple bond correlation
HSQC	heteronuclear single quantum correlation
Hz	hertz
J	coupling constant
Lit.	Literature
IC_{50}	inhibitory concentration at which 50% inhibition is achieved
NOESY	nuclear Overhauser effect spectroscopy
m	multiplet
mp	melting point
m/z	mass-to-charge-ratio
ppm	parts per million
q	quartet
R_f	retention factor
s	singlet
t	triplet
RI	resistance index
SI	selectivity index
TLC	thin layer chromatography

cm	centimeters
h	hours
kV	kilovolts
mg	milligrams
mg/L	milligrams per liter
mm	millimeters
mmol	millimoles

ng/ml	nanograms per milliliter
nm	nanometers
μM	micromolar
μg/ml	micrograms per milliliter
g/L	grams per liter

spp.	species
subsp.	subspecies

et al.	and others
i.e.	that is
viz.	namely

CONTENTS

CHAPTER 2

Sesquiterpene lactones

CHAPTER 3

Antiplasmodial Activity of *Vernonia staehelinoides*

CHAPTER 4

Antiplasmodial Activity of *Oncosiphon piluliferum*

CHAPTER 5
Experimental

CHAPTER 1

Malaria and antimalarials from plants

1.1 History of Malaria

Malaria, a life-threatening disease that is transmitted by Anopheles mosquitoes, is probably one of the oldest diseases known to mankind. Mentions of this disease can be found in ancient Chinese, Indian and Egyptian manuscripts. In the 5th century BC Hippocrates, the Greek physician, was the first to describe the manifestations of the disease. In the 7th century AD, the Italians named the disease *mal'aria* meaning bad air, due to its association with ill-smelling vapours from the swamp near Rome.

The first recorded treatment of malaria dates back to 1600 when the bark of the Cinchona tree was first used by the native Peruvian Indians to treat the intermittent fevers associated with this illness.[1] It was not until 1889 that Alphonse Laveran discovered the protozoal (single celled parasite) cause of malaria and not until 1897 that Ronald Ross demonstrated that the Anopheles mosquito was the vector for the disease.[2] His pioneering work on establishing the main features of the parasitic life cycle earned Ross the Nobel Prize in Medicine in 1902.

Over the next century significant advances were made towards attempts to eradicate malaria particularly with respect to controlling mosquitoes, understanding the parasite and developing drugs to treat the disease.[3] The greatest challenge lies in the parasites ability to quickly adapt and overcome eradication efforts when these are fragmented and uncoordinated. Malaria quickly rebounded from the mass insecticide spraying campaigns in the 1950s and 1960s. Since the 1980s parasite resistance to chloroquine, the most commonly available antimalarial drug, has emerged as a major challenge.

---

[1] M.R. Lee, *J. R. Coll. Physicians Edinb.*, 2002, **32**, 300.
[2] A. Robert, B. Françoise, O. Dechy-Cabaret and B. Meunier, *Pure Appl. Chem.*, 2001, **73**, 1173.
[3] London School of Hygiene and Tropical Medicine, 'Malaria : Waiting for the Vaccine', John Wiley & Sons, Chichester, 1991.

1.2 Malaria Today

Malaria is one of the biggest killers in the world. Current estimates place the clinical caseload at between 300 and 500 million people annually and nine out of ten of these cases occur in sub-Saharan Africa.[4] This is due to the majority of infections in Africa being caused by *Plasmodium falciparum*, the most dangerous of the human malaria parasites. It is also because the most effective and most difficult to control malaria vector - the mosquito *Anopheles gambiae* - is the most widespread in Africa. Climatic conditions over a large part of Africa favour malaria transmission and global warming together with changes in land use are extending the areas of transmission. Moreover, many countries in Africa lacked the infrastructures and resources necessary to mount sustainable campaigns against malaria and as a result few benefited from historical efforts to eradicate malaria. Also, methods aimed at eradicating the disease have been hindered by lack of governmental commitment, failure to use existing resources and poor health care facilities.

Today approximately forty percent of the world's population is at risk to malaria. Malaria is endemic in Africa, much of South and Southeast Asia, Central America, and northern South America (Figure1.1).[5]

In South Africa malaria is mainly transmitted in the low altitude areas of the northeastern parts of Southern Africa; this includes the lowveld region of Mpumalanga, Limpopo Province and the northeastern parts of KwaZulu-Natal. Malaria transmission is seasonal with the greatest number of cases occurring between October and May with a significant inter-annual variation in the number of malaria cases. In the year 2002 the annual number of reported malaria cases was approximately 15 582 while in 2003 it was 4392.[6] This variation is mainly attributed to favourable climatic conditions, population migration and the emergence of drug resistant parasites. The South African government has increased efforts to control malaria particularly due to its devastating impact on the economy.

---

[4] World Health Organisation Fact Sheet No. 94, 2003, WHO information. http://www.int/inf~fs/en/fact094.html

[5] World Health Organisation, World Health Report, 2003. http://www.d2ol.com/malaria.html

[6] South African Department of Health, National Health Report, 2003. http://www.doh.gov.za/issues/malaria/year00_03.pdf

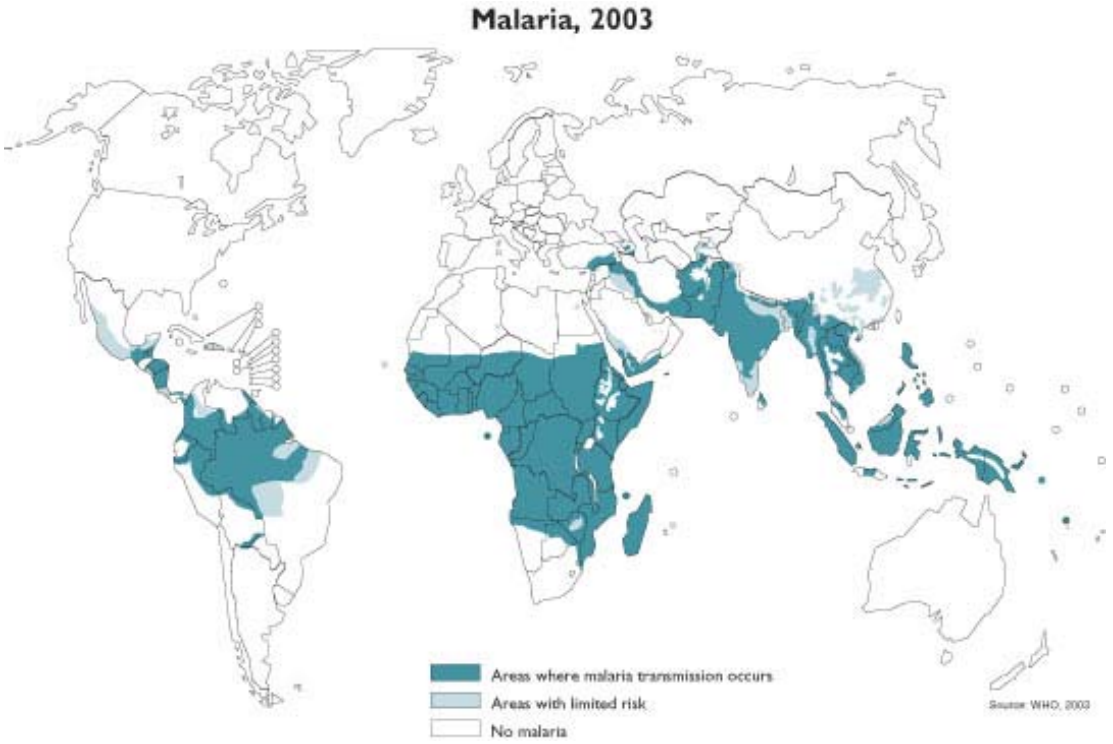

Figure 1.1 Malaria-endemic regions.

Annual economic growth in countries with high malaria transmission has historically been lower than in countries without malaria. The direct costs of malaria include a combination of personal and public expenditures on both prevention and treatment of the disease. The indirect costs of malaria include lost productivity or income associated with illness or death. Also, the prevalence of malaria in a country can lead to a decline in international trade and tourism and foreign investment, which are vital for economic growth.

1.3 The Malaria Parasite

The malaria parasite*, Plasmodium falciparum*, is a very small, single-cell blood organism, or 'protozoan'. There are three other parasite species (*P. malariae*, *P. vivax* and *P. ovale*) that also cause malaria but they are rare in South Africa. The parasite is transmitted to humans by a vector, namely the female *Anopheles* mosquito.

Knowledge of the life cycle of the malaria parasite is fundamental to understanding the methods of prevention, treatment and research pursuits. Interrupting the life

cycle will prevent malaria, but this has proven more difficult than anticipated. The *Plasmodium* parasite spends part of its life cycle in humans and partly in mosquitoes (Figure 1.2).[7,8]

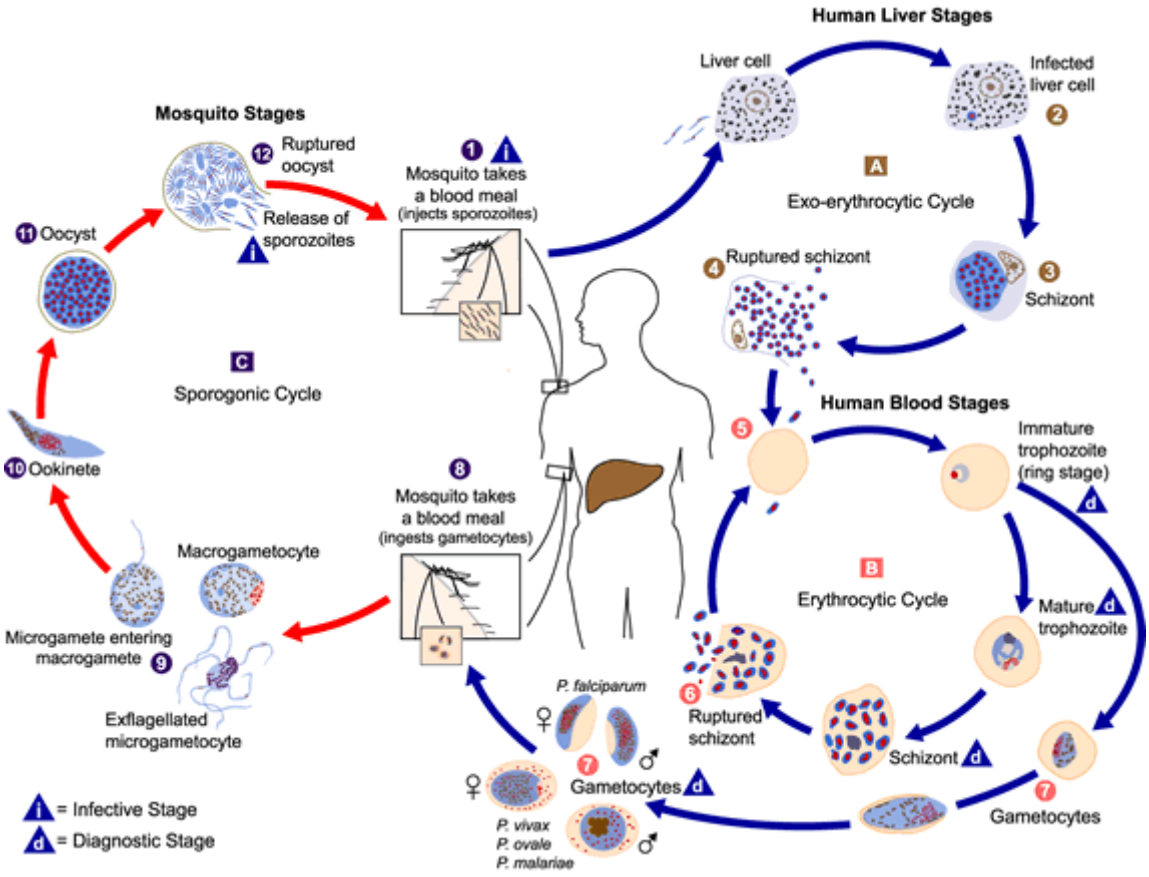

Figure 1.2 Life cycle of *Plasmodium* spp.[9]

While ingesting a blood meal, an infected mosquito injects sporozoites into a human host (1). Sporozoites move to the liver and infect liver cells (2) where they reproduce by mitosis and develop into schizonts (3), which rupture and release merozoites (4). Following this initial replication in the liver (exo-erythrocytic schizogony (A)), the merozoites are released into the bloodstream where they undergo asexual multiplication in the erythrocytes (erythrocytic schizogony (B)).

Merozoites infect red blood cells (5). The ring stage trophozoites mature into schizonts, which rupture releasing merozoites (6). Two out of every three red blood

[7] R. Caniato and L. Puricelli, *Crit. Rev. Plant Sci.*, 2003, **22**, 79.
[8] G. Taubes, *Science*, 2000, **290**, 435.
[9] http://www.netdoctor.co.uk/travel/disease/lifecycle of the malarial parasite.htm

cells soon become infected. The periodic fever and chills associated with malaria occur when the red blood cells rupture and release the merozoites. This is the blood stage of the disease. A fraction of the merozoites differentiate into gamete producing cells (gametocytes) (7).

The gametocytes, male (microgametocytes) and female (macrogametocytes), are ingested by an Anopheles mosquito during a blood meal (8). The parasites' multiplication in the mosquito is known as the sporogenic cycle (C). While in the mosquito's stomach, the male gametes fertilize the female gametes generating zygotes (9). The zygotes in turn become ookinetes (10) which invade the midgut wall of the mosquito where they develop into oocysts (11). The oocysts grow, rupture and release sporozoites (12), which make their way to the mosquito's salivary glands. Inoculation of the sporozoites into a new human host occurs and the cycle begins again (1).

1.4 Malaria Prevention and Control

There are a number of approaches towards the prevention and control of malaria and the choice of intervention in a country or region are usually most dependent on cost-effectiveness.[3]

The early diagnosis of malaria and prompt treatment with antimalarial drugs is essential in controlling the spread of the disease. By reducing the number of infected humans, the number of infected mosquitoes is effectively reduced. This type of control is especially important when outbreaks of malaria occur. When humans are treated the life cycle of the parasite is essentially interrupted.

Another approach is the use of personal protection. The first objective of this is to protect people from being bitten by an infected mosquito. Mosquito nets, screening doors and windows, wearing protective clothing, using insect repellants, coils and vapourizers are all ways of doing this. The other objective of personal control is the use of preventative or prophylactic drug treatment. For instance, travelers to regions where malaria is present often take prophylactics which help prevent the

development of the disease but not the initial infection. Cost and availability of drugs can be dictating factors in many countries.

A third approach is vector or mosquito control. Spraying of insecticides to kill the adult or larval mosquitoes can be quite effective. Managing the environment by reducing the mosquito breeding sites has helped to eliminate malaria in some areas. Using natural biological controls such as mosquito predators is also promising. In the last few years there has been growing interest in bioengineering insects that are unable to transmit the malaria parasite.[10] This is vector manipulation.

Ideally, a protective vaccine would be the most effective approach to controlling malaria. Attempts to develop a vaccine, however, have been hindered by the great genetic diversity of the parasite, its multistage life cycle, as well as the complex and inefficient human immune response.[11] It is anticipated that a vaccine will be available within the next ten years.[3]

1.5 Malaria Treatment

Drugs used for the treatment of malaria do not assist the natural healing processes of the body; instead they act chemically on the parasite as a controlled poison. In most cases antimalarial drugs target the asexual erythrocytic stage of the parasite. The parasite degrades haemoglobin in its acidic food vacuole, producing free haeme able to react with molecular oxygen and thus generating reactive oxygen species as toxic by-products. A major pathway of detoxification of haeme moieties is polymerization as malaria pigment. Most antimalarial drugs act by disturbing the polymerization of haeme, thus killing the parasite with its own metabolic waste. Antimalarial drugs fall into several chemical groups. The first and most commonly used are the quinoline based antimalarials, which include quinine **(1)** and its derivatives chloroquine **(2)**, amodiaquine **(3)** and mefloquine **(4)** (Figure 1.3).

[10] http://ecology.cwru.edu/malaria
[11] P. Newton and N. White, *Annu. Rev. Med.*, 1999, **50**, 179.

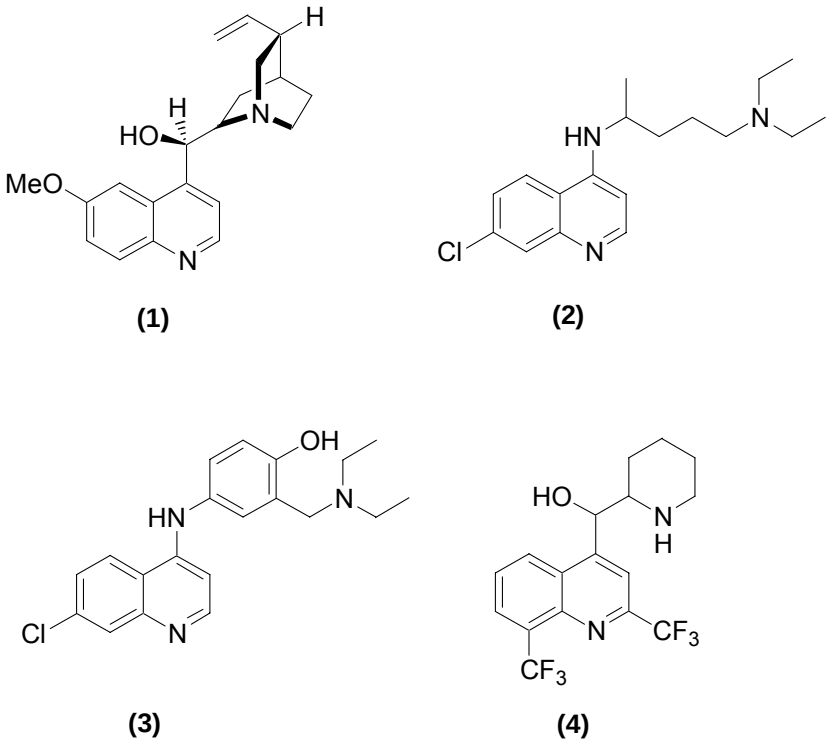

Figure 1.3 Quinoline based antimalarials.

Quinine **(1)** has been used for more than three centuries and until the 1930s was the only effective agent for the treatment of malaria. Of the 36 alkaloids found in the bark of the Cinchona tree, only four possess antimalarial properties, with quinine being the most effective.[1] It is able to bind strongly to blood proteins and forms complexes that are toxic to the malarial parasite. Due to its undesirable side effects it is now only used as an intravenous injection to treat severe malaria.

Chloroquine **(2)** was introduced in 1944 and soon became the mainstay of therapy and prevention, since this drug was cheap, non-toxic and effective against all strains of the parasite.[2] It is capable of blocking the polymerisation of haem to haemozoin (malaria pigment).[12] It is a chemically synthesized drug and remains the most widely used drug in the treatment of malaria, despite increasing parasite resistance. Chloroquine's reduced efficacy led to the development of the synthetic analogues amodiaquine **(3)** and mefloquine **(4)** that are used to treat cases of uncomplicated malaria in areas where chloroquine resistance is prevalent.

[12] J. Zhang, M. Krugliak and H. Ginsburg, *Mol. Biochem. Parasitol*., 1999, **99**, 129.

The second class of common antimalarials is the folate antagonists (Figure 1.4). These compounds inhibit the synthesis of parasitic pyrimidines and thus of parasitic DNA.[2] There are two types of antifolates, the dihydrofolate reductase (DHFR) inhibitors pyrimethamine **(5)** and proguanil **(6)**, and the dihydropteroate synthetase (DHPS) inhibitors, which include the sulphonamide drugs, sulphadoxine **(7)** and dapsone **(8)**. Due to a marked synergistic effect, a drug of the first group is usually used in combination with a drug of the second one. Pyrimethamine-sulphadoxine (SP), or Fansidar®, is the most widely used combination.[11]

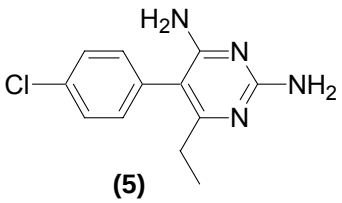

(5)

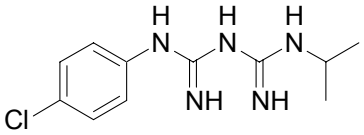

(6)

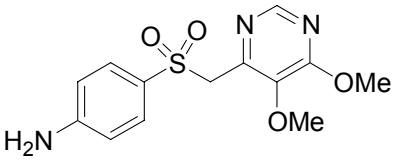

(7)

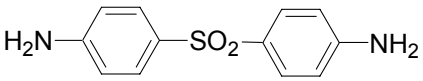

(8)

Figure 1.4 DHPS and DHFR inhibitors.

The third class of antimalarials is based on the natural endoperoxide artemisinin **(9)** which was first extracted from the Chinese traditional medicine, *Artemisia annua*, in 1972.[13] Artemisinin is not soluble in water or oil and because of this poor solubility the drug absorption and its bioavailability are also poor. However, since the peroxide bridge of the compound is stable under various chemical reactions, several oil and water-soluble derivatives of artemisinin have since been synthesized.[14] These include dihydroartemisinin (DHA) **(10)**, artemether **(11)**, arteether **(12)**, artesunate **(13)** and artelinic acid **(14)** (Figure 1.5).[2] The semi-

[13] J.A. Vroman, M. Alvim-Gaston and Mitchel A. Avery, *Curr. Pharm. Design*, 1999, **5**, 101.
[14] M.R. Lee, *J.R. Physicians Edinb.*, 2002, **32**, 300.

synthetic derivatives of artemisinin have improved pharmacokinetic properties and are also of current clinical use.

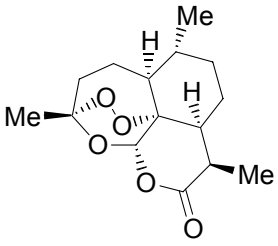

(9)

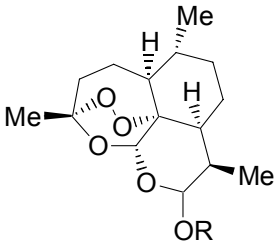

(10) R = H
(11) R = Me
(12) R = Et
(13) R = $CO(CH_2)_2COONa$
(14) R = $CH_2(p\text{-}C_6H_4)CO_2H$

Figure 1.5 Artemisinin and its semisynthetic derivatives.

Since an artemisinin derivative lacking the endoperoxide bridge (deoxyartemisinin) is devoid of antimalarial activity, the possible reactivity of this peroxide function within the parasite is the key factor of the pharmacological activity of these molecules.[15] This group of antimalarials is the most rapidly acting and is effective against multi-drug resistant strains of the parasite. Although the precise mode of action of artemisinin and its derivatives is not completely understood, it is proposed that the endoperoxide bridge is cleaved to generate free radicals. The free radicals are strong alkylating agents and form covalent bonds with various parasite proteins.

In addition to destroying the parasite, health care providers are attentive to treating the multiple symptoms of malaria. These symptoms include fever, chills, headaches, malaise, weakness, hepatomegaly (enlarged liver), splenomegaly (enlarged spleen) and dehydration. Malaria can also cause anemia, anorexia, nausea, vomiting, abdominal pain and diarrhoea. Deaths from malaria are normally caused by cerebral, renal or pulmonary fever, or a combination of the three.[16]

[15] D.L. Klayman, *Science*, 1985, **228**, 1049.
[16] G.T. Strickland and K.W. Hunter, 'The Pathophysiology of Human Malaria', Praeger, Westport, 1982.

1.6 Resistance to Antimalarial Drugs

Whilst the number of effective drugs to treat a malaria infection is limited, the rapid emergence of drug resistant strains of the parasite is outpacing the development of new antimalarials. The reasons for the development and spread of drug resistance involve the interaction of drug-use patterns, characteristics of the drug itself, human host factors, parasite characteristics, and vector and environmental factors.[17] However, only gene mutations confer resistance to the parasites in nature.

The rate of spread of resistance to a particular drug will depend on a number of factors including the starting frequency of resistant mutations to that drug, the intensity of malaria transmission, immunity of population, drug pressure and the pharmacokinetic/pharmacodynamic properties of the drug.

Chloroquine **(2)** is by far the most used antimalarial in conventional malaria therapy due to it being relatively inexpensive and readily available in many endemic areas. However, owing to widespread drug resistance, the drug is becoming increasingly ineffective in many parts of the world. The generally accepted explanation for chloroquine resistance is that resistant parasites accumulate less chloroquine than sensitive parasites. Thus lethal concentrations of the drug are prevented from reaching the parasitic food vacuole. The decrease in chloroquine accumulation can be attributed to a higher rate of chloroquine efflux, a lower rate of chloroquine uptake, or varying combinations of both these processes.[18]

There is also evidence of increasing antifolate resistance in malaria parasites. Antifolate resistance is generally due to a combination of mutations in the target enzymes and the use of an alternative pathway to recover folate. There is no solid data supporting the existence of resistance to artemisinin, although recurrence is associated with the monotherapy of artemisinin and its derivatives at a high rate.

---

[17] R.G. Ridley, *Nature*, 2002, **415**, 686.
[18] K.J. Saliba, P.I. Folb and P.J. Smith, *Biochem. Pharmacol.*, 1998, **56**, 313.

In order to prevent this return artemisinins are used with longer-acting antimalarial medications in combined treatments.[19]

1.7 Need for New Antimalarials

Growing resistance to antimalarial drugs is perhaps the most important factor contributing to the current resurgence of malaria. The escalating mortality rate among African children is directly attributable to malaria and more specifically to the rapidly increasing resistance to antimalarial drugs. The number of effective drugs available to treat malaria is limited and the rate at which resistance is mounting is outpacing the development of new antimalarials. Nearly all the antimalarials that are in use today were developed almost thirty years ago and, in general, the pharmaceutical companies, particularly the multinationals, have little interest in developing a new cure despite the immense need.[20]

Most of the available drugs were developed through synthesis and screening – an approach which has proved inefficient and costly. With no vaccine on the immediate horizon, chemotherapy and chemoprophylaxis remain the major methods of controlling malaria. However, with the increase in cases of drug resistance there is an urgent need for new drugs with novel modes of action.

One of the biggest obstacles in the battle against malaria in areas where the disease is most prevalent is poverty. Thus there is a real need to find simple, affordable antimalarial medicines. One approach to this is the investigation of medicinal plants and natural products.

1.8 Traditional Medicine

Traditional medicine is the embodiment of the knowledge, skills and practices based on the theories, beliefs and experiences indigenous to different cultures that have been handed down from generation to generation. They are used in the maintenance of health as well as in the prevention, diagnosis, improvement or treatment of physical and mental illness.

---

[19] P.B. Bloland, 'Drug resistance in malaria', Geneva: World Health Organisation, 2001.
[20] R. Ramachandran, *Frontline*, 2002, **19** http://www.frontlineonnet,com/fl1913/19130870.htm

In the last decade, there has been a global upsurge in the use of traditional medicine and complementary and alternative medicine in both developed and developing countries. Various reasons have been proposed for this increase, including affordability, but also changing needs and beliefs. The most widely used traditional medicine and complementary and alternative medicine therapies are herbal medicines and acupuncture.

Traditional medicine has been described by the World Health Organisation (WHO) as one of the surest means to achieve total health care coverage of the world's population. In spite of the marginalisation of traditional medicine practiced in the past, the attention currently given by governments to widespread health care application has stimulated research, investments and programme design in this field in several developing countries.[21] So far countries that have successfully integrated traditional medicine into their primary health care systems are China, North and South Korea and Vietnam.

In South Africa there are an estimated 200 000 practicing traditional healers. A traditional healer is the general term used to describe a practitioner of indigenous medicine. The popularity of traditional healers in South Africa is considered due to the strong cultural belief system and modern medical facilities often being inaccessible or unaffordable. A number of initiatives have been taken by the South African National Department of Health to investigate traditional medicines for efficacy, safety and quality with the aim to incorporate their use in the national health care delivery system.

1.9 Medicinal Plants

Plants of medicinal value have been used effectively for centuries in traditional medicine. Traditional health care systems using medicinal plants can be recognized and used as a starting point for the development of novel drug leads. Medicinal plants are considered a major source of biologically active natural products that may serve as commercially significant entities themselves or provide

[21] Conserve Africa Organisation, 'Overview on Medicinal Plants and Traditional Medicine in Africa', 2004 http://www.conserveafrica.org/medicinal_plants.rtf

lead structures for the development of modified derivatives possessing enhanced activity and/or reduced toxicity.

Traditional medicines include crude plant extracts, or combinations of several medicinal plants, which contain numerous components that are thought to contribute to the overall therapeutic effect. Because the chemical compounds in the different plant components are often quite different, usually only a specified plant part is used medicinally (*viz.* leaves, roots, bark or fruit). The method of preparation is crucial. Activities including the addition of appropriate volumes of solvents such as water or alcohol to a specified amount of fresh or dry plant material, boiling for a specified length of time or partial burning to achieve a desired colour are important and can serve to neutralize certain toxins. Dosage forms (*viz*. tinctures, extracts, ointments or enemas) as well as the method of administration (*viz*. orally, topically or nasally) are also critical and are conveyed by the healer.[22]

Plant-based traditional medicine systems continue to play an essential role in healthcare, and it has been estimated by the WHO that approximately 80% of the world's inhabitants use plants for their primary healthcare.[23] Because of the importance of medicinal plants the WHO encourages their use not only under an empirical basis, but also under a scientific approach. The profits gained from a scientific approach to traditional plant remedies in developing countries, where they have fundamental importance, are numerous.

Firstly it would allow natives to gain some independence from developed countries in the preparation of plant-derived medications, and it would promote the establishment of sustainable supply and extraction industries, which could prove to be a vital aspect for economic development. Proving the efficacy of traditional medicines, would also allow the local medium-large scale cultivation of medicinal plants with an obvious benefit for the national economy. Finally, from an environmental point of view, the proof of therapeutic value of selected medicinal

[22] B.E. van Wyk, B. van Oudtshoorn and N. Gericke, 'Medicinal Plants of South Africa', Briza Publications, Pretoria, 2000.
[23] World Health Organisation, 'Traditional Practitioners as Primary Health Care Workers', WHO/SHS/DHS/TRM/95.6, Geneva, 1995.

plants would help to conserve species that would otherwise be depleted by unsustainable harvesting activities.[7]

An estimated 70% of South Africans regularly use traditional medicines, most of which are derived from plant species indigenous to the region. South Africa represents only 0.04% of the land surface area of the world, yet nearly 10% of all known plant species occur here. There are over 24 000 plants indigenous to South Africa. Approximately 3000 species of plants are used as medicines, and some 350 of these are the most commonly used and traded medicinal plants. South African medicinal plants that are popular worldwide include Cape aloes (*Aloe ferox*), buchu (*Agathosma betulina*) and devil's claw (*Harpagophytum procumbens*).[22]

1.10 Drugs from Plants

There are two basic approaches to drug discovery: rational drug design and the traditional method of random screening. Rational design-engineering of new drug molecules from scratch with the aid of computers and molecular biology requires knowledge of the drug target such as a receptor or an enzyme. So far, it has had only limited payoffs, although it has promising potential. In random screening many synthetic chemicals or natural products are indiscriminately tested for biological activity. Because this method is both costly and time-consuming, there has been a great need for better efficacy in strategic research and development planning for pharmaceutical companies. The strategy of developing new drugs based on medicinal plants has an advantage over random screening, since it is guided by experience from a long history of clinical practice.

In 1819, the isolation of the analgesic morphine **(15)** from the opium poppy (*Papaver somniferum*) laid the foundation for the purification of pharmacologically active compounds from medicinal plants.[24] More than 50% of all drugs in clinical use today originated from plants or are derivatives of natural products. Well known examples include quinine **(1)**, extracted from the bark of the *Cinchona* species; the anticancer drug, taxol **(16)**, from the bark of *Taxus brevifolia*; and salicylic acid **(17)**

[24]M.S. Butler, *J. Nat. Prod*., 2004, **67**, 2141.

which served as a template for aspirin **(18)**, originally isolated from the bark of the *Salix* species. In addition, crude herbal preparations such as *Oenothera biennis* (Evening primrose), *Hypericum perforatum* (St John's wort), and *Panax ginseng* (Ginseng) are also popular. The isolation of an active compound, or the use of a herbal preparation with therapeutic efficacy is particularly relevant to diseases lacking effective chemotherapeutic agents.

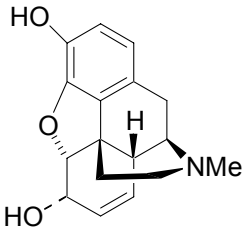

(15)

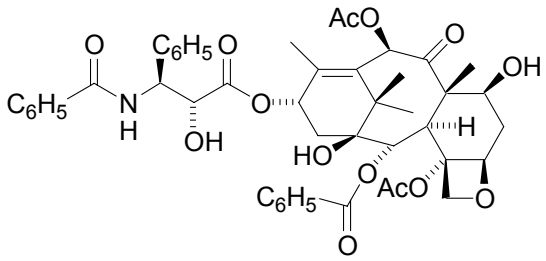

(16)

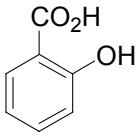

(17)

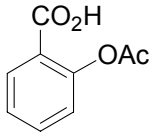

(18)

Figure 1.6 Examples of plant-derived drugs.

The active ingredients in medicinal plants are chemical compounds that act directly or indirectly to prevent or treat a disease or ailment and maintain health. Plants investigated for pharmacologically active compounds are usually selected on the basis of ethnomedicinal information as there is a correlation between biological activity and the traditional use of the plant. In selecting plants that may contain biological agents, generally a targeted approach to plant collection is adopted based on the belief that plants that have acquired the status of a traditional herbal remedy have reasonable proof of safety and efficacy from their history of use and have a higher probability of yielding an active substance.

The chemical diversity and stereospecificity of complex natural products are the main attractions of working with plants as opposed to synthetic chemistry approaches. In addition plant constituents often occur as a group of structurally

related metabolites, making it possible to isolate analogues of the active compound and obtain information on structure-activity relations. Only a small percentage of the estimated 250 000 higher plant species have been investigated for pharmacological activity thus it is most likely that plants will continue to offer novel leads for drug development.

1.11 Antimalarials from Plants

Historically the majority of the antimalarial drugs have been derived from medicinal plants or from structures modeled on plant lead compounds. Quinine **(1)**, the first effective antimalarial drug is still in clinical use today and the more recently discovered artemisinin **(9)** has proved to be an incentive for further research into plants.

The investigation of a range of plants from various countries used in traditional medicine for the treatment of malaria has led to the discovery of a large number of antimalarial compounds with significant structural variety.[25] Table 1.1 lists some of these compounds which belong to different secondary metabolite classes and the traditional medicines from which they were isolated.[7] Some of these compounds are not particularly active, but are nevertheless interesting because they might strengthen chloroquine activity or restore chloroquine sensitivity in resistant strains of *P. falciparum*.

In researching plants which are frequently mentioned as antimalarials in literature it is often found that these do not necessarily show high activity in *in vitro* tests. This can partly be explained by the fact that many plants are used in the treatment of malaria, not for their antiparasitic effects but because of other therapeutic activities. These include reducing fever, calming convulsions and headache, and possibly even immuno-stimulatory effects. Another problem is that some plants are given in a mixture and are possibly only active in this combination due to synergistic effects. Also, an *in vitro* assay cannot precisely reproduce the *in vivo* situation. Certain plant extract components might only become active after specific metabolic processes *in vivo*.[26]

---

[25] S. Schwikkard and F.R. van Heerden, *Nat. Prod. Rep.*, 2002, **19**, 675.
[26] M.C. Gessler, M.H.H. Nkunya, L.B. Mwasumbi, M.Heinrich and M.Tanner, *Acta Trop.*, 1994, **56**, 65.

Table 1.1 Examples of classes of compounds with antimalarial activity isolated from traditional medicines

Class of compound	Compound	Plant	Part of plant	Country
Quinones	1-hydroxybenzoiso-chromanquinone	*Psychotria camponutans*	Stem and roots	Panama
Triterpenes	Lupeol	*Vernonia brasiliana*	Leaves	Brazil
Sesquiterpenoids	16,17-Dihydrobrachy-calyxolide	*Vernonia brachycalyx*	Leaves	Kenya
Quassinoids	Bruceolide	*Brucea javanica*	Fruits	China
Liminoids	Fissinolide	*Khaya Senegalensis*	Bark	Sudan
Alkaloids	Ancistroheynine A	*Ancistocladus heyneanus*	Roots	India
Lignans	(+)-Nyasol	*Asparagus africanus*	Roots	Kenya
Coumarins	O-Methylexostemin	*Exostema mexicanum*	Stem bark	Latin America

Other problems commonly encountered when investigating medicinal plants as a source of antimalarial drugs is that crude extracts or compounds show *in vitro* activity but are extremely toxic or those which are active *in vitro* fail to display *in vivo* activity. If a compound destroys parasites, it is logical to screen for toxicity *in vitro* using human cells in culture. When a compound is found to destroy human cells at similar concentrations its potential as a useful drug is limited as the safety margins will be too slender. The difficulty arises from the fact that protozoa share many biochemical pathways with the human host thereby limiting the antimalarial drug's selectivity to kill the parasite without harming mammalian cells. The pharmacokinetic and pharmacodynamic properties of the extract or compound determine whether it will display *in vivo* activity. This includes absorption, distribution to the active site and whether the compound is metabolized too rapidly or to a less active form.[27] Out of the numerous potential antimalarial drugs discovered, only a limited number achieve drug candidate status.

[27] G.C Kirby, *Trans. R. Soc. Trop. Med. Hyg.*, 1996, **90**, 605.

1.12 Antimalarial Drug Discovery

In the drug discovery process, when a compound is identified in primary screens to have antiparasitic activity and lack of host toxicity, extensive biochemical studies are conducted to determine the mode of action. In terms of developing a drug from a plant-derived lead compound, attempts may be made to produce chemical analogues of the active principle with enhanced antiplasmodial activity and reduced host toxicity. Guides for conducting this work are often obtained from the original plant source since many plant compounds exist as groups of structurally related metabolites within a single species or within related species and genera of one or more families. Before a compound can be used as a drug it is essential to know its likely effects when used in humans. This is achieved after extensive laboratory testing followed by the application of clinical trials.

Biological testing for antimalarial activity in plants has progressed over the years. In the 1950s, the screening of crude plant extracts was based on avian malarias using *in vivo* tests against *P. gallinaceum* in chicks and against *P. cathemerium* and *P. lophurae* in ducklings. In the 1970s, *in vitro* procedures were developed utilizing *P. falciparum* cultures in human red blood cells, a technique that enabled the development of a microdilution assay. This technique, compared to previous ones active on human malarias, is useful to assess *in vitro* antimalarial activity of crude extracts prior to the isolation of active principles.[7]

One such *in vitro* assay is the parasite lactate dehydrogenase (pLDH) assay. pLDH is a terminal enzyme in the glycolytic pathway of *Plasmodium spp.* and plays an important role in the parasites anaerobic carbohydrate metabolism. As malaria parasites principally rely on anaerobic glycolysis, they require the regeneration of nicotinamide adenine dinucleotide (NAD) for the continuous flux of glucose through this pathway.[28] On the basis of the discovery that pLDH is distinguishable from host LDH using the 3-acetylpyridine dinucleotide analogue of NAD (APAD), Makler *et al*.[29] developed a drug-sensitivity assay that determines inhibition profiles by measuring the enzymatic activity of pLDH.

---

[28] H. Noedl, C. Wongsrichanalai and W.H. Wernsdorfer, *Trends Parasitol.*, 2003, **19**, 175.
[29] M.T. Makler J.M. Ries, J.A. Williams, J.E. Bancroft, R.C. Piper, B.L. Gibbins and D.J. Hinrichs, *Am. J. Trop. Med. Hyg.*, 1993, **48**, 739.

An *in vivo* screening is possible in mice using a natural infection with *P. berghei*. These methods allow the development of strains resistant to chloroquine or to other antimalarials by a passage in the presence of increasing concentrations of the drug. *In vitro* tests are considered more practical, quicker and less expensive than *in vivo* cultures and not all antimalarial drugs are active in the *P. berghei* mouse model. In addition, the *in vivo* model requires significantly higher amounts of drugs (at least 1 g of extract) when compared to the *in vitro* assays which require a few mg of extract. The advantage of the *in vivo* model is that at the same time it gives a measure of toxicity.

Detailed evaluation of antimalarial drugs is done in the Aotus monkey (*Aotus trivirgatus*) using *P. falciparum* infection or in the Rhesus monkey (*Macaca mulata*) with *P. cynomolgi* B infection.[7] Of the numerous extracts and compounds studied in primary screens *in vitro*, very few reach this stage of investigation.

1.13 Scope of this Study

South Africa boasts remarkable biodiversity and a rich cultural heritage of medicinal plant use. A number of extracts from South African plants have been evaluated for *in vitro* antimalarial activity but little is known about their active constituents.[30] In light of this and the pressing need for new antimalarial drugs, the South African Department of Arts, Culture, Science and Technology (now the Department of Science and Technology) awarded an Innovation Fund to five South African institutions - the Medical Research Council, South African National Botanical Institute, Council for Scientific and Industrial Research, University of Cape Town and University of Pretoria - to scientifically validate South African medicinal plants for the treatment of malaria.[31]

Extracts of approximately 140 plant taxa, which were selected semi-quantitatively using weighted criteria, were tested *in vitro* against the D10 *P. falciparum* strain using the pLDH assay. Approximately 50% of these showed promising antiplasmodial activity ($IC_{50} \leq 10\mu g/ml$). Several South African plant species and

---

[30] E.A. Prozesky, J.J.M. Meyer, and A.I. Louw, *J. Ethnopharmacol.*, 2001, **76**, 239.
[31] C. Clarkson V.J. Maharaj, N.R. Crouch, O.M. Grace, P. Pillay, M.G. Matsabisa, N. Bhagwandhin, P.J. Smith, P.I. Folb., *J. Ethnopharmacol.*, 2004, **92**, 177.

genera were shown for the first time to possess *in vitro* antiplasmodial activity. This study reports on two of the plants identified as potential sources of new antimalarial drugs and was aimed at:

1. Investigating the *in vitro* antiplasmodial activity of these two plant species (*Vernonia staehelinoides* and *Oncosiphon piluliferum*)
2. Identifying, isolating and characterising compounds with *in vitro* antiplasmodial activity from these two plants

CHAPTER 2

Sesquiterpene lactones

2.1. Secondary Plant Metabolites

A characteristic feature of plants is their ability to synthesize a large variety of low molecular weight compounds, the so-called secondary metabolites. By definition secondary plant metabolites do not play a role in the primary metabolic processes essential for the maintenance of life in an individual plant, but many may be absolutely essential to the survival of the species as a whole in a given natural habitat. Secondary metabolites may function as signal molecules within the plant or between the plant producing them and other plants, microbes, herbivores, pollinating or seed-dispersing animals. More often, they serve as chemical defense compounds against herbivorous animals, microbes, viruses or competing plants.

It is suggested that during the course of evolution millions of secondary products have been synthesized from time to time by different species of plants and when the presence of a particular secondary product conferred a selectionary advantage on the plant containing it, then the chances of survival of the plant, its offspring and the secondary product itself will have been enhanced.[1]

Since the 1850s organic chemists have extensively investigated the chemical properties of these novel phytochemicals. Studies of natural products stimulated the development of separation techniques, spectroscopic approaches to structure elucidation, and synthetic methodologies that now constitute the foundation of contemporary organic chemistry. Interest in natural products was prompted by their immense utility as dyes, fibers, glues, polymers, oils, waxes, flavouring agents, perfumes and drugs. Recognition of the biological properties of numerous natural products has fueled the current focus of this field, namely the search for new drugs, antibiotics, insecticides and herbicides.

[1] E.A. Bell and B.V. Charlwood, 'Secondary Plant Products', Springer-Verlag, Berlin Heidelberg, 1980.

2.2. Terpenoids

The largest class of plant secondary metabolites is undoubtedly that of the terpenoids or isoprenoids. Terpenoids are not only numerous but also extremely variable in structure, exhibiting hundreds of different carbon skeletons and a large assortment of functional groups. In spite of such diversity, the simple unifying feature of all terpenoids is that these compounds are derived from the simple process of assembly of a C_5 unit *i.e*. the isoprene **(19)** unit.[2]

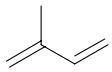

(19)

This leads to a rational classification of the terpenoids depending upon the number of such isoprene units incorporated in the molecular skeleton (Table 2.1).

Table 2.1 Classification of terpenoids

Terpenoids	Isoprene units	Carbon atoms
Monoterpenes	2	10
Sesquiterpenes	3	15
Diterpenes	4	20
Sesterterpenes	5	25
Triterpenes	6	30
Carotenoids	8	40
Rubber	>100	>500

The biosynthetic pathway to terpenoids (Figure 2.1) comprises four basic stages, the first of which involves the formation of isopentenyl pyrophosphate (IPP) **(20)**, the biological C_5 isoprene unit. IPP and its allylic isomer, dimethylallyl pyrophosphate (DMAPP) **(21)** are synthesized by plants via one of two routes: the well-established mevalonic acid pathway; or the newly-discovered glyceraldehyde phosphate/pyruvate pathway.

[2] A.A. Newman, 'Chemistry of Terpenes and Terpenoids', Academic Press, London and New York, 1970.

In the mevalonate pathway for IPP biosynthesis **(A)**, three acetyl coenzyme A (acetyl-CoA) **(22)** units are joined successively to form 3-hydroxy-3-methylglutaryl coenzyme A (HMG-CoA) **(24)**. HMG-CoA is then reduced to mevalonate (MVA) **(25)**, which is subsequently phosphorylated, decarboxylated and dehydrated to form IPP **(20)**.[3,4] The first intermediate in the non-mevalonate pathway **(B)**, 1-desoxy-D-xylulose-5-phospate **(28)**, is assembled by condensation of glyceraldehyde 3-phoshate (GAP) **(26)** and pyruvate **(27)**. A skeletal rearrangement coupled with a reduction step yields the branched-chain polyol, 2C-methyl-D-erythritol 4-phosphate **(29)**, which is subsequently converted into a cyclic 2,4-diphospate **(30)**, by a series of enzymes via nucleotide diphosphate intermediates.[5,6]

In the second stage, the basic C_5 units condense to generate geranyl pyrophosphate (GPP, C_{10}) **(31)**, farnesyl pyrophosphate (FPP, C_{15}) **(32)** and geranylgeranyl pyrophosphate (GGPP, C_{20}) **(33)**. In the third stage the C_{10}-C_{20} pyrophosphates undergo a variety of cyclizations and rearrangements to produce the parent carbon skeletons of each terpene class. GPP is converted to the monoterpenes, FPP is converted to the sesquiterpenes and GGPP is converted to the diterpenes. FPP and GGPP can also dimerize in a head-to-head fashion to form the precursors of the C_{30} and C_{40} terpenoids, respectively. The fourth stage encompasses a range of oxidations, reductions, isomerizations, conjugations and other transformations by which the parent skeletons of each terpene class are converted to thousands of distinct terpene metabolites.[2]

There are over 30 000 terpenoid natural products known. Many of these are from plants, where they play important roles in the ecological chemistry involved in interactions with insects and pathogens. Many terpenoids have been shown to have important biological activities. There are a number of antibiotics amongst the sesquiterpenes and diterpenes. Some sesquiterpenes and diterpenes are insect and plant hormones, respectively.

---

[3] A. L. Lehninger, 'Biochemistry', 2nd edition, Worth Publishers, New York, 1975, 681.
[4] E.I. Wilding, J.R. Brown, A.P. Bryant, A.F. Chalker, D.J. Holmes, K.A. Ingraham, S. Iordanescu, C.Y. So, M. Rosenberg and M.N. Gwynn, *J. Bacteriol*., 2000, **182**, 4319.
[5] F. Rohdich, K. Kis, A. Bacher and W. Eisenreich, *Curr. Opin. Chem. Biol.*, 2001, **5**, 535.
[6] A. Disch, J. Schwender, C. Müller, H.K. Lichtenthaler and M. Rohmer, *Biochem. J*., 1998, **333**, 381.

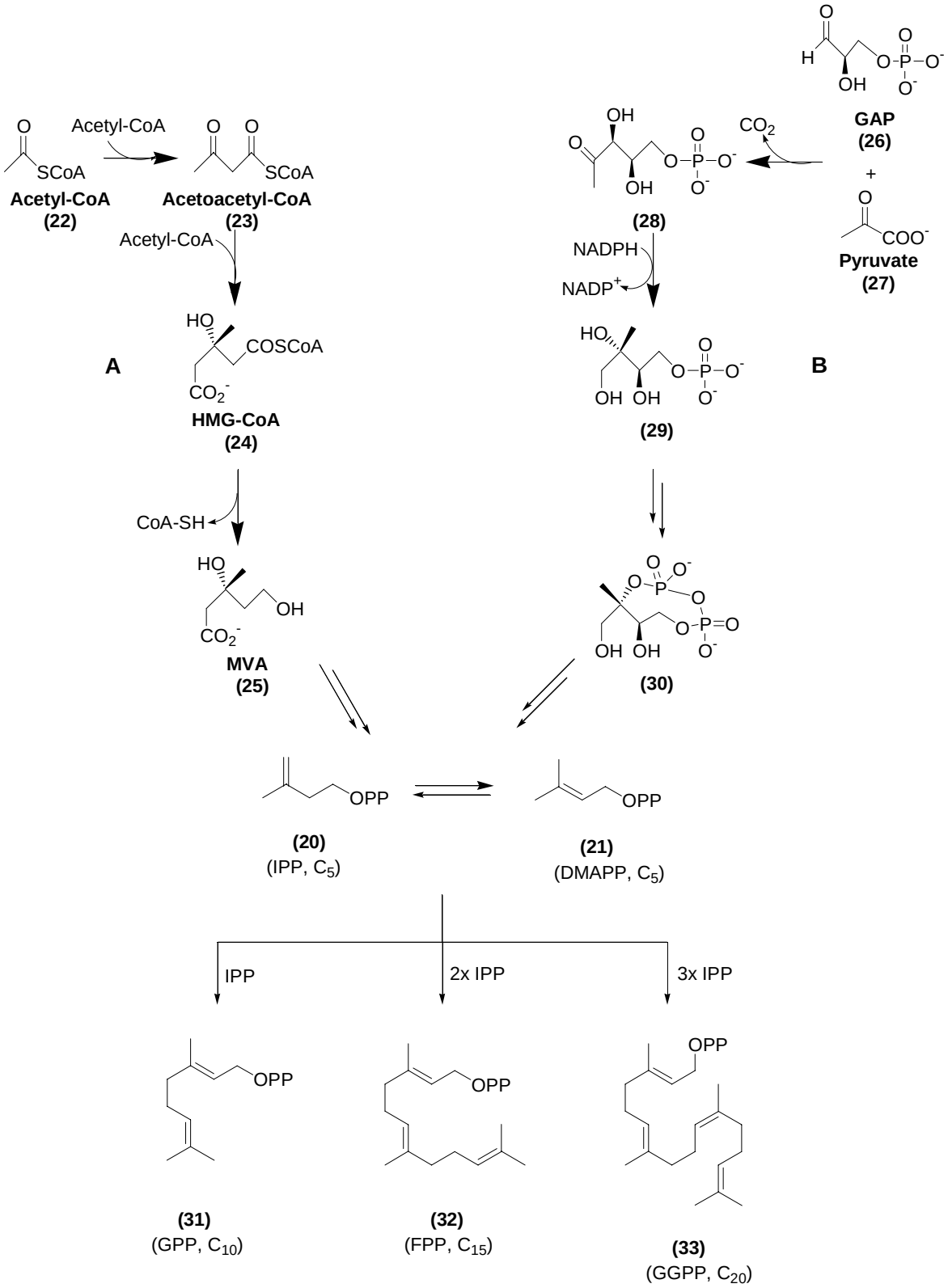

Figure 2.1 Overview of terpenoid biosynthesis in plants, showing the mevalonate **(A)** and GAP/pyruvate **(B)** pathways for the production of IPP, as well as the generation of the higher order terpenoid building blocks

Terpenoids can accumulate to high levels in some plant species and are significant components of essential oils that have found important uses in the flavour and fragrance industry. Many terpenoids find use in industry as raw materials in the manufacture of adhesives, coatings, emulsifiers and speciality chemicals, whilst others are of commercial importance as insecticides or as pharmaceuticals.

2.3. Sesquiterpene Lactone Skeleton

The sesquiterpene lactones are considered as a major class of secondary metabolites, which mainly occur in the *Asteraceae*. They are typically colourless, bitter, relatively stable, lipophilic constituents that often contain as a major structural feature an α,β-unsaturated-γ-lactone. They are biogenetically derived from *trans*,*trans*-farnesyl pyrophosphate **(32)** following an initial cyclisation and ensuing oxidative modifications. The typical lactones resulting from these enzyme-mediated cyclisations are primarily classified on the basis of their carbocyclic skeletons as germacranolides, guaianolides, pseudoguaianolides and eudesmanolides. However, sesquiterpene lactones exhibit a variety of other skeletal arrangements.

Generally the α,β-unsaturated lactone is either *cis*- or *trans*-fused to the C(5)-C(6), C(6)-C(7) or C(7)-C(8) positions of the carbocyclic skeleton containing, in many cases, an α-methylene group. Structural modification of the basic sesquiterpene skeleton involves incorporation of an epoxide ring, hydroxyl groups (generally esterified), and/or a C_5-acid such as tiglic or angelic acid. A few sesquiterpene lactones occur in glycosidic form and some contain halogens or sulphur.[7]

Over 4000 different sesquiterpene lactone structures are known, but the majority of them have a guaiane, eudesmane or germacrene framework (Figure 2.2). It is generally accepted that biogenetically the germacranolides represent the most primitive class and that all other sesquiterpene lactones evolved from them.[8]

---

[7] A.K. Picman, *Biochem. Syst. Ecol.*, 1986, **14**, 255.
[8] http://www.ansci.cornell.edu/plants/toxicagents/sesqlactone/structure1.gif

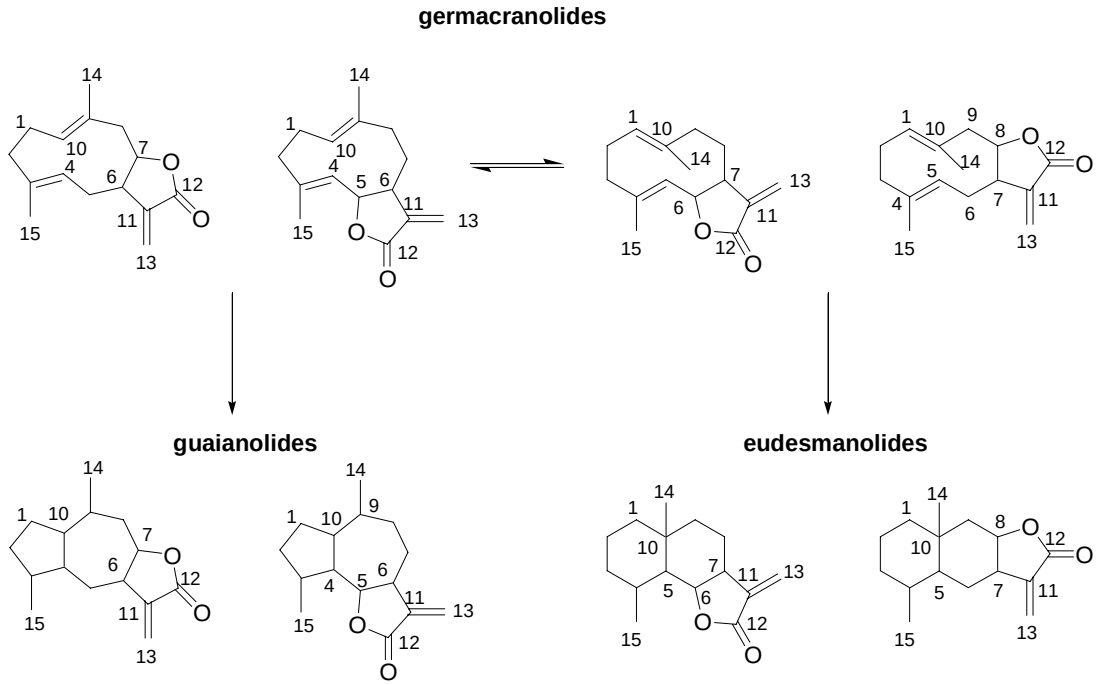

Figure 2.2 Germacranolide, guaianolide and eudesmanolide skeletal types.

2.4. Sesquiterpene Lactone Biosynthesis

By far the largest group of naturally occurring sesquiterpene lactones is the germacranolides, and the majority of sesquiterpene lactones are thought to evolve from this class. The simplest member of the germacranolides (+)-costunolide **(34)** is generally accepted as the common intermediate of all germacranolide-derived lactones. Figure 2.3 depicts the proposed biosynthetic route for the germacrene-derived sesquiterpene lactones as established in chicory (*Cichorium Intybus*) roots.[9]

The committed step in the biosythesis of (+)-costunolide **(34)** is the cyclization of farnesyl pyrophosphate (FPP) **(32)** to (+)-germacrene A **(35)** by a sesquiterpene synthase (**I**). Formation of the lactone ring involves the introduction of a carboxylic acid function in the isopropenyl group of (+)-germacrene A. This process starts with the hydroxylation of (+)-germacrene A **(35)** to germacra-1(10),4,11(13)-trien-12-ol **(36)** by (+)-germacrene A hydroxylase, a cytochrome P450 enzyme (**II**).

[9] J. de Kraker, M. C.R. Franssen, M.C. Dalm, A. de Groot and H.J. Bouwmeester., *Plant Physiol.*, 2001, **125**, 1930.

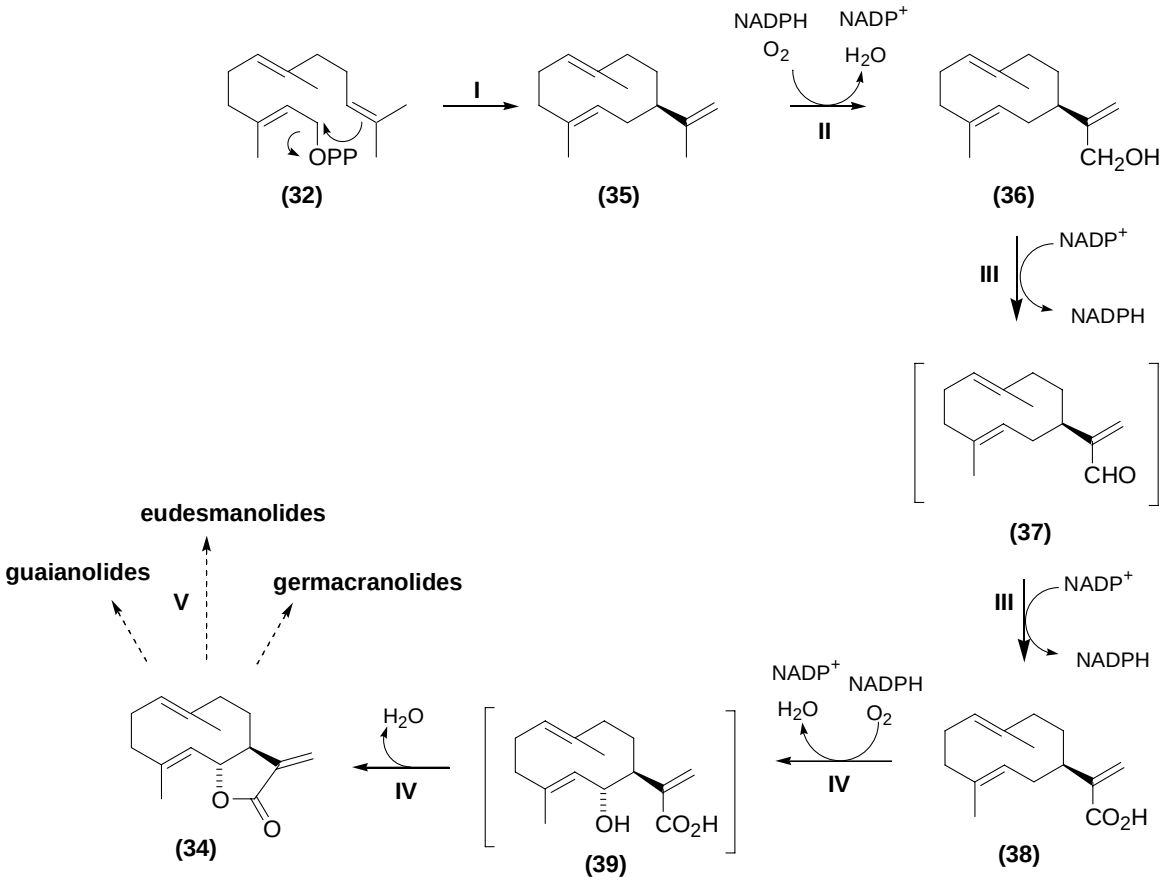

Figure 2.3 Proposed biosynthetic route for the germacrene-derived sesquiterpene lactones present in chicory.

Germacratrien-12-ol **(36)** is subsequently oxidized to germacra-1(10),4,11(13)-trien-12-oic acid **(38)** via the germacra-1(10),4,11(13)-trien-12-al **(37)** intermediate by $NADP^+$-dependent dehydrogenases (**III**). Conversion of germacratrien-12-oic acid **(38)** to (+)-costunolide **(34)** is proposed to proceed *via* a hydroxylation at the C(6)-position of the germacrene acid **(38)** and subsequent attack of the hydroxyl group on the carboxyl group at C(12) (**IV**). This is followed by the postulated formation of guaiane, eudesmane and germacrane lactones (**V**).

2.5. Biological Activities of Sesquiterpene Lactones

The sesquiterpene lactones from plants comprise a group of substances with a variety of biological effects. These include antibacterial, antifungal, antitumour, antiplasmodial, anthelminthic, schistosomicidal, cytotoxic, phytotoxic and

analgesic activities.[10] They are also known to poison livestock, to act as insect feeding deterrents and to cause allergic contact dermatitis in humans. The variety of activities displayed by sesquiterpene lactones against numerous types of organisms suggests that the individual lactones from this group of plant secondary metabolites may play a role in the plant's defense against pathogens, herbivorous insects and mammals, and in competition with other plants.[11]

The biological activities are generally the result of reaction of sesquiterpene lactones with the thiol groups of vitally important compounds such as enzymes. No major generalizations have emerged from various studies aimed at examining the relationship between biological activities and chemical structure of these compounds. This is because in addition to the α-methylene-γ-lactone moiety **(40)**, which has been suspected to be responsible for several activities, a number of other groups of sesquiterpene lactones as well as variation in physiology and biochemistry between diverse organisms affected by these compounds must be considered. [7]

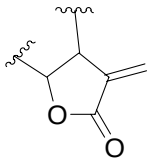

(40)

Detailed investigations on the biological activities of sesquiterpene lactones provides useful information in our understanding of the adaptive role of these compounds in plants and contribute to a general perception of their activities in related disciplines of medicine, pharmacology and agriculture.

2.5.1. Antitumour and Cytotoxic Activity

Plant extracts that exhibit anti-cancer activity have received considerable attention particularly in the last 40 years.[11] Sesquiterpene lactones are amongst the biggest class of cytotoxic and antitumour compounds of plant origin. Various studies on the relationship between chemical structure and cytotoxic activity of sesquiterpene lactones revealed that the presence of an exo-methylene group is an essential

[10] R.V. Burim, R. Canalle, J.L.C. Lopes and C.S. Takahashi, *Genet. Mol. Biol.*, 1999, **22**, 2
[11] E. Rodriguez, G.H.N. Towers and J.C. Mitchell, *Phytochemistry*, 1976, **15**, 1573.

requisite for cytotoxicity. Loss of cytotoxicity and tumour inhibition was observed with changes such as saturation or addition to the methylene group. An additional conjugated ester, cyclopentenone, an epoxy group or a second α,β-unsaturated lactone appeared to enhance cytotoxicity.[7]

Studies of structure–antitumour activity established that the presence of an α-methylene-γ-lactone moiety, a β-unsaturated cyclopentenone ring or an α-epoxycyclopentenone system gives rise to significant *in vivo* antitumour activity.[7] The reactivity of sesquiterpene lactones exhibiting antitumour activity may be associated with selective alkylation of nucleophilic groups in biological growth-regulatory macromolecules such as key enzymes which control cell division. For instance vernolepin **(41)**, an eudesmanolide, has been shown to inhibit phosphofructokinase, an enzyme that has many –SH groups.[11]

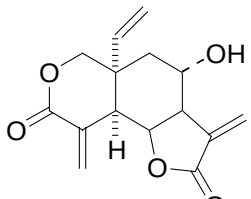

(41)

2.5.2. Antiplasmodial Activity of Sesquiterpene Lactones

After the discovery of the antiplasmodial properties of the endoperoxide sesquiterpene lactone artemisinin **(9)**, many other sesquiterpene lactones have been investigated as antimalarial agents. Some examples of these are illustrated below.

Two sesquiterpene lactones of the germacranolide type neurolenin A **(42)** and neurolenin B **(43)** obtained from *Neurolaena lobata* showed interesting *in vitro* activity against *P. falciparum* (IC_{50} 0.92 μM and 0.62 μM, respectively) if compared with that of the reference antimalarial agents, artemisinin **(9)** (IC_{50} 0.14 μM) and quinine **(1)** (IC_{50} 0.19 μM).

Structure-activity studies suggested that the α,β-unsaturated-keto function and a free hydroxyl function at C(8) increased the antiplasmodial activity. The

compounds were found to be cytotoxic, though their IC_{50}'s on both tumour cell lines tested were significantly higher than their IC_{50} values for activity against the parasite. The authors hypothesized that the antiplasmodial effects of the neurolenins are not due to their general cytoxicity, caused by the alkylating properties of the exocyclic methylene group fused to the lactone ring, but are rather dependent on a more specific mechanism of action.[12] These results may explain the traditional use of decoctions of *Neurolaena lobata* in Central America to treat malaria.

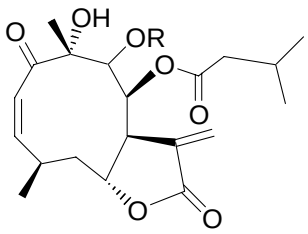

(42) R = H
(43) R = Ac

The sesquiterpene dilactone 16,17-dihydrobrachycalyxolide **(44)** from *Vernonia brachycalyx*, a Kenyan plant used to treat malaria, showed strong antiplasmodial activity (IC_{50} 5.9 to 32 μM, on different *P. falciparum* strains). It was however found to strongly inhibit the proliferation of human lymphocytes at the same concentrations, so it suppresses the body's immune mechanism if administered to humans.[13]

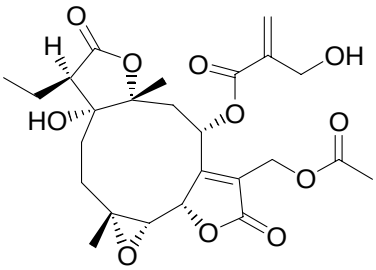

(44)

[12] G. Francois, C.M. Passreiter, H.J. Woerdenbag and M.V. Looveren, *Planta Med.*, 1996, **62**, 126.
[13] H.A. Oketch-Rabah, S.B. Christensen, K. Frydenvang, S.F. Dossaji, T.G. Theander, C. Cornett, W.M. Watkins, A. Kharazmi and E. Lemmich, *Planta Med.*, 1998, **64**, 559.

Brevilin A **(45)** which was isolated from the Chinese medicinal plant, *Centipeda minima*, was found to have activity against *P.falciparum*.[14]

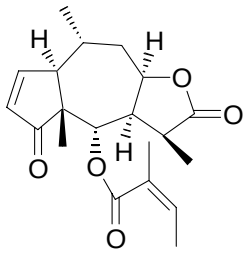

(45)

The sesquiterpene lactone, parthenin **(46)**, identified as the major active amoebicidal compound of *Parthenium hysterophorus*, was also shown to be active *in vitro* (IC_{50} 1.29 μg/ml) against a multi-drug resistant (K1) strain of *P. falciparum*.[15] A series of semi-synthetic derivatives of parthenin has been prepared which have varying activities against *P. falciparum in vitro* and it has been shown that the active moieties are the exocyclic methylene of the lactone ring and the cyclopentenone A ring.

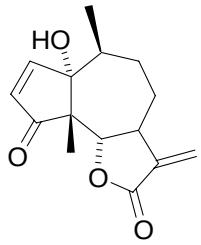

(46)

A series of sesquiterpene lactones, including vernodalin **(47)**, from *Vernonia amygdalina* is active against *P. falciparum in vitro*.[16]

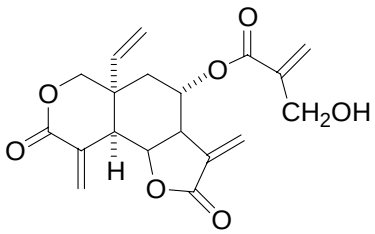

(47)

[14] S. Schwikkard and F.R. van Heerden, *Nat. Prod. Rep.*, 2002, **19**, 675.
[15] J.D. Phillipson and C.W. Wright, *J. Ethnopharm.*, 1991, **32**, 155.
[16] W.C. Evans, 'Trease and Evans´ Pharmacognosy', 14th Ed, WB Saunders, London, 1996, 429.

2.5.3. Other Pharmacological Activities of Sesquiterpene Lactones

A wide variety of sesquiterpene lactones isolated from plant extracts have been demonstrated to show various other pharmacological activities which include expectorant, blood pressure lowering, cholinergic, hypoglycaemic, anti-asthmatic and anti-inflammatory activity. Inulicin **(48)**, for instance, is a sesquiterpene lactone from *Inula japonica* which acts as a stimulant of the central nervous system and smooth muscles of the intestine, has anti-ulcer activity and capillary-strengthening diuretic properties. High doses of inulicin inhibit cardiac activity but low doses have no effect.[7]

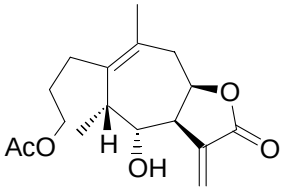

(48)

The wide variety of pharmacological activities of sesquiterpene lactones show that these compounds could have significant promise for practical utility in medicine.

CHAPTER 3

Antiplasmodial Activity of *Vernonia staehelinoides*

3.1 *Vernonia staehelinoides* Harv.

Vernonia belongs to the botanical family Asteraceae and there are over 1000 different species of which approximately 50 species occur in Southern Africa.[1] *Vernonia* species have been used traditionally to treat rheumatism, dysentery, diabetes, jaundice as well as malaria.[2] Many *Vernonia* species have been studied chemically. Highly oxygenated germacranolides such as glaucolides and hirsutinolides seem to be characteristic for many members of this genus, though many other compounds have also been isolated.[3]

Vernonia staehelinoides, commonly known as "blouteebossie", is a multi-stemmed perennial shrublet. Stems and leaves are covered with numerous short hairs, giving it a greyish appearance. Leaves are very narrow and long flexuous stems give rise to numerous flower heads. It is indigenous to South Africa and grows on rocky ridges in summit grasslands predominantly in Gauteng as well as in parts of Mpumalanga and the Limpopo Province.

Figure 3.1 *Vernonia staehelinoides* growing at Klapperkop, Pretoria. Photo by Jean Meyer (SANBI)

---

[1] http://www.plantzafrica.com/planttuv/vernonhirsut.htm

[2] B.E. van Wyk, B. van Oudtshoorn and N. Gericke, 'Medicinal Plants', Briza Publications, Pretoria, 2000, 268.

[3] F. Bohlmann, C. Zdero, R.M. King and H. Robinson, *Phytochemistry*, 1982, **21**, 695.

V. staehelinoides is reported to be used medicinally but no details have been specified.[4] Previous chemical investigations of this plant revealed that the roots contain squalene, stigmasterol and sitosterol while the aerial parts afforded caryophyllene, α-humulene, germacrene D and a novel glaucolide, 3β-hydroxy-stilpnotomentolide-8-*O*-(5-acetoxysenecioate) **(49)**.[5]

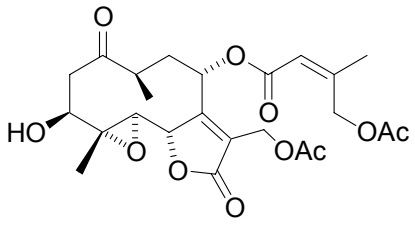

(49)

3.2 *In vitro* Antiplasmodial Activity of *V. staehelinoides* Extracts

A dichloromethane, a 1:1 dichloromethane/methanol and an aqueous extract were prepared from the leaves of *V. staehelinoides* (Table 3.1).

Table 3.1 Yield of extracts obtained from *V. staehelinoides* leaves

Extract code	Extract description	% Yield
P01009A	Dichloromethane	3.3
P01009B	Dichloromethane/Methanol (1:1)	3.8
P01009C	Water	1.3

The concentrated *V. staehelinoides* extracts were tested *in vitro* against a chloroquine-sensitive (D10) strain in duplicate (Table 3.2). Those extracts showing a D10 IC_{50} of less than 10 μg/ml were tested against the chloroquine-resistant (K1) strain of *P. falciparum*.

The antiplasmodial component in the leaves of *Vernonia staehelinoides* was concentrated in the organic extracts. P01009A and P01009B, were found to be significantly active against both strains of the parasite having 50% inhibitory concentrations (IC_{50}) values of less than 10μg/ml. The dichloromethane extract was to some extent more active than the dichloromethane/methanol (1:1) extract

[4] J.M. Watt and M.G. Breyer-Brandwyk, 'The Medicinal and Poisonous Plants of Southern Africa', 2nd Edition. Livingstone, London, 1962.
[5] F. Bohlmann, M. Wallmeyer and J. Jakupovic, *Phytochemistry*, 1982, **21**, 1445.

against both the D10 and K1 strains of *P. falciparum*. The aqueous extract, P01009C, was found to be relatively inactive.

Table 3.2 *In vitro* antiplasmodial activity of *V. staehelinoides* extracts

Extract	D10 (Experiment 1) IC_{50} (μg/ml)	D10 (Experiment 2) IC_{50} (μg/ml)	K1 IC_{50} (μg/ml)
P01009A	2.0	4.0	2.8
P01009B	3.0	9.0	4.5
P01009C	>10	>10	-

3.3 Bioassay-guided Fractionation of the *V. staehelinoides* Extracts

Bioassay-guided fractionation based on *in vitro* antiplasmodial activity against the D10 *P. falciparum* strain was used to identify the compounds from the organic extracts of *V. staehelinoides* which are responsible for the observed activity. Details of the purification techniques are given in Chapter 5 (Experimental).

3.3.1 Bioassay-guided Fractionation of P01009A

Figure 3.2 outlines the stepwise fractionation of the dichloromethane extract, P01009A, guided by observed antiplasmodial activity against the D10 *P. falciparum* strain. Enhanced antiplasmodial activity was observed for fractions 1C, 1D and 1E. Based on their similar TLC profiles and the yield of the three fractions, fraction 1D was selected for further purification. This process led to the identification (by TLC analysis) of two semi-pure compounds in fractions 2C and 2D with significant antiplasmodial activity (0.65 and 0.8 μg/ml, respectively). The two compounds gave distinctive colours (orange and brown) with vanillin spray reagent and were therefore easily discernible. Further purification of the two compounds for structure determination was impractical due to the low yields of fractions 2C and 2D.

3.3.2 Bioassay-guided Fractionation of P01009B

Figure 3.3 summarizes the stepwise fractionation of the 1:1 dichloromethane/ methanol extract, P01009B, which was guided by the observed antiplasmodial activity against the D10 *P. falciparum* strain. Increased antiplasmodial activity was

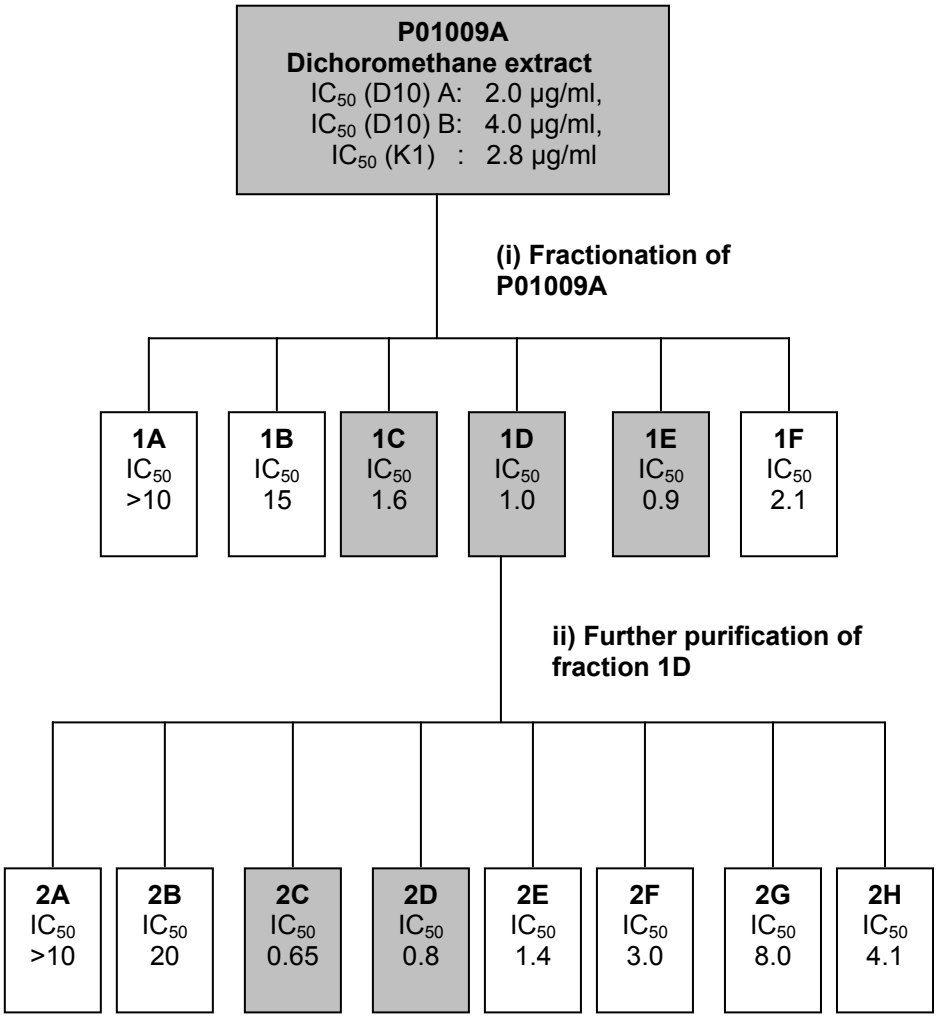

Figure 3.2 Fractionation of the dichloromethane extract of *V. staehelinoides.* IC_{50} values are in µg/ml.

observed in fractions 3D and 3E. Based on the similar TLC profiles and the yields of the two fractions, fraction 3E was selected for further purification. This resulted in a single fraction, 4C, with improved antiplasmodial activity. TLC analysis of fraction 4C revealed that it contained two major compounds: the same compounds identified in fractions 2C and 2D of the dichloromethane extract. Due to the low yield of fraction 4C, further purification was not feasible.

3.4 Targeted Purification of Active Compounds from *V. staehelinoides*

Once it was established that essentially the same two compounds were responsible for the antiplasmodial activity in both the dichloromethane (P01009A) and the 1:1 dichloromethane/methanol (P01009B) extracts of *V. staehelinoides*,

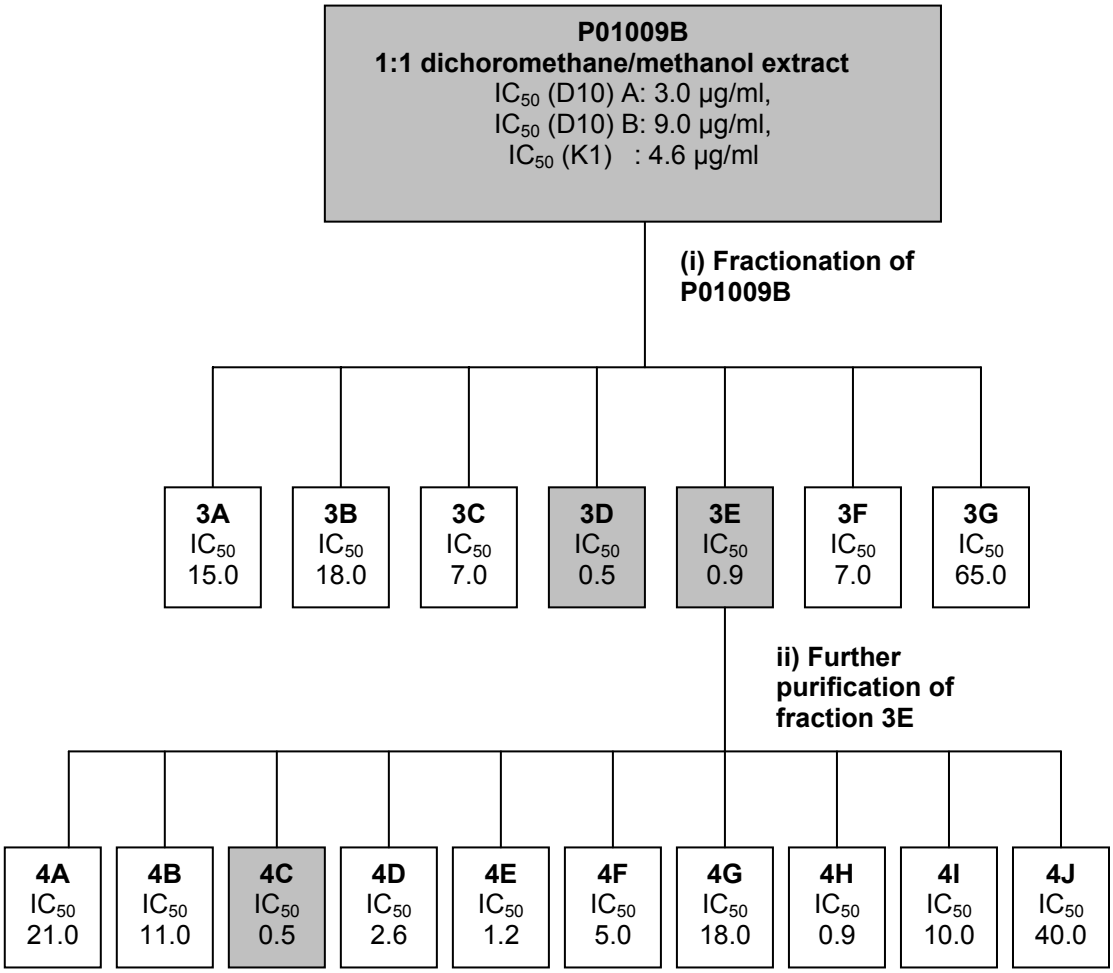

Figure 3.3 Fractionation of the dichloromethane/methanol (1:1) extract of *V. staehelinoides.* IC_{50} values are in µg/ml.

targeted isolation of the active compounds from P01009A was conducted. Liquid-liquid partitioning of the crude extract served to concentrate the active components in a less complex matrix. TLC analysis of the three fractions generated from liquid/liquid partitioning of the crude extract revealed that the target compounds were concentrated in the dichloromethane-soluble fraction, (5A). This fraction was subjected to a series of successive flash silica gel purifications to yield compounds **(50)** and **(51)** (Figure 3.4). This proved to be an effective and time economical method for the isolation of the active compounds.

The yield of **(50)** was 0.39% by weight of the dichloromethane extract and 0.01% by weight of the dried ground plant material. For **(51)** the yields were marginally higher; 0.56% and 0.02% respectively. The relatively low yields of the active compounds indicate that the antiplasmodial component was probably a minor

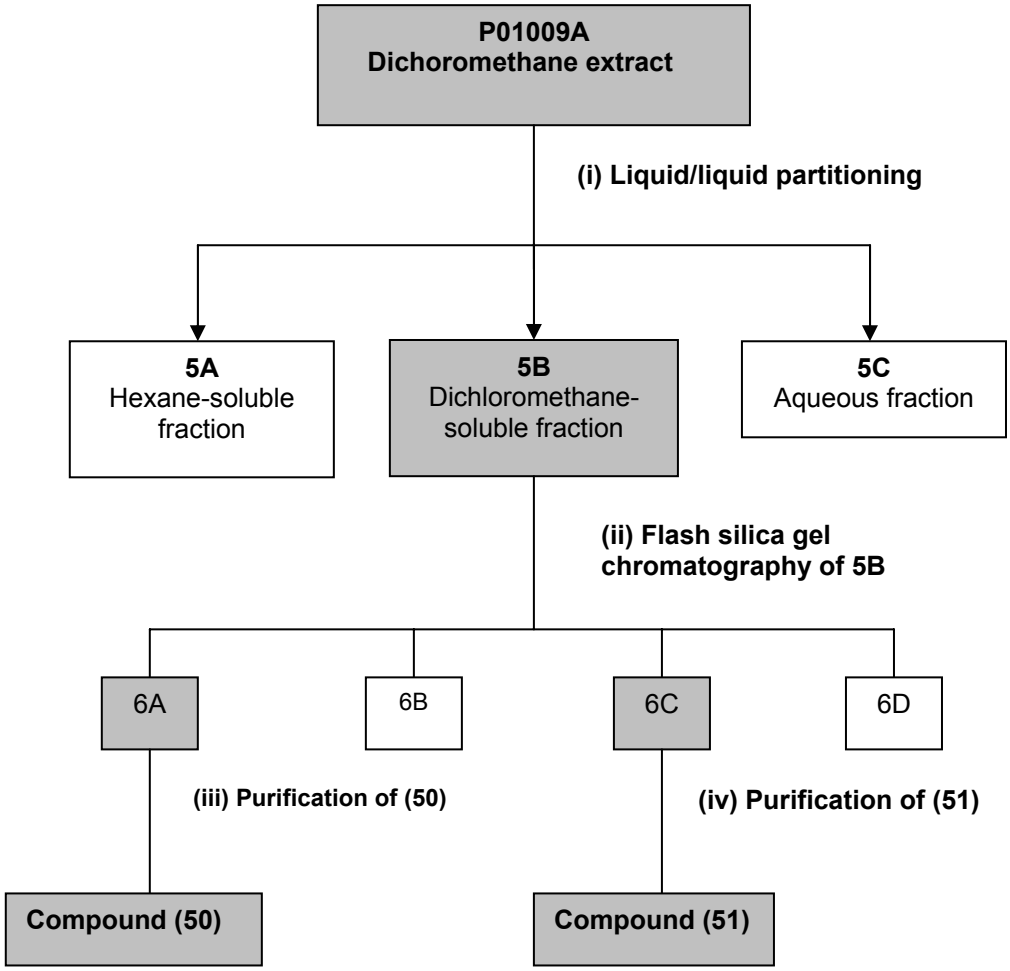

Figure 3.4 Targeted purification of compounds **(50)** and **(51)** from P01009A

constituent of the leaves of the plant. The low yields could also be attributed to the fact that compounds **(50)** and **(51)** are relatively unstable and showed evidence of decomposition during silica gel purification and on standing. The yields could possibly be improved to some extent by optimising the extraction and separation procedures. Despite the low yields, the quantities of **(50)** and **(51)** isolated were sufficient for structure elucidation and *in vitro* assaying.

3.5 Identification and Characterization of Compounds (50) and (51) from *V. staehelinoides*

Compounds **(50)** and **(51)** were identified and characterized by mass spectrometry (HR EI-MS) and NMR experiments. The structural assignments of **(50)** and **(51)** are based on detailed studies of the high-field ^{1}H and ^{13}C NMR spectral data

(chemical shifts and coupling constants) and the following two-dimensional (2D) NMR techniques.[6,7]

The proton-proton connectivity patterns were established by 2D (^{1}H,^{1}H) correlation spectroscopy (COSY) experiments. The multiplicities of the different resonances in the ^{13}C spectra were deduced from the proton-decoupled CH, CH_2 and CH_3 subspectra obtained using the DEPT (distortionless enhancement by polarisation transfer) pulse sequence. The ^{13}C resonances were partly assigned by correlation of the proton-bearing carbon atoms with specific proton resonances in 2D (^{13}C,^{1}H) heteronuclear single quantum correlation (HSQC) experiments. The assignment of the quaternary carbon atoms and the deduction of the long-range (more than one bond) connectivity pattern was facilitated by 2D (^{13}C,^{1}H) heteronuclear multiple bond correlation (HMBC) experiments. Correlations observed in nuclear Overhauser effect spectroscopy (NOESY) experiments provided information on the relative stereochemistry of the compounds.

3.5.1 Structural Elucidation of 13-Acetoxy-1,4*β*-epoxy-8*α*-(2-methylpropenoyl)-3-oxo-1,5,7(11)-germacratrien-12,6-olide (50)

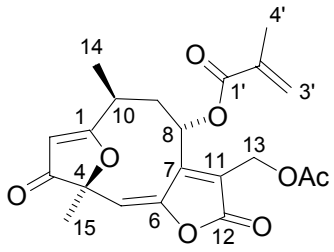

(50)

Compound **(50)** was isolated as a colourless gum and had $[\alpha]_D$ –77.4 (*c* 0.31, $CHCl_3$). The HR EI-MS did not show the molecular ion peak but showed a $[M–C_3H_5COOH]^+$ fragment at *m/z* 316.0868. The molecular formula of **(50)** was deduced to be $C_{21}H_{22}O_8$, corresponding to a molecular weight of 402 Dalton. The ^{1}H, ^{13}C, HSQC, HMBC, COSY and NOESY data are summarized in Table 3.3.

---

[6] W. R. Croasmun and R.M.K. Carlson, "Two Dimensional NMR Spectroscopy: Applications for Chemists and Biochemists", VCH Publishers, New York, 1987.

[7] J.M. Saunders and B.K. Hunter, "Modern NMR Spectroscopy. A Guide for Chemists", Oxford University Press, Oxford, 1987.

The ^{1}H NMR spectrum of (**50**) showed a pair of broad doublets (J 13.2 Hz) at δ_H 4.91 and 5.09, which were assigned to the C(13) (δ_C 55.65T) protons. The chemical shift of this AB system suggested that the C(13) protons were allylic and this was confirmed by their HMBC correlations to the olefinic carbons, C(7) (δ_C 151.12S) and C(11) (δ_C 132.66S). H(13) also showed an HMBC correlation to an ester carbonyl carbon atom at δ_C 170.15S, which in turn was correlated to a methyl signal in the acetate region (δ_H 2.03) indicating that there was an *O*-acetate group at C(13). The HMBC correlation of H(13) with another ester carbonyl, C(12) (δ_C 166.14S), as well as the correlation between C(7) and the C(5) (δ_C 117.89D) olefinic proton at δ_H 5.89 which was in turn correlated to the olefinic carbon atom C(6) (δ_C 146.19S), established the presence of an enol 2(5H)-furanone moiety **(50 i)** in the compound.

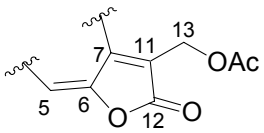

50 i

The methyl resonance at δ_H 1.58, assigned to H(15), correlated with the signal at δ_C 86.90S, assigned to an oxygen-substituted quaternary carbon, in the HMBC spectrum and placed the methyl group at C(4). H(15) also showed an HMBC correlation with a ketone carbonyl carbon at δ_C 202.27S, which was subsequently identified as C(3). The correlation of an olefinic proton signal at δ_H 5.40, H(2), with C(3) and an oxygen-bearing olefinic carbon, C(1), at δ_C 194.93S, revealed the presence of a dihydrofuran-4-one moiety **(50 ii)** formed by an oxygen bridge between C(1) and C(4).

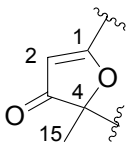

50 ii

The two furanone moieties **(50 i)** and **(50 ii)** were subsequently linked by the long-range (HMBC) correlations between the C(5) and H(15) signals to generate the fragment **(50 iii)**.

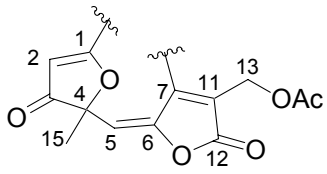

50 iii

The signal for C(1) showed HMBC correlations to a proton resonating at δ_H 3.01, identified as H(10), as well as to a methyl signal resonating at δ_H 1.26, H(14). The methyl group, H(14), was subsequently located at C(10) (δ_C 31.31D). HMBC correlations also linked C(1) with two proton signals at δ_H 2.77 and 1.70, which were assigned to the C(9) (δ_C 40.23T) methylene protons. The (^{1}H,^{1}H) COSY spectrum showed cross peaks between H(14) and H(10), as well as between H(10) and H(9), supporting the observed multiplicities of H(14) as a doublet ($J_{10,14}$ 7.0 Hz) and H(10) as a multiplet (ddq) signal ($J_{10,14}$ 7.0 Hz, $J_{10,9a}$ 5.1 Hz $J_{10,9b}$ 11.0 Hz).

The chemical shift value for H(8), a broad doublet resonating at δ_H 6.45, suggested that this proton is dehielded by the neighbouring double bond π-system. In addition the C(8) signal appeared at δ_C 65.70D, and represents an oxygen-bearing carbon atom. The C(8) proton displayed a coupling (J 9.0 Hz) only with H(9a) (δ_H 2.77 ddd, $J_{9a,10}$ 5.1, $J_{8,9a}$ 9.0, $J_{9a,9b}$ 14.9 Hz). The dihedral angle between H(8) and H(9b) obtained from a molecular model was close to 90°, and based on the Karplus equation[8] explains the absence of vicinal coupling with H(9b). This absence of coupling was confirmed by the COSY correlation of H(8) only with H(9a) and by the observed multiplicities of H(9a) and H(9b) (δ_H 1.70 dd, $J_{9b,10}$ 11.0, $J_{9a.9b}$ 14.9 Hz). Geminal coupling between H-9a and H-9b (J 14.9 Hz) was also observed.

The HMBC data linking C(7) and C(8) with H(9a), together with the above corroborations and published data,[9,10] led to the deduction that a sesquiterpene

[8] R.J. Abraham, " Introduction to NMR spectroscopy.", John Wiley & Sons, Essex, 1988.
[9] S. Borkosky, A. Bardón, César, A.N. Catalán, J.G. Díaz and W. Herz, *Phytochemistry*, 1997, **44**, 465.
[10] F. Bohlmann, G. Brindöpke and R.C. Rastogi, *Phytochemistry*, 1978, **17**, 475.

lactone skeleton such as **(50 iv)**, commonly isolated from *Vernonia* spp. and named as a hirsutinolide type sesquiterpene, was present.

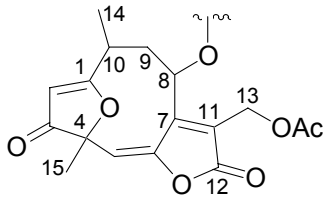

50 iv

The unaccounted ^{13}C and ^{1}H resonances were assigned to a 2-methylpropenoyl moiety **(50 v)** located at C(8). This was demonstrated by the HMBC correlation between the pair of broad signals at δ_H 5.63 and 6.22, identified as H(3′), and the signals for a carbonyl carbon atom (δ_C 166.90S, C(1′)), an olefinic quaternary carbon (δ_C 135.67S, C(2′)) and a methyl carbon atom at δ_C 18.12Q, identified as C(4′). These data were supported by the observed multiplicities and COSY correlations between the C(3′) and C(4′) protons. H(3′a) (δ_H 5.63) was observed as a doublet of quartets and showed a geminal coupling (J 1.6 Hz) to H(3′b) (δ_H 6.22) typical of a terminal methylene group, and allylic coupling (J 1.6 Hz) to H(4′). Allylic coupling (J 1.0 Hz) was also observed between H(3′b) and H(4′).

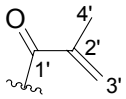

50 v

Inspection of a molecular model and the observed proton-proton couplings indicated that the ester group at C(8) was probably α-orientated. The stereochemistry at C(10) and C(4) followed from a molecular model and the observed NOESY correlations between H(2) and H(14) and that between H(5) and H(15). Thus compound **(50)** was identified as 13-acetoxy-1,4*β*-epoxy-8*α*-(2-methylpropenoyl)-3-oxo-1,5,7(11)-germacratrien-12,6-olide.

A search of the chemical literature revealed that **(50)** is a known compound, previously isolated from *Vernonia poskeana* and referred to as 8*α*-(2-methylacryl-

oyloxy)-3-oxo-1-desoxy-1,2-dehydrohirsutinolide-13-*O*-acetate.[11] The ^{1}H NMR data compared favourably with published data.[11]

Table 3.3 ^{1}H and ^{13}C NMR data (in $CDCl_3$) for 13-acetoxy-1,4*β*-epoxy-8*α*-(2-methylpropenoyl)-3-oxo-1,5,7(11)-germacratrien-12,6-olide **(50)**

Atom	^{1}H δ_H (J in Hz)	^{13}C δ_C	HMBC ^{13}C↔^{1}H	COSY ^{1}H↔^{1}H	NOESY ^{1}H↔^{1}H
1		194.93 S	H(14),H(9a),H(10), H(2)		
2	5.40 (s)	98.28 D			H(14)
3		202.27 S	H(15), H(2)		
4		86.90 S	H(15), H(2), H(5)		
5	5.89 (s)	117.89 D	H(15)		H(15)
6		146.19 S	H(15), H(5)		
7		151.12 S	H(9a), H(13), H(5)		
8	6.45 (br d) (J 9.0)	65.70 D	H(9a)	H(9a)	H(9a),H(9b). H(13a),H(13b)
9	H(9a) 2.77 (ddd) (J 5.1, 9.0, 14.9) H(9b) 1.70 (dd) (J 11.0, 14.9)	40.23 T	H(14)	H(10), H(8), H(9b) H(10), H(9a)	H(14),H(9b), H(10), H(8) H(14); H(9a); H(8)
10	3.01 (ddq) (J 5.1, 11.0, 7.0)	31.31 D	H(14), H(9a)	H(9a), H(9b), H(14)	H(14), H(9a)
11		132.66 S	H(13)		
12		166.14 S	H(13)		
13	H(13a) 4.91 (d) (J 13.2) H(13b) 5.09 (d) (J 13.2)	55.65 T	13-OCOC**H**$_3$	H(13b) H(13a)	H(13b), H(8) H(13a), H(8)
14	1.26 (d) (J 7.0)	15.52 Q	H(9a), H(10)	H(10)	H(9a), H(9b), H(10), H(2)
15	1.58 (s)	20.68 Q	H(5)		H(5)
1′		166.90 S	H(4′); H(3′)		
2′		135.67 S	H(4′); H(3′)		
3′	H(3′a) 5.63 (dq) (J 1.6,1.6)	126.98 T	H(4')	H(3′b), H(4′)	H(3′b)

[11] F. Bohlmann, N. Ates (Gören) and J. Jakupovic, *Phytochemistry*, 1983, **22**, 1159.

	H(3′b) 6.22 (br dq) (J 1.6; 1.0)			H(3′a); H(4′)	H(3′a)
4′	1.93 (dd) (J 1.6,1.0)	18.12 Q	H(3′)	H(3′)	H(3′a)
13-*O*-**C**OCH$_3$		170.15 S	13-OCOC**H**$_3$); H(13)		
13-*O*-CO**CH**$_3$	2.03 (s)	20.68 Q			

3.5.2 Structural Elucidation of 13-Acetoxy-8*α*-(4-acetoxy-3-methyl-2*Z*-buten-oyl)-1,4*β*-epoxy-3-oxo-1,5,7(11)-germacratrien-12,6-olide (51)

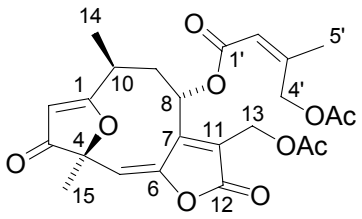

(51)

Compound **(51)** {[α]$_D$ -209.8 (*c* 0.51, $CHCl_3$)} was isolated as a colourless gum. The EI-MS spectrum of **(51),** as in the case of **(50)**, did not show a molecular ion peak but rather showed a fragment at *m/z* 316.0885, corresponding to the loss of a $C_7H_{10}O_4$ fragment *i.e.* 4-acetoxy-3-methyl-2*Z*-butenoic acid, from the molecular ion peak. The molecular formula of **(51)** was established as $C_{24}H_{26}O_{10}$ and corresponded to a molecular weight of 474 Dalton. The ^{1}H, ^{13}C, HSQC, HMBC, COSY and NOESY data of this compound are summarized in Table 3.4.

The ^{1}H NMR spectrum of compound **(51)** closely resembled that of compound **(50)**. The most obvious differences were the additional methyl signal in the acetate region (δ_H 2.05) and the additional olefinic proton at δ_H 5.75 in the ^{1}H spectrum of **(51)**. A thorough investigation of the ^{1}H, ^{13}C, HSQC, HMBC, COSY and NOESY experiments performed on this compound showed that the main skeleton was identical to that of **(50)** and that only the ester group at C(8) was different.

The olefinic proton H(2′) (δ_H 5.75) appeared as a broad multiplet and showed HMBC correlations to a broad methyl signal (δ_H 1.91) assigned as H(5′) and to a

pair of broad doublets (J 15.5 Hz) resonating at δ_H 5.12 and δ_H 5.22. Closer inspection of the pair of doublets, identified as H(4′), revealed that it was not an ideal AB system, and each signal was a multiplet due to allylic coupling (J ~1Hz) with H(5′) and H(2′). This was supported by cross peaks observed in the COSY spectrum.

An HMBC correlation between H(4′) with a carbonyl carbon atom at δ_C 170.54, which in turn correlated to the methyl signal at δ_H 2.05, revealed that there was an acetate at C(4′). This led to the conclusion that there was a 4-acetoxy-3-methyl-2-butenoyl moiety attached to C(8) as shown in **(51 i)**.

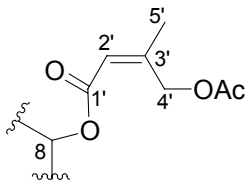

51 i

The *Z* configuration of the 2′ double bond followed from the strong NOE observed between H(2′) and H(5′). This was confirmed by comparison of the H(4′) chemical shift (δ_H 5.17) with published data for methyl *Z*- and *E*-4-acetoxy-3-methyl-2-butenoates: the *Z*-CH_2 signals were shown to occur at δ_H 5.15 whereas the *E*-CH_2 signals were observed at δ_H 4.56.[12]

Compound **(51)** was previously isolated from *V. poskeana*[11]and *V. erinacea*.[12] A comparison of the data for (**51**) with the published ^{1}H NMR data[11] revealed that the authors had transposed the H-13 and H-4' resonances. In this account an unequivocal assignment of these resonances based on 2D NMR data, which the original reporters did not have access to, is reported. All other data compared favourably, indicating that **(51)** was identical to 8α-(5'-acetoxysenecioyloxy)-3-oxo-1-desoxy-1,2-dehydrohirsutinolide-13-*O*-acetate.

[12] L.E. Tully, M.S. Carson and T.B.H. McMurray, *Tetrahedron Lett.*, 1987, **28**, 5925.

Table 3.4 ^{1}H and ^{13}C NMR data (in $CDCl_3$) for 13-acetoxy-8*α*-(4-acetoxy-3-methyl-2*Z*-butenoyl)-1,4*β*-epoxy-3-oxo-1,5,7(11)-germacratrien-12,6-olide **(51)**

Atom	^{1}H δ_H (J in Hz)	^{13}C δ_C	HMBC $^{13}C \leftrightarrow {}^{1}H$	COSY $^{1}H \leftrightarrow {}^{1}H$	NOESY $^{1}H \leftrightarrow {}^{1}H$
1		194.92 S	H(14), H(9a)		
2	5.43 (s)	99.93 D			H(14)
3		202.16 S	H(15)		
4		86.93 S	H(15), H(5)		
5	5.88 (s)	117.35 D	H(15)		H(15)
6		146.19 S	H(15), H(5)		
7		151.19 S	H(9a), H(13), H(5)		
8	6.23 (br d) (J 8.0)	65.61 D	H(9a)	H(9a)	H(9a),H(9b), H(13)
9	H(9a) 2.75 (ddd) (J 5.5, 8.0, 14.7) H(9b) 1.70 (dd) (J 9.0, 14.7)	40.09 T	H(14), H(10)	H(10), H(8), H(9b) H(10), H(9a)	H(14),H(9b), H(10), H(8) H(14), H(9a), H(8)
10	3.01 (ddq) (J 5.5; 9.0; 7.0)	31.92 D	H(14), H(9a)	H(9a), H(9b), H(14)	H(14), H(9a)
11		131.79 S	H(13a)		
12		166.23 S	H(13)		
13	H(13a) 4.93 (d) (J 13.1) H(13b) 5.02 (d) (J 13.1)	55.79 T	13-OCOC**H**$_3$	H(13b) H-13a	H(13b), H(8) H(13a), H(8)
14	1.25 (d) (J 7.0)	15.38 Q	H(9a), H(10)	H(10)	H(9a),H(9b), H(10), H(2)
15	1.59 (s)	20.64 Q	H(5)		H(5)
1′		164.04 S			
2′	5.75 (br m*)	116.49 D	H(5′), H(4′)	H(4′), H(5′)	H(5′)
3′		156.77 S	H(5′), H(4′)		
4′	H(4′a) 5.12 (br dm*) (J 15.5) H(4′b) 5.22 (br dm*) (J 15.5)	63.60 T	H(5′), H(2′)	H(4′b), H(2′); H(5′) H(4′a), H(2′); H(5′)	H(5′)
5′	1.91 (br m*)	21.48 Q	H(4′)	H(2′), H(4′)	H(2′)

13-*O*-**C**OCH_3		170.18 S	13-OCOC**H**$_3$, H(13)		
13-*O*-CO**CH**$_3$	2.03 (s)	20.69 Q			
4′-O **C**OCH_3		170.54 S	4′-OCOC**H**$_3$, H(4′)		
4′-*O*-CO**CH**$_3$	2.05 (s)	20.69 Q			

* allylic coupling of ~1Hz

3.5.3 Characterization and Biosynthesis of Compounds (50) and (51)

Although **(50)** and **(51)** have been isolated previously from other South African *Vernonia* species,[11,12] this is the first report on the isolation of these compounds from *V. staehelinoides*. Compounds **(50)** and **(51)** fall into a class of sesquiterpene lactones which are typically isolated from *Vernonia* species and named as hirsutinolides.[9,10]

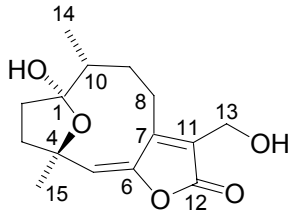

Figure 3.5 Basic hirsutinolide skeleton

Thus **(50)** and **(51)** are ketohirsutinolides in which the C(8) hydroxyl group is utilized for ester formation with two different acids. As plant metabolites often exist as part of a family of related compounds it is likely that other less active analogues and precursors were also present in the crude extract. In order to isolate sufficient material for structural characterization the focus in this investigation remained on **(50)** and **(51)** as these compounds showed the greatest antiplasmodial activity.

It has been suggested that hirsutinolides are not natural products but are rather artifacts formed from glaucolides on exposure to slightly acidic silica gel during chromatography.[9,12] Thus the glaucolide **(49)** could be chemically transformed into the hirsutinolide **(52)** by treatment with slightly acidic silica gel as depicted in Figure 3.6.[5]

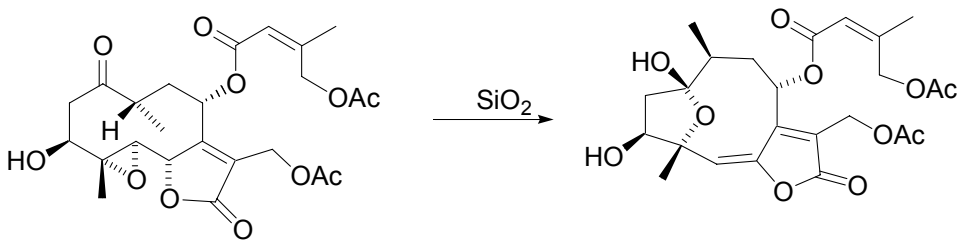

(49) **(52)**

Figure 3.6 Silica gel induced transformation of glaucolide **(49)** to hirsutinolide **(52)**

Contrary to this suggestion, **(50)** and **(51)** were easily detected through their characteristic colours and R_f values by TLC analysis of the dichloromethane-soluble fraction (5B) following liquid/liquid partitioning of the crude dichloro-methane extract. This detection prior to any silica gel chromatography suggests that **(50)** and **(51)** were originally present in the dichloromethane extract of *V. staehelinoides*.

The demonstrated transformation of glaucolide **(49)** into hirsultinolide **(52)** provides some insight into the biosynthesis of compounds **(50)** and **(51)**. Glaucolide **(49)** was previously isolated from the roots of *V. staehelinoides* and hirsutinolide **(52)** can be considered a precursor of compound **(51)**. Based on this and literature precedent a biosynthetic pathway to the formation of compounds **(50)** and **(51)** is postulated in Figure 3.7. In recognising compounds **(50)** and **(51)** as 6,7-germacranolide derivatives it is safe to assume that they are formed from the most elementary germacrene sesquiterpene lactone, costunolide **(25)**. Epoxidation of the 1,10 and 4,5 double bonds of **(25)** and hydroxylation at the C(7) allylic position would yield the diepoxide **(53)**. Subsequent rearrangement and esterifications of **(53)** would result in the formation of **(54)**. Selective hydrolysis of the 1,10 epoxide would afford **(55)**, which could dehydrate to give **(56)**. Hydrolysis at the C(3) position of **(56)** would yield the glaucolide **(57)**. This glaucolide could then, as demonstrated, be transformed into hirsutinolide **(58)**. An ensuing dehydration at C(1) and oxidation of the C(3) hydroxyl would yield compound **(50)** or compound **(51).**

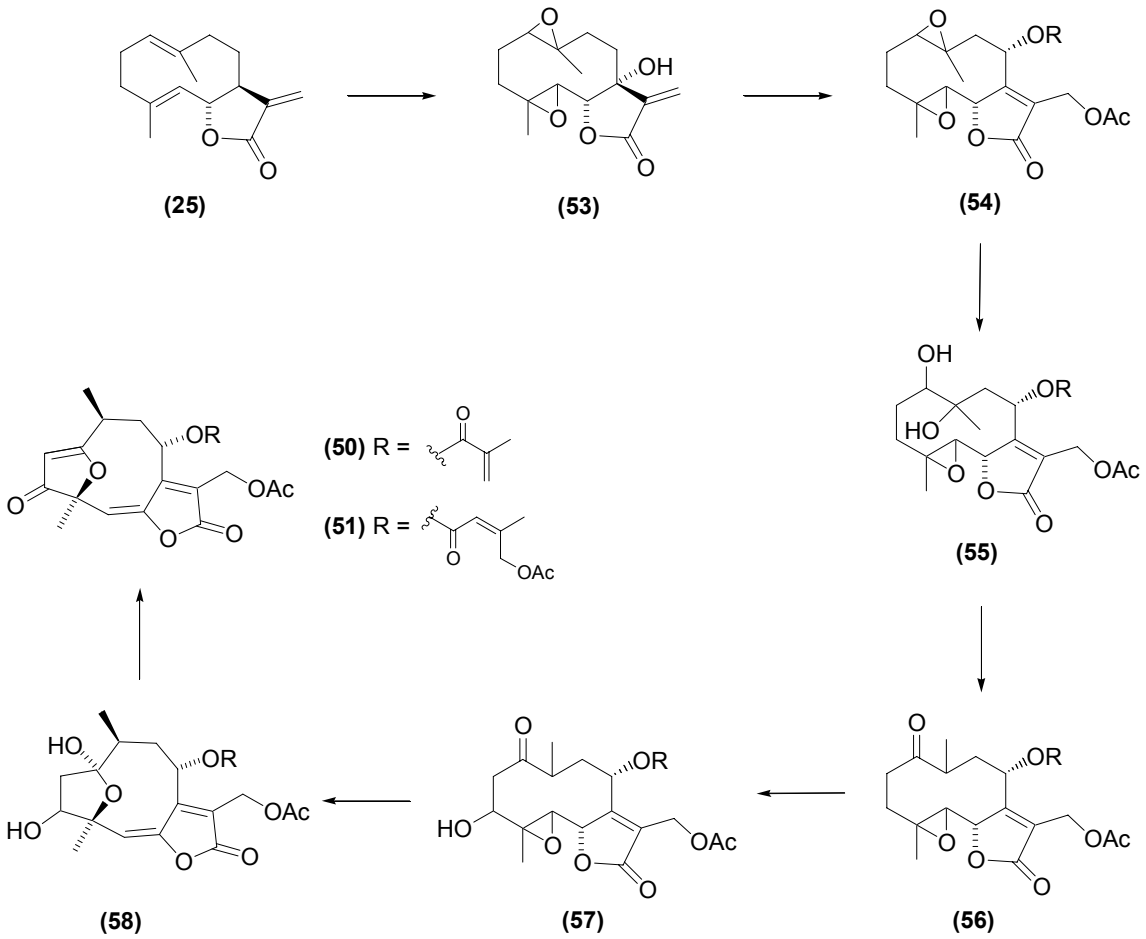

Figure 3.7 Postulated biosynthesis of compounds **(50)** and **(51)**.

3.6 *In vitro* Antiplasmodial Activity and Cytotoxicity of Compounds (50) and (51)

Compounds **(50)** and **(51)** were tested for *in vitro* antiplasmodial activity against the D10 and K1 *P. falciparum* strains. The sensitivity of the two strains to chloroquine **(2)** was also evaluated. The corresponding IC_{50} values are listed in Table 3.5.

Table 3.5 *In vitro* antiplasmodial activity of chloroquine and **(50)** and **(51)**

Tested sample	**D10 IC_{50} (μg/ml)**	**K1 IC_{50} (μg/ml)**	**RI***
Chloroquine	11.83×10^{-3}	181.76×10^{-3}	15.36
Compound **(50)**	0.26	1.80	6.92
Compound **(51)**	0.24	2.60	10.83

* RI = K_1 IC_{50} / D_{10} IC_{50}

There are no previous reports of **(50)** and **(51)** having been investigated for any biological activity. In this account the compounds are demonstrated to have *in vitro* antiplasmodial activity against two strains of *P. falciparum*. The difference in their C(8) ester groups does not appear to significantly influence the observed antiplasmodial activities of **(50)** and **(51)** as they were equipotent against the chloroquine sensitive D10 strain. There was a marginal difference in their observed activity against the chloroquine resistant K1 strain.

Both compounds, like chloroquine, showed greater activity against the D10 strain than against the K1 strain as indicated by their resistance index values being greater than 1. Compounds **(50)** and **(51)** are, however, in all respects significantly less active than chloroquine against both strains. They were found to be more than 20 times less active than chloroquine against the D10 strain. The difference in activity between chloroquine and **(50)** against the K_1 strain was 10 fold and for **(51)** this difference was approximately 14 fold.

The *in vitro* cytotoxicity of the compounds was determined against Chinese Hamster Ovarian (CHO) cells using the MTT assay. The IC_{50} values of the positive control (Emetine), chloroquine and compounds **(50)** and **(51)** are summarised in Table 3.6.

Table 3.6 *In vitro* cytotoxicity results

Tested sample	**CHO IC_{50} (μg/ml)**
Emetine	0.03
Chloroquine	18.53
Compound **(50)**	2.89
Compound **(51)**	0.97

Although both compounds had significantly higher IC_{50} values than Emetine, they can still be considered as cytotoxic to CHO cells. This data suggests that **(50)** and **(51)** were cytotoxic to mammalian cells at similar concentrations, indicating that the observed antiplasmodial activity could be due to general toxicity. Further

investigation would be required to confirm this but the fact that **(50)** and **(51)** have similar IC_{50}'s against the D10 strain but show a notable difference in their activity against the K1 strain, suggests that there may be more than general cytotoxicity coming into play.

The apparent non-selectivity of **(50)** and **(51)** is emphasised by the selectivity index values for the two compounds, summarised in Table 3.7. The selectivity index (SI) is a ratio of cytotoxicity to antiplasmodial activity and gives a general indication of the specific activity.

Table 3.7 Selectivity index values for chloroquine and compounds **(50)** and **(51)**

Tested sample	**SI***
Chloroquine	1566
Compound **(50)**	11.12
Compound **(51)**	4.04

* SI = cytotoxicity CHO IC_{50} / antiplasmodial D_{10} IC_{50}

The SI value for **(50)** indicates that it is approximately 11 times more potent to the parasites than to mammalian cells. For **(51)** this ratio is of the order of 4, indicating less selectivity.

In considering a recent publication[13] outlining criteria for antiparasitic drug discovery, a compound can be considered a hit if it is:

- Active *in vitro* against whole protozoa with an IC_{50} of ≤ 1 µg/ml
- Selective (at least tenfold more active against the parasite than against a mammalian cell line)

Based on these criteria and taking into account the activity of the compounds against the D10 *P. falciparum* strain, **(50)** can be considered a hit. Compound **(51)** was not sufficiently selective to kill the parasites without damaging mammalian cells.

[13] R. Pink, A. Hudson, M. Mouriès and M. Bendig, *Nature Rev. Drug Discov.*, 2005, **4**, 727.

3.7 Conclusion and Research Prospects

Although *Vernonia staehelinoides* is used traditionally to treat malaria and compounds showing significant *in vitro* antiplasmodial activity have been isolated from extracts of the plant; the active components, **(50)** and **(51)**, cannot be considered as viable antimalarial drugs – as their activity does not compare to that of chloroquine and **(51)** is non-selective (SI 4) while **(50)** showed only limited selectivity (SI 11). Ideally, for an effective therapeutic window, selectivity index values should be greater than 100 - the SI value for chloroquine is in excess of 1500.

The hirsutinolides could, however, prove to be attractive scaffolds for chemical modification with the view of exploring structure-activity relationships. Medicinal chemistry approaches could be used to modify the natural product core structure so as to optimise the activity of these compounds and reduce their cytotoxicity, generating lead compounds for antimalarial drug development. The hirsutinolide skeleton could be modified through hydrogenation of the double bonds and hydrolysis of the ester groups. Alternatively potential pharmacaphores or substructures which may be responsible for the observed antiplasmodial activity, can be used as scaffolds for new derivatives. The 2(5H)-furanone and dihydrofuran-4-one (Figure 3.8) are two such privileged substructures identified for derivatisation and antimalarial drug lead development. This research prospect has been taken up by the University of Cape Town, Department of Chemistry.

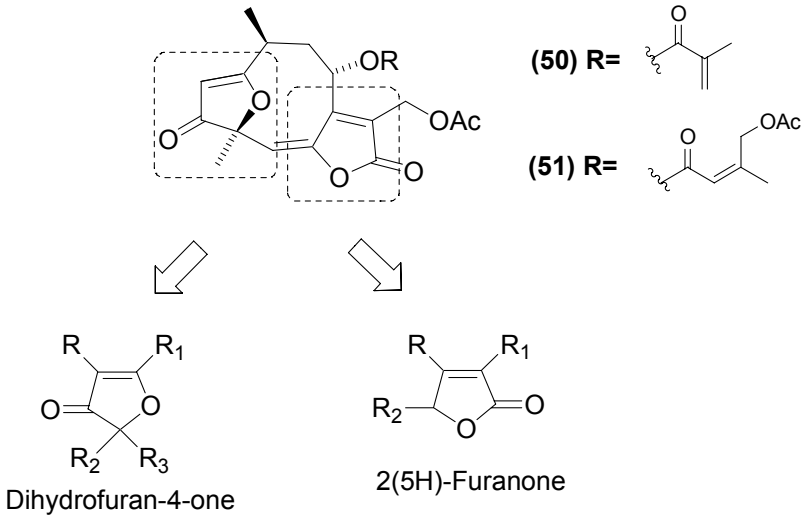

Figure 3.8 Potential pharmacophores in compounds **(50)** and **(51)**

CHAPTER 4

Antiplasmodial Activity of *Oncosiphon piluliferum*

4.1 *Oncosiphon piluliferum*

The historical name of this plant is *Pentzia globifera* and it belongs to the botanical family *Asteraceae*. The Europeans administered an infusion of the plant for convulsions and the Hottentots used an infusion of the flower and leaf for typhoid and other fevers. A decoction of the plant is an old fashioned "Dutch" remedy to bring out the rash in measles and both the Xhosa and Mfengu use it as an antifebrile. Extracts of the plant are reported to have given "negative results in experimental malaria".[1]

The plant is very bitter and has a "heavy smell" from the volatile oil which it contains; hence its common name stinkkruid. It is a bushy annual herb with stalkless leaves deeply dissected with two stipule-like lobes at the base and the flower heads sit on solitary long erect leaveless stalks. It grows mainly in the Witwatersrand region but also occurs in the Eastern Cape.

Figure 4.1 *Oncosiphon piluliferum* growing in Graaff-Reinet. Photo by Jean Meyer (SANBI)

[1] J.M. Watt and M.G. Breyer-Brandwyk, 'The Medicinal and Poisonous Plants of Southern and Eastern Africa', 2nd edition, Livingston, London, 1962, 254.

There are no reports on the chemical components of this plant to date. Chemical investigation of other *Pentzia* species has identified acetylenes, glaucolides, fulvenoguaianolides and other sesquiterpene lactones as constituents.[2]

4.2 *In vitro* Antiplasmodial Activity of *O. piluliferum* Extracts

A dichloromethane and a 1:1 dichloromethane/methanol extract were prepared from the aerial parts of the *O. piluliferum* plant (Table 4.1).

Table 4.1 Yield of extracts obtained from *O. piluliferum*

Extract Code	Extract description	% Yield
P01609A	Dichloromethane	2.2
P01609B	Dichloromethane/methanol (1:1)	3.3

The concentrated *O. piluliferum* extracts were tested *in vitro* in duplicate against a chloroquine-sensitive strain (D10) and the active dichloromethane extract was tested against the chloroquine-resistant (K1) strain of *P. falciparum*. (Table 4.2)

Table 4.2 *In vitro* antiplasmodial activity of *O. piluliferum* extracts

Extract	D10 (Experiment 1) IC_{50} (μg/ml)	D10 (Experiment 2) IC_{50} (μg/ml)	K1 IC_{50} (μg/ml)
P01609A	2.0	1.0	2.0
P01609B	>10	10.0	

The dichloromethane extract, P01609A, was found to be significantly active against both strains of the parasite having a 50% inhibitory concentration (IC_{50}) value of 2 μg/ml against the chloroquine-resistant (K1) strain. The 1:1 dichloromethane/methanol extract was found to be relatively inactive.

A bulk collection of plant material was undertaken to produce sufficient dichloromethane extract for bioassay-guided fractionation. This extract was bioassayed against the D10 strain and its activity (Table 4.3) compared favourably with that observed for the original extract.

[2] C. Zdero and F. Bohlmann, *Phytochemistry*, 1990, **29**, 189.

Table 4.3 *In vitro* antiplasmodial activity of extract of bulk plant material

Extract	D10 (Experiment 1) IC_{50} (μg/ml)	D10 (Experiment 2) IC_{50} (μg/ml)
P01609A (bulk)	2.6	3.1

4.3 Bioassay-guided Fractionation of the *O. piluliferum* Dichloromethane Extract

Bioassay-guided fractionation techniques based on antiplasmodial activity were used to identify and isolate the active compounds from the dichloromethane extract of *O. piluliferum*. Details of the purification techniques are given in Chapter 5 (Experimental).

4.3.1 Primary Fractionation of P01609A

Primary fractionation of the crude dichloromethane extract (P01609A) of O. *piluliferum* yielded a total of 32 pooled fractions. These fractions were bioassayed against *P. falciparum* D10. Due to difficulties experienced with the solubility of and the poor activity observed for the first 12 fractions these results were disregarded. The IC_{50} values for the remaining 20 fractions (7A - 7T) are summarised in Figure 4.2. Enhanced antiplasmodial activity was observed primarily in the region of fractions 7H - 7P. The identification of the compounds responsible for the observed activity is best illustrated by the further purification of fractions 7I, 7M and 7O. Further purification of the other active fractions resulted in the loss of observed antiplasmodial activity or pointed to the same active compounds.

4.3.2 Further Purification of Fraction 7I

Figure 4.3 summarizes the steps employed to further purify fraction 7I, guided by observed antiplasmodial activity against the D10 *P. falciparum* strain. Only fraction 8D was found to retain the activity of the parent fraction, 6I. Further fractionation of 8D led to the identification of a semi-pure compound, 9B, with enriched antiplasmodial activity. The compound was easily discernible on TLC by its characteristic dark pink colour when sprayed with vanillin spray reagent. Further purification of 9B yielded compound **(59).**

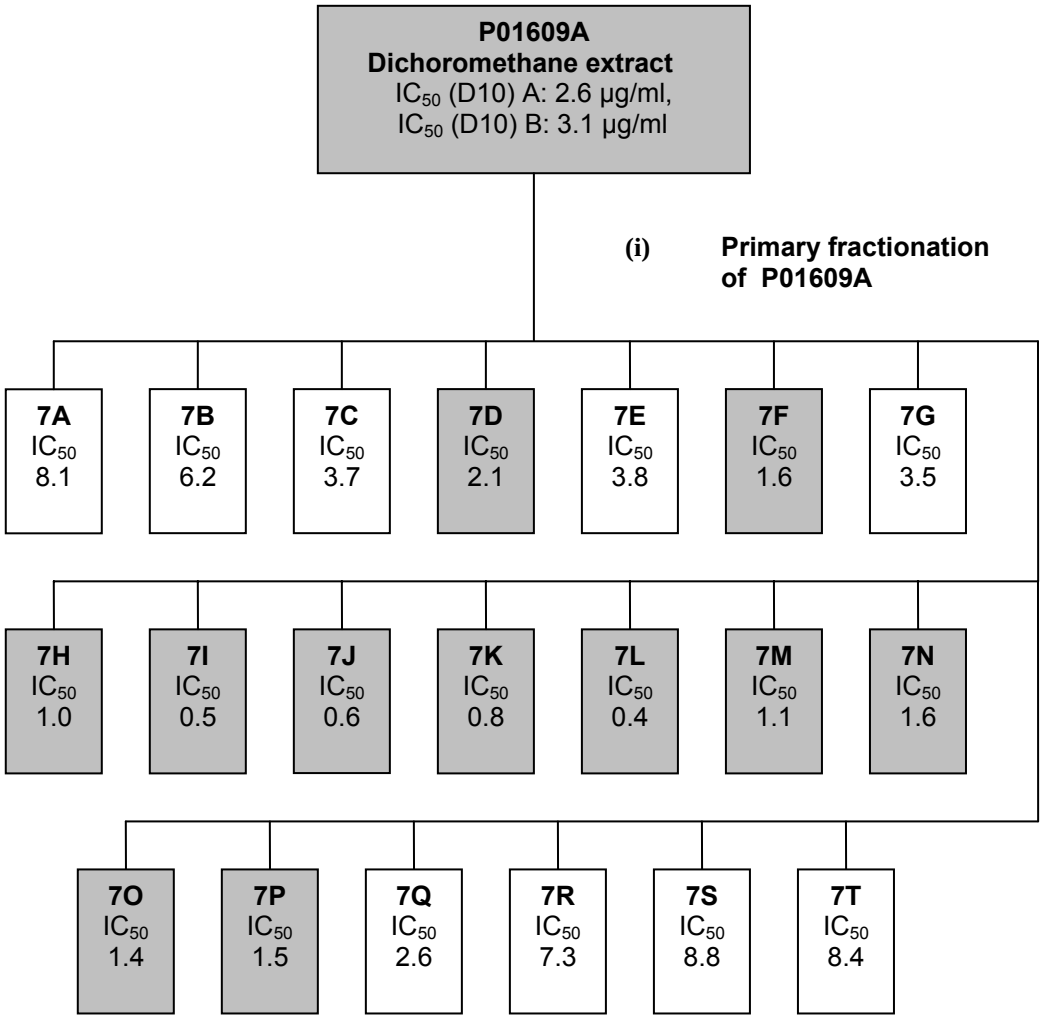

Figure 4.2 Summary of IC_{50} values of the primary fractions generated from silica gel column chromatography of P01609A. IC_{50} values are in µg/ml.

This compound, however, proved to be unstable and decomposed during NMR analysis, providing insufficient data for complete structural elucidation. Due to the observed instability of **(59)** and its low yield it was decided that a targeted purification of this compound from an adequate quantity of crude extract would be more practical than trying to re-isolate it from existing fractions containing minimal traces of it.

4.3.3 Further Purification of Fraction 7M

Figure 4.4 summarizes the steps employed to further purify fraction 7M. The crystalline fraction 11A was identified as the major constituent of 7M and was submitted for bioassaying. NMR Analysis of 11A, however, revealed that it was a

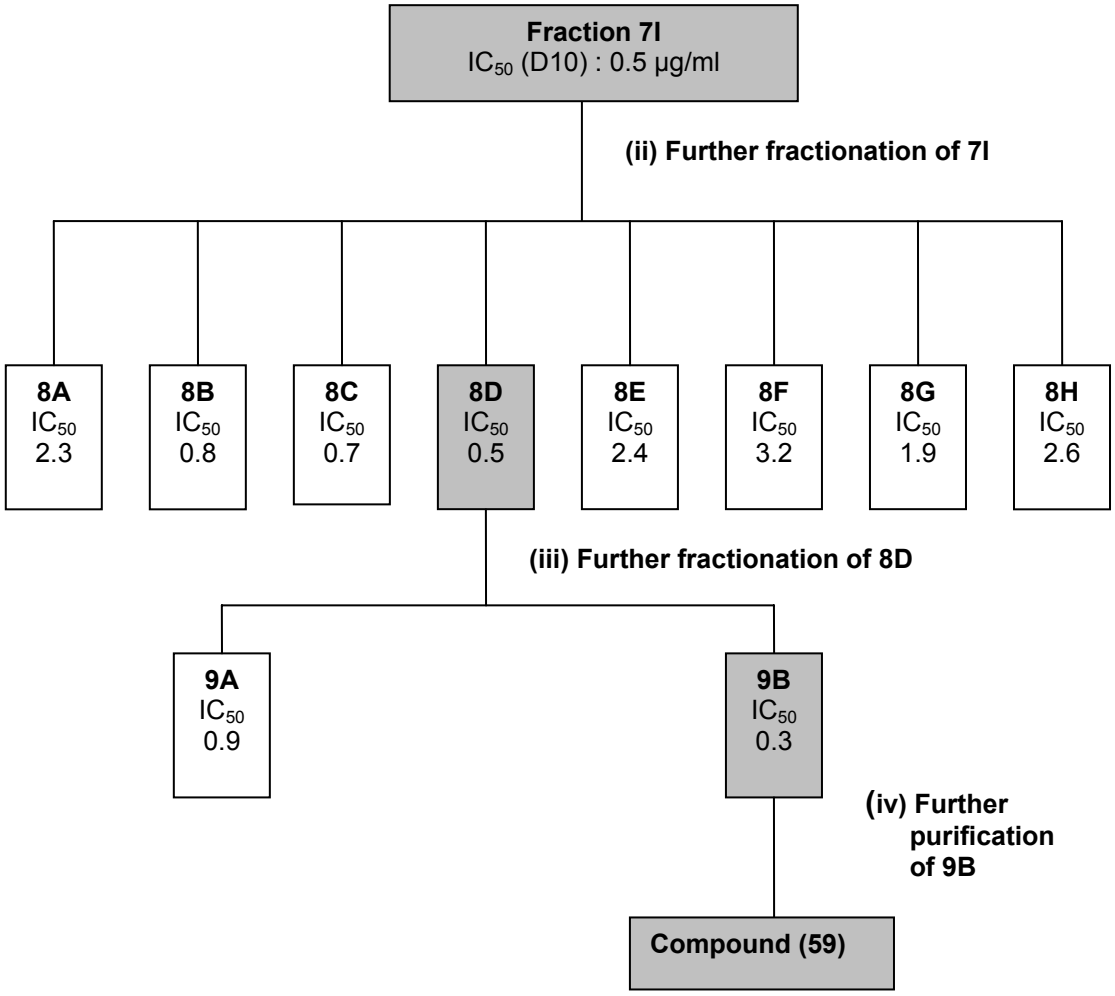

Figure 4.3 Further purification of fraction 7I. IC_{50} values are in µg/ml.

mixture of at least two closely related compounds. Further purification of 11A led to the isolation of the crystalline compound **(60)**, which had a characteristic blue-grey colour on TLC with vanillin spray reagent. The crystalline fraction 12A was found to contain a trace quantity of a closely related compound **(61)** and a major compound **(62)**. Despite their very close R_f values on TLC, compound **(61)** and **(62)** could be distinguished by their respective brown and pink colours when sprayed with vanillin reagent. The yield of 12A was too low to attempt the difficult purification required to separate compounds **(61)** and **(62)** with the aim of isolating sufficient quantities of each for structural elucidation and bioassaying. Thus, a targeted purification of these compounds from a larger quantity of crude extract was opted for.

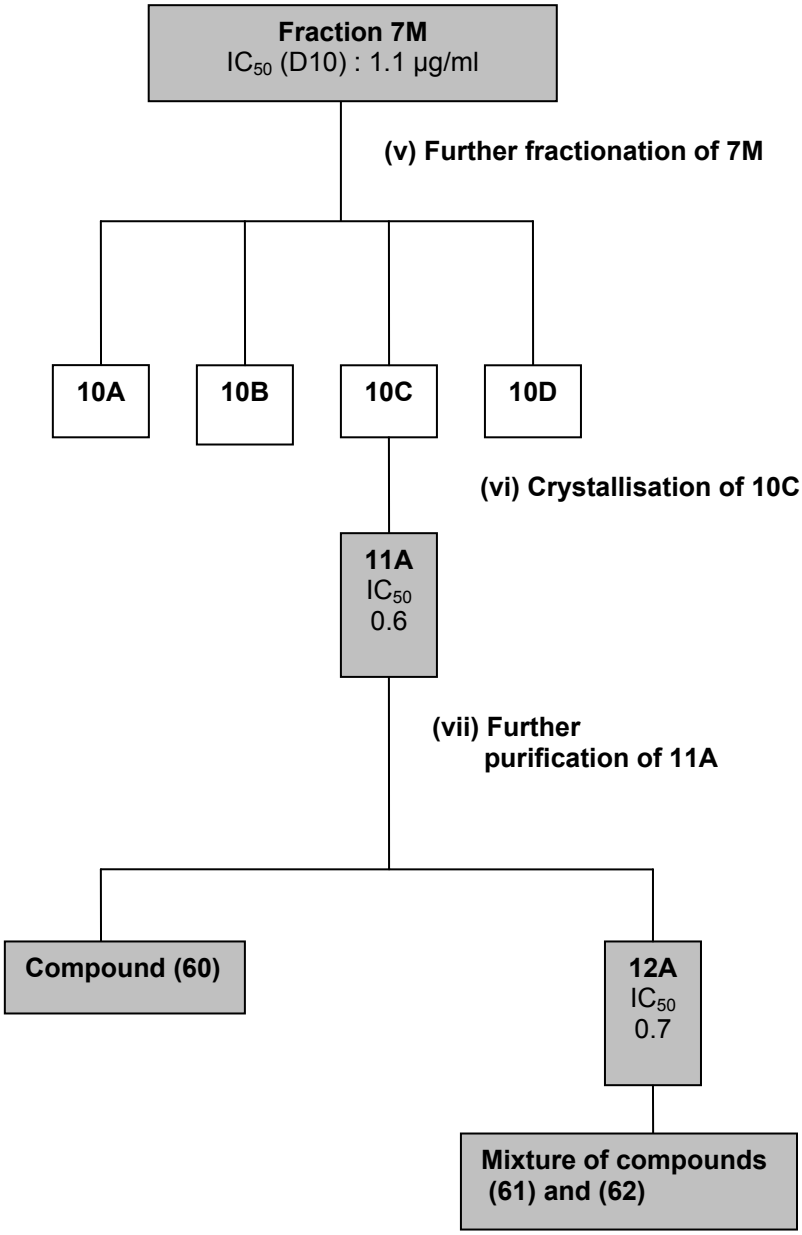

Figure 4.4 Further purification of fraction 7M. IC_{50} values are in µg/ml

4.3.4 Further Purification of Fraction 7O

Fraction 7O was found to contain one major compound, easily discernible by its dark pink colour on TLC with vanillin spray reagent. Further purification of 7O led to the isolation of the crystalline compound **(63)** (Figure 4.5). Although the yield of **(63)** was sufficient for structural elucidation and bioassaying, it was anticipated that more would be required for further characterization and thus a targeted purification of this compound from a larger quantity of crude extract was also deemed necessary.

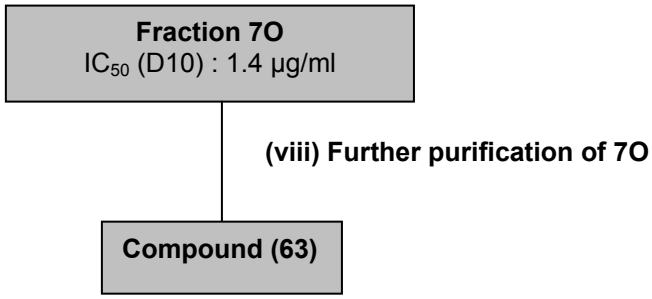

Figure 4.5 Further purification of fraction 7O. IC_{50} values are in µg/ml

4.4 Targeted Purification of Compounds (59)-(63) from P01609A

Bioassay guided fractionation of the dichloromethane extract P01609A, led to the identification of at least 5 structurally related compounds responsible for the observed activity of this extract. It was evident, however, that less active analogues of these compounds were present in the crude extract and that the overall antiplasmodial activity of the extract and several of the fractions generated were due to the synergistic effect of a number of compounds. Purification was, however, focused on those fractions showing significant enrichment of antiplasmodial activity upon fractionation so as to isolate the compounds primarily responsible for the observed biological activity. Also, low yields and marked instability rendered isolation of additional compounds from active fractions impractical.

To isolate sufficient quantities of compounds **(59)**–**(63)** for structural elucidation, characterization and bioassaying the dichloromethane extract was subjected to targeted purification techniques. Liquid-liquid partitioning of the crude dichloromethane extract once again served to concentrate the active components in a simpler matrix and proved to be an efficient method for targeting the isolation of these compounds.

TLC analysis of the three fractions generated from liquid/liquid partitioning of the crude extract revealed that the target compounds were concentrated in the dichloromethane-soluble fraction, 13B, which was then fractionated. The target compounds, identified by their characteristic R_f values and colours on TLC, were found to be present in three of the fractions generated (14B, 14E and 14F). Figure

4.6 summarises the steps employed to isolate additional quantities of compounds **(59)**, **(60)**, **(61)**, **(62)** and **(63)** for structure elucidation, derivatisation and bio-assaying. Details of the purification techniques are given in Chapter 5 (Experimental).

Compound **(59)** was isolated from fraction 14B by successive flash silica gel purifications. Once isolated, **(59)** was again observed to be unstable during NMR analysis. The acetate of **(59)**, compound **(64)**, was subsequently prepared and proved to be more stable and structure elucidation was conducted on this derivative. More material was subsequently isolated from a sub-fraction of 14B to prepare the crystalline *p*-nitrobenzoate ester of compound **(59)**, compound **(65),** for its characterization by X-ray crystallography.

Compounds **(60)**, **(61)** and **(62)** were isolated from fraction 14E by a series of crystallisations and flash silica gel purifications. The acetate of **(62)**, compound **(66),** was prepared in order to compare its X-ray structure with that of the original compound.

Compound **(63)** was isolated from fraction 14F by flash silica gel chromatography. The (*R*)- and (*S*)-Mosher ester [α-methoxy-α-trifluoromethylphenylacetate or MTPA] derivatives of **(63),** compounds **(67)**-**(72),** were prepared to determine the absolute configuration of the stereogenic centers bearing hydroxyl groups. The sodium borohydride ($NaBH_4$) reduction of **(63)** produced compound **(73)**, which was prepared to investigate a structure-activity relationship.

In contrast to a yield of almost 3% by weight of the dichloromethane extract for compound **(63),** the yields of compounds **(59)**, **(60)**, **(61)** and **(62)** were relatively low. This indicated that the antiplasmodial component was a minor constituent of the aerial parts of the plant. The low yield of compound **(59)** could be attributed to the fact that it was relatively unstable and showed evidence of decomposition during silica gel purification and on standing. The yields of all the compounds identified could possibly be improved to some extent by optimising the extraction and separation procedures. Despite the low yields the quantities of compounds

(59)–**(63)** isolated were sufficient for structure elucidation, selected derivatisations and *in vitro* assaying.

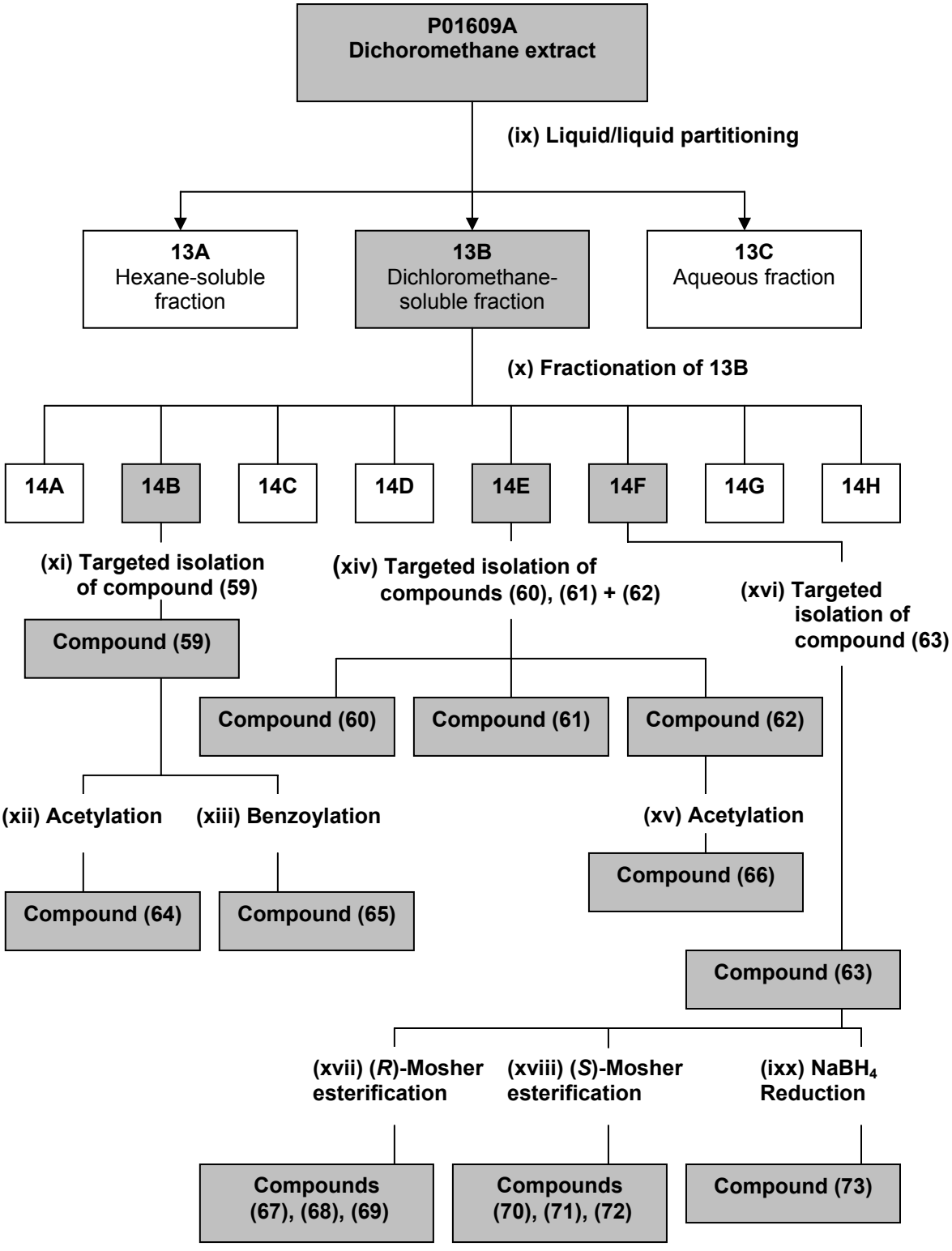

Figure 4.6 Summary of targeted purification and selected derivatisation of compounds **(59)**–**(63).**

4.5 Identification and Characterization of Compounds (59)–(63) from *O. piluliferum*

Compounds **(59)**–**(63)** were identified and characterized by mass spectrometry, specific rotation, melting points, X-ray crystallography, selected derivatisations, and ^{1}H, ^{13}C, DEPT, HSQC, HMBC, COSY and NOESY NMR experiments (as discussed in section 3.5).

4.5.1 Structure Elucidation of 4,5*α*-epoxy-6*α*-hydroxy-1(10)*E*,11(13)-germacradien-12,8*α*-olide (59).

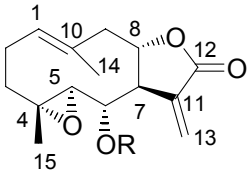

(59) R = H

(64) R = Ac

(65) R = 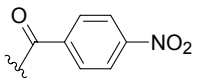

Compound **(59)** was isolated as a transparent gum. The compound showed a tendency to deteriorate on standing and this was most evident by the decomposition observed during NMR analysis. For this reason a complete set of NMR data for structure elucidation of **(59)** was not obtained. The ^{1}H NMR data of **(59)** are summarised in Table 4.4. The acetate of **(59)** was prepared and proved to be more stable, thus structural elucidation was completed on this derivative.

Compound **(64)** was obtained as a yellow gum, $[\alpha]_D$ +41.2 (*c* 0.34, $CHCl_3$). Attempts at crystallisation were unsuccessful. The ^{1}H spectrum of **(64)** revealed that a single hydroxyl group had been acetylated. The high resolution EI-MS showed an ion at *m/z* 264.1313, corresponding to the $[M - (CH_2{=}C{=}O)]^+$ fragment, which is typical of an acetate functionality. The fragment ion at *m/z* 246.1224 $[M - (CH_2{=}C{=}O) - H_2O]^+$ was also indicative of the initial loss of the ketene group. On the basis of this the molecular formula of **(64)** was deduced to be $C_{17}H_{22}O_5$.

The ^{1}H, ^{13}C, HSQC, HMBC, COSY and NOESY data of **(64)** are summarized in Table 4.5. Many of the NMR resonances were broad and unresolved and several obvious HSQC and HMBC contours were weak or undetected. Comparison with published data[3,4,5] and a few significant correlations, however, identified **(64)** as a germacranolide and facilitated its complete structural elucidation.

The C(13) (δ_C 127.27T) protons of **(64)** appeared as a pair of double doublets at δ_H 5.78 and 6.34 typical of the signals of an α-methylene-γ-lactone functionality. This was substantiated by HMBC correlations linking H(13) to C(11) (δ_C 134.33S), C(7) (δ_C 43.96D) and the lactone carbonyl carbon atom, C(12) (δ_C 168.85S). The H(13) protons showed both geminal ($J_{13,13}$ 0.7 Hz) and allylic coupling ($J_{7,13}$ ~2 Hz).

The H(7) signal (δ_H 3.00) was broadened but its multiplicity was supported by cross peaks in the COSY spectrum with H(6), H(8), H(13a) and H(13b). The one-bond correlations for H(6) (δ_H 5.23, dd, $J_{5,6}$ 3.7 Hz, $J_{6,7}$ 11.5 Hz) and H(8)(δ_H 4.48) and the signals in the HSQC spectrum at δ_C 69.25D and 77.53D, respectively, identified C(6) and C(8). The chemical shift values pointed to the presence of an oxygen atom at each of these carbon atoms. In the ^{1}H spectrum of the parent compound **(59)** (Table 4.4) the H(6) signal appeared more downfield at δ_H 4.08. This downfield shift observed for the C(6) proton on acetylation located the *O*-acetate group at C(6) (δ_C 69.25D). This was confirmed by the HMBC correlation between H(6) and the acetate carbonyl carbon atom at δ_C 168.89S. It therefore follows that the C(8) (δ_C 77.53D) oxygen atom is involved in lactone formation as shown in **(64 i)**.

Analysis of the ^{1}H NMR spectrum revealed that the H(6) signal at δ_H 5.23 (dd, $J_{5,6}$ 3.7 Hz, $J_{6,7}$ 11.5 Hz) was coupled to both H(7) and H(5). The latter signal

[3] F. Bohlmann, J. Jakupovic, M. Ahmed and A. Schuster, *Phytochemistry*, 1983, **22**, 1623.
[4] F. Bohlmann, A. Alder, J. Jakupovic, R.M. King and H. Robinson, *Phytochemistry*, 1982, **21**, 1349.
[5] F. Shafizadeh and N.R. Bhadane, *Phytochemistry*, 1973, **12**, 857.

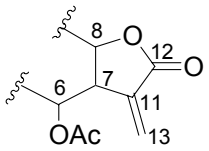

(64 i)

appeared as a doublet at δ_H 2.64 ($J_{5,6}$ 3.7 Hz). In addition HMBC correlations linked H-6 to the signals at δ_C 59.58S [C(4)] and δ_C 62.28D [C(5)]. The chemical shift values for C(4) and C(5) pointed to the presence of an oxygen atom at both these carbon atoms. The magnitude of the one-bond (^{1}H,^{13}C) coupling constant, $^1J(^1H,^{13}C)$ of 164 Hz in the coupled ^{13}C spectrum of **(64)** is typical of an epoxide methine carbon atom and established the presence of a 4,5-epoxide moiety.

Two additional HMBC correlations for the C(4) signal were observed: the one with a singlet resonating at δ_H 1.23, H(15), indicated that there was a methyl group at C(4) and the second with the protons at δ_H 1.17 and δ_H 2.03, assigned as H(3a) and H(3b), respectively. C(3) (δ_C 37.39) in turn, showed an HMBC correlation with H(2), which appeared as a broad multiplet at δ_H 2.28 and integrated for two protons. Although C(2) (δ_C 23.49T) showed no HMBC correlations, a cross peak in the COSY spectrum linked H(2) to another broad multiplet at δ_H 5.31 assigned to H(1). These results identify the fragment **(64 ii).**

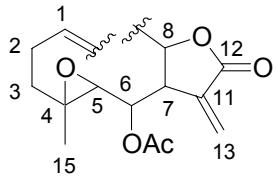

(64 ii)

The chemical shift of H(1) and the corresponding carbon atom C(1) (δ_C 127.84D) suggested that these atoms formed part of a double bond and more specifically a trisubstituted double bond. This was confirmed by the HMBC correlations between C(1) and the broad singlet at δ_H 1.72 [H(14)], which in turn was correlated to the olefinic tertiary carbon, C(10) (δ_C 129.99S). The C(14) (δ_C 19.65Q) resonance was weak and appeared as a broad hump in the ^{13}C spectrum. The absence of an

NOE between H(1) and H(14) pointed to the *E* configuration for the 1(10) double bond.

The remaining ^{1}H resonances, two broad double doublets at δ_H 1.92 and 2.82 were assigned to the C(9) protons. The corresponding carbon atom, C(9), appeared as a weak broad signal at δ_C 43.04T although no HSQC correlations were detected linking these resonances. No HMBC correlations were detected for C(9) either. The COSY spectrum did, however, indicate that the C(9) protons were coupled to each other as well as to a broad signal at δ_H 4.48, identified as H-8. This assignment completed the elucidation of the 10-membered ring of **(64)**, identifying it as a 12,8-germacranolide with an acetate at C(6), a 4,5-epoxide and a 1,10-double bond.

The relative stereochemistry of **(64)** is based on the observed coupling constants and NOE correlations and by comparison with published data.[6] Based on the Karplus equation,[7] the magnitude of the coupling constant between H(6) and H(5) (J 3.7 Hz) suggests a dihedral angle of approximately 40°. This was supported by the observed NOE correlation between H(5) and H(6). Similarly, the coupling constant between H(6) and H(7) (J 11.5 Hz) and the absence of an NOE correlation between these two protons suggests that H(6) and H(7) are antiperiplanar. Furthermore, the lactone ring fusion was shown to be trans by the absence of an NOE between H(7) and H(8) whereas the NOE observed between H(6) and H(8) indicated that both these hydrogen atoms are on the same side of the 10-membered ring. Since the configuration of H(7) is generally α in sesquiterpene lactones from higher plants;[8] H(5), H(6) and H(8) must be β-orientated. Further NOE correlations indicated that H(3a) and H(9b) were β-orientated, while H(3b) and H(9a) were α-orientated. The stereochemistry of **(64)** was thus assigned as 4,5*α*-epoxy-6*α*-hydroxygermacra-1(10)E, 11(13)-dien-12,8*α*-olide.

---

[6] F. Bohlmann and C. Zdero, *Phytochemistry*, 1977, **16**, 776.
[7] R.J. Abraham, " Introduction to NMR spectroscopy.", John Wiley & Sons, Essex, 1988.
[8] E.J. Park and J. Kim, *Planta Med.*, 1998, **64**, 752.

The *p*-nitrobenzoyl ester of **(59)** was prepared in order to obtain crystals suitable for characterisation by X-ray crystallography. The derivative **(65)** proved to be highly unstable and this not only resulted in a poor yield but also foiled attempts to recrystallize the recovered product in order to obtain crystals suitable for X-ray analysis. The ^{1}H NMR data of **(65)** are summarised in Table 4.4.

Compound **(59)** was ultimately identified as 4,5*α*-epoxy-6*α*-hydroxy-1(10)*E*, 11(13)-germacradien-12,8*α*-olide, a compound previously isolated from *Artemisia arbuscula* and *A. tridentata* as well as *Mikania pohli.* The authors of these reports depicted the epoxide moiety as 4*α*,5*β*-orientated which is impossible. The reports did, however, substantiate the observed instability of **(59)**.

Table 4.4 ^{1}H data (in $CDCl_3$) for 4,5*α*-epoxy-6*α*-hydroxy-1(10)E,11(13)-germacradien-12,8*α*-olide **(59)** and the 6-*O*-*p*-nitrobenzoyl derivative **(65)**

	(59)	**(65)**
Proton	**δ_H (J in Hz)**	**δ_H (J in Hz)**
H-1	5.33 (br m*)	5.39 (br m*)
H-2	2.30 (br m*)	2.36 (br m*)
H-3a	1.23 (dm*) (J 12.2)	1.26 (br m*)
H-3b	2.07 (ddd) (J 12.8, 3.5, 4.1)	2.10 (ddd) (J 13.0, 3.8, 4.0)
H-5	2.32 (br d*)	2.85 (br d*)
H-6	4.08 (dd) (J 3.6, 10.8)	5.59 (dd) (J 3.8, 11.5)
H-7	2.85 (br m*)	3.25 (dm*) (J 12.3)
H-8	4.42 (br m*)	4.63 (br dm*) (J 10.3)
H-9a	1.98 (br dd*)	2.02 (br dd*)
H-9b	2.85 (br dd*)	2.94 (br dd*) (J 12.0)
H-13a	6.13 (br m*)	5.77 (dd*) (J 1.6)
H-13b	6.41 (dd) (J 1.1, 2.5)	6.35 (dd*) (J 2.4)
H-14	1.74 (s)	1.83 (s)
H-15	1.40 (s)	1.48 (s)
p-nitro-Bz	-	8.16 – 8.33

* broadened signals: multiplicities and J's could not be determined

Table 4.5 ^{1}H and ^{13}C NMR data (in $CDCl_3$) for 6*α*-acetoxy-4,5*α*-epoxy-1(10)E, 11(13)-germacradien-12,8*α*-olide **(64)**

Atom	^{1}H δ_H (J in Hz)	^{13}C δ_C	HMBC $^{13}C \leftrightarrow {}^{1}H$	COSY $^{1}H \leftrightarrow {}^{1}H$	NOESY $^{1}H \leftrightarrow {}^{1}H$
1	5.31 (br m*)	127.84 D	H(14)	H(2)	H(3a); H(9a); H(2);H(7), H(8)
2	2.28 (br m*)	23.49 T		H(3a); H(1)	H-3(a); H(1)
3	H(3a) 1.17 (ddd) (J 9.5, 12.8, 10.5) H(3b) 2.03 (m#)	37.39 T	H(15), H(2), H(1)	H(3b), H(2) H(3a)	H(3b), H(2), H(5) H(3a)
4		59.58 S	H(6), H(3), H(15)		
5	2.64 (d) (J 3.7)	62.28 D	H(6), H(3b), H(15)	H(6)	H(3a), H(8), H(6), H(1)
6	5.23 (dd) (J 3.7, 11.5)	69.25 D	H(5), H(13)	H(5), H(7)	H(5), H(8)
7	3.00 (br dddd*) (J 11.5, 2.1, 2.3)	43.96 D	H(13), H(6)	H(6), H(8), H(13)	H(3b), H(1)
8	4.48 (br ddd*) (J 11.3)	77.53 D	H(6)	H(9), H(7)	H(14), H(5), H(9b), H(6), H(1)
9	H(9a) 1.92 (br dd*) (J 12.6) H(9b) 2.82 (dd) (J 12.6, 11.3)	43.04 T		H(9b), H(8) H(9a), H(8)	H(9b), H(7), H(1) H(9a), H(8)
10		129.99 S	H(14)		
11		134.33 S	H(13), H(6)		
12		168.85 S	H(13)		
13	H(13a) 5.78 (dd) (J 0.7, 2.1) H(13b) 6.34 (dd) (0.7, 2.4)	127.27 T		H(13b), H(7) H(13a), H(7)	H(13b) H(13a)
14	1.72 (br s)	19.65 Q			
15	1.23 (s)	15.81 Q	H(3a)		
6-O-CO**CH**$_3$	2.02 (s)	20.55 Q			
6-O **C**OCH$_3$		168.89 S	H(6), 6-OCOC**H**$_3$		

* broadened signals: all J's could not be determined

\# overlap with acetate peak

4.5.2 Structure Elucidation of 1*β*,6*α*-dihydroxy-4(15),11(13)-eudesmadien-12,8*α*-olide (60)

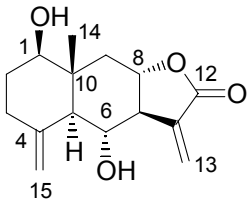

(60)

Compound **(60)** was obtained as colourless crystals, mp 278 - 280 ºC, $[\alpha]_D$ +2.0 (*c* 0.49, MeOH). The high resolution EI-MS of **(60)** showed the molecular ion peak at *m/z* 264.1347 which corresponds to a molecular formula $C_{15}H_{20}O_4$. The ^1H, ^{13}C, HSQC, HMBC, COSY and NOESY data of **(60)** are summarized in Table 4.6. The resonances of **(60)** were sharper and better resolved then was the case for (**59**), and suggested that **(60)** was structurally related to compound **(59)**. The ^{13}C spectrum of (**60**) confirmed that it had a C_{15}-skeleton, typical of germacranolide type sesquiterpene lactones.

The ^1H NMR of **(60)** exhibited four olefinic proton signals. The downfield pair of double doublets (J ~3 Hz, J 1.4 Hz) at δ_H 5.93 and δ_H 5.98 were identified as the C(13) protons, characteristic of the α-methylene-γ-lactone functionality. The upfield pair of signals at δ_H 4.83 and 4.98 were assigned to the exocyclic methylene protons H(15a) and H(15b), respectively, and both signals correlated with the δ_C 145.32S signal which is thus assigned to C(4) of the exocyclic methylene group. The H(15) signals were broadened due to both geminal coupling (J ~1 Hz) and allylic coupling (J ~1 Hz) with H(3) and H(5).

The multitude of HMBC correlations for C(5) (δ_C 57.90D) and C(10) (δ_C 43.70S), particularly those linking both these carbons to H(1), H(14), H(9) and H(6) indicated that a carbon-carbon bond existed between C(5) and C(10). Compound **(60)** was subsequently identified as an eudesmanolide with a 12,8-lactone ring.

The fragments at *m/z* 246 $[M - H_2O]^+$ and 228 $[M - H_2O - H_2O]^+$ suggested the presence of two hydroxyl functions. The two hydroxyl protons, represented by the doublets at δ_H 3.83 (J 5.3 Hz) and δ_H 3.70 (J 5.8 Hz) showed cross peaks in the

COSY spectrum with H(1) (δ_H 3.56) and H(6) (δ_H 4.13) and were consequently assigned as 1-OH and 6-OH, respectively. H(1), H(6) and H(8) were all identified and interpreted as ABX systems although some overlap of signals occurred. For instance, H(1) appeared as a dt due to coupling with H(2a) (J 11.3 Hz) and two similar couplings with H(2b) (J 5.1 Hz) and 1-OH (J 5.3 Hz). Likewise, in theory H(7) (δ_H 2.60) should be a dddd signal but appeared as a ddt due to vicinal coupling with H(8) (J 11.2 Hz) and H(6) (J 9.8 Hz) and almost equivalent allylic coupling with both H(13a) (J 3.1 Hz) and H(13b) (J 3.2 Hz).

The relative stereochemistry of **(60)** followed from comparison with compound **(64)** and published data.[9,10] The magnitude of the coupling constant of H(6) with H(5) ($J_{5,6}$ 9.9 Hz) and H(7) ($J_{6,7}$ 9.8 Hz) suggests a antiperiplanar relationship between them. The *trans* relationship between H(7) and H(8) followed from the magnitude of the coupling constant ($J_{7,8}$ 11.2 Hz). These relative configurations were confirmed by the observed NOE correlation between H(5) and H(7) and that between H(6) and H(8). As established for **(64)**, H(7) and H(5) are most likely α-orientated,[8] therefore H(6) and H(8) must be β-orientated.

The configurations at C(1) and C(10) followed from the NOEs observed between H(5) and H(1) and those between H(14), H(6) and H(8). Further NOESY correlations defined H(9b) (δ_H 2.46) and H(2a) (δ_H 1.60) as β-orientated and H(9a) (δ_H 1.53) and H(2b) (δ_H 1.82) as α-orienated. The stereochemistry of **(60)** was assigned as 1*β*,6*α*-dihydroxy-4(15),11(13)-germacradien-12,8*α*-olide.

The X-ray structural investigation of **(60)** confirmed its structure and relative stereochemistry. The conformation shown in Figure 4.7 is for the enantiomer with the lower Flack parameter. The crystals were orthorhombic and the structure was found to have the P $2_12_12_1$ space group. The cyclohexane system adopts a full chair conformation despite the sp^2 hybridization at C(4). The 4,15-*exo*-methylene group and the methyl group at C(10) are both located on the β-face and adopt an axial orientation, while both the hydroxyl groups lie in a *pseudo*-equatorial position

[9] M.L Cardona, I. Fernández, B. Garcia and J. R. Pedro, *J. Nat. Prod.*, 1990, **53**, 1042.
[10] J. Triana, M. López, M. Rico, J. González-Platas, J. Quintana, F. Estévez, F. Léon and J. Bermejo, *J. Nat. Prod.*, 2003, **66**, 943.

to minimise transannular interactions. Crystallographic data for **(60)** are tabulated in *Appendix (A)*.

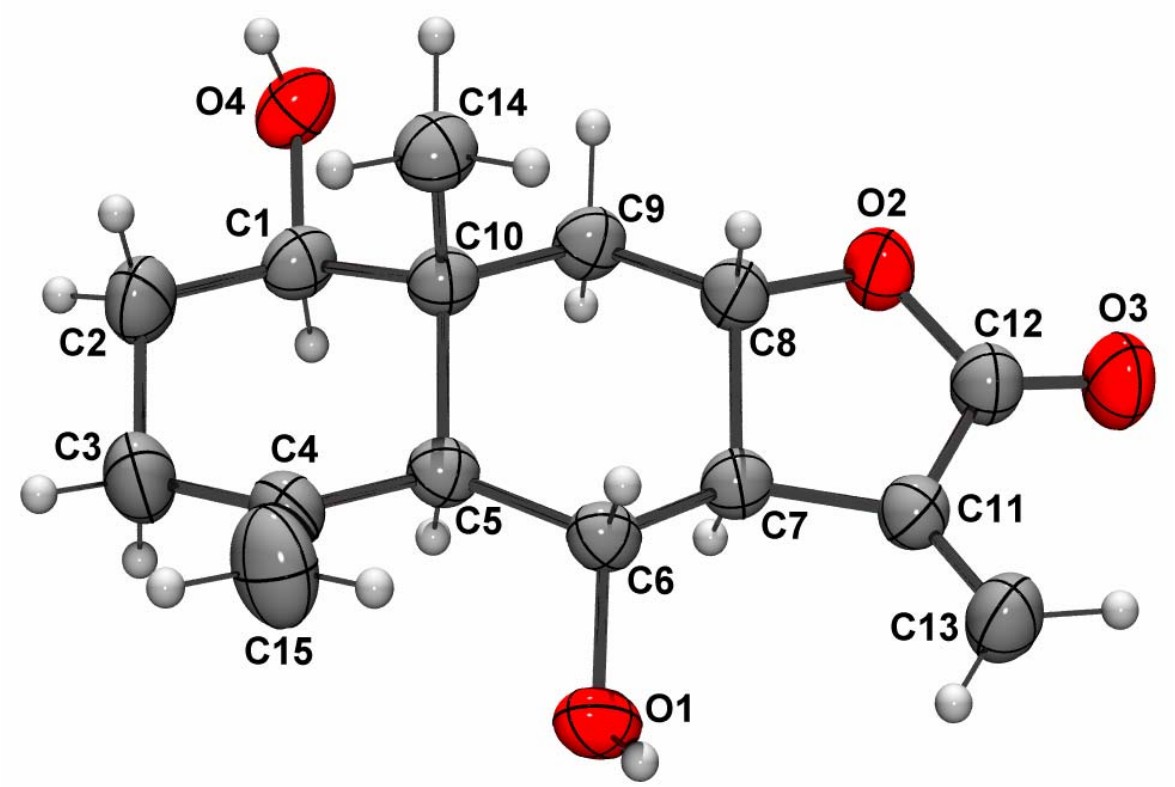

Figure 4.7 X-ray crystal structure of **(60)**

Compound **(60)** was identified as desacetyl-*β*-cyclopyrethrosin previously isolated from several other plant species such as *Mikania pohlii* and *Brocchia cinerea*.[11] The ^{1}H NMR data reported in this dissertation compared well with those reported for this compound.[9]

[11]J. Jakupovic, M.A. Aad, F. Eid, F. Bohlmann, S. El-Dahmy and T. Sarg., *Phytochemistry*, 1988, **27**, 2219.

Table 4.6 ^{1}H and ^{13}C NMR data (in acetone-d_6) for 1*β*,6*α*-dihydroxy-4(15),11(13)-eudesmadien-12,8*α*-olide **(60)**

Atom	^{1}H δ_H (J in Hz)	^{13}C δ_C	HMBC $^{13}C \leftrightarrow {}^{1}H$	COSY $^{1}H \leftrightarrow {}^{1}H$	NOESY $^{1}H \leftrightarrow {}^{1}H$
1	3.56 (ddd) (J 11.3, 5.1, 5.3)	78.51 D	H(14), H(2), H(3), 1-O**H**	H(2a), H(2b), 1-O**H**	H(9a), H(2b), H(5)
2	H(2a) 1.60 (dddd) (J 11.3, 12.9, 13.4, 5.3) H(2b) 1.82 (dddd) (J 2.0, 5.1, 12.0, 12.9)	32.54 T	H(3), H(1), 1-O**H**	H(1), H(2b), H(3b), H(3a) H(3b), H(1), H(2a)	H(14), H(2b) H(1), H(2a)
3	H(3a) 2.09 # H(3b) 2.30 (ddd) (J 2.0; 5.3; 13.4)	35.63 T	H(2), H(5), H(15)	H(2a),H(2b), H(3b),H(15b) H(2b), H(3a), H(2a)	H(3b) H(3a), H(15b)
4		145.32 S	H(2b), H(3), H(5), H(6), H(15)		
5	2.01 (br d) (J 9.9)	57.90 D	H(14), H(3), H(15), H(9b), H(1); 6-O**H**; H(6)	H(6), H(15a)	H(7), H(1)
6	4.13 (ddd) (J 5.8, 9.9; 9.8)	68.00 D	6-O**H**;H(5), H(7), H(8)	6-O**H**, H(5), H(7)	H(14), H(15a)
7	2.60 (dddd) (J 3.1, 3.2, 9.8, 11.2)	55.66 D	H(9),H(6),H(5), 6-O**H**, H(13)	H(13a), H(13b), H(6), H(8)	H(9a), H(5)
8	4.03 (ddd) (J 3.7, 11.2, 12.2)	77.65 D	H(9), H(7), H(6)	H(9b), H(7), H(9a)	H(14); H(9b)
9	H(9a) 1.53 (dd) (J 11.7, 12.2) H(9b) 2.46 (dd) (J 11.7; 3.7)	41.41 T	H(14), H(7), H(1)	H(9b), H(8) H(9a), H(8)	H(9b), H(7), H(1) H(14), H(9a), H(8)
10		43.70 S	H(15), H(9), H(2), H(6), H(1), 1-O**H**		
11		140.26 S	H(7), H(6), H(8), H(13)		
12		170.74 S	H(13)		
13	H(13a) 5.93(dd) (J 3.1; 1.4) H(13b)	118.75 T	H(7)	H(13b), H(7) H(13a), H(7)	

	5.98 (dd) (J 3.2; 1.4)				
14	0.84 (s)	14.20 Q	H(9), H(5), H(1)		H(9b), H(6), H(8), H(2a)
15	H(15a) 4.83 (br m*) H(15b) 4.98 (br m*)	109.36 T	H(3), H(6)	H(5), H(15b) H(3a), H(15a)	H(15b), H(6) H(15a)
1-O**H**	3.83 (d) (J 5.3)			H(1)	
6-O**H**	3.70 (d) (J 5.8)			H(6)	

obscured by solvent signal

* allylic coupling of ~1 Hz

4.5.3 Structure Elucidation of 1*β*,6*α*-dihydroxy-3,11(13)-eudesmadien-12,8*α*-olide (61)

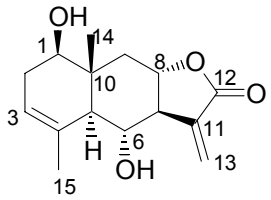

(61)

Compound **(61)** was isolated as white crystals, mp 234 - 236 ºC, $[\alpha]_D$ –38.5 (*c* 0.39, MeOH). A molecular ion peak at *m/z* 264.1261 was observed in the high resolution EI-MS of **(61)**, analyzing for $C_{15}H_{20}O_4$. Initial inspection of the ^1H and ^{13}C spectra of **(61)**, indicated that it was a close analogue of **(60)**. Thorough analysis of the ^1H, ^{13}C, HSQC, HMBC, COSY and NOESY data of **(61)**, summarized in Table 4.7, confirmed that it was also a 12,8*α*-eudesmanolide with an exocyclic double bond conjugated with the lactone carbonyl group.

The appearance of the C(3) (δ_C 122.34D) proton as a broad multiplet at δ_H 5.28 and its HMBC and COSY correlations with a broad methyl signal at δ_H 1.90, led to the deduction that there was a 3,4-double bond and a methyl group at C(4) (δ_C 134.83S). The signals were broadened due to allylic coupling of ~1Hz.

The fragments at *m/z* 246 $[M - H_2O]^+$ and 228 $[M - H_2O - H_2O]^+$ pointed to the presence of two hydroxyl groups in **(61)**. Although both C(1) (δ_C 75.14D) and C(6)

(δ_C 69.10D) are oxygen-bearing carbon atoms only the 1-OH proton resonance, represented by the doublet (J 5.4 Hz) at δ_H 3.79, could be observed. Closer inspection of the complex multiplet between δ_H 3.98 and 4.10 indicated that the H(8), H(6) and 6-OH signals overlapped. Addition of D_2O to the sample simplified its ^{1}H NMR and not only resolved the H(8) and H(6) signals but also simplified the H(6) and H(1) signals and enabled their analysis.

The observed NOESY correlations and proton-proton couplings similar to those described for **(60)**, led to the stereochemical assignments of compound **(61)**. The H(7), H(5), H(1), H(2b) and H(9a) protons were all defined as *α*-orientated, and as a consequence the H(6), H(3), H(15), H(2a), H(15), H(9b) and H(8) protons must be β-orientated. Thus **(61)** was identified as 1*β*,6*α*-dihydroxy-3,11(13)-eudesma-dien-12,8*α*-olide.

The low yield and poor crystals of **(61)** meant that no X-ray crystallography was conducted on this compound. A literature search revealed that **(61)** is a known compound commonly called sivasinolide and first isolated from *Tanacetum densum* subsp. *sivasicum.*[12] The ^{1}H NMR data of **(61)** are in agreement with published data for sivasinolide.[12]

Table 4.7 ^{1}H and ^{13}C NMR data (in acetone-d_6) for 1*β*,6*α*-dihydroxy-3, 11(13)-eudesmadien-12,8*α*-olide **(61)**

Atom	**^{1}H δ_H (J in Hz)**	**^{13}C δ_C**	**HMBC ^{13}C↔^{1}H**	**COSY ^{1}H↔^{1}H**	**NOESY ^{1}H↔^{1}H**
1	3.64 (ddd) (J 5.4, 7.0, 9.5)	75.14 D	H(14), H(2), H(3),1-O**H** H(9)	H(2a), 1-O**H**	H(2b), H(5)
2	H(2a) 1.95 (m) H(2b) 2.33 (m)	33.31 T	 H(3), 1-O**H**	H(1), H(2b) H(1), H(2a)	H(14), H(2b) H(1), H(2a), H(3)
3	5.28 (br m*)	122.34 D	H(2), H(5), H(15)	H(2b), H(15)	H(2b), H(15)
4		134.83 S	H(2b), H(5), H(6), H(15)		
5	2.13 (br dm*)	54.10 D	H(14), H(15),	H(6)	H(7), H(1),

[12] N. Gören, C. Bozak-Johansson, J. Jakupovic, L. Lin, H. Shieh, G. A. Cordell and N. Celik, *Phyto-chemistry*, 1992, **31**, 101.

	(J 10.0)		H(9b), H(1), 6-O**H**, H(6)		6-O**H**
6	4.02 (ddd) (J 8.7, 10.0, 9.8)	69.10 D	6-OH, H(5), H(7), H(8)	H(5)	H(14), H(15)
7	2.51 (dddd) (J 3.1, 3.2, 9.8, 11.5)	56.42 D	H(9), H(6), 6-O**H**, H(8), H(13)	H(13a), H(13b), H-6, H(8)	H(9a), H(5)
8	4.07 (ddd) (J 3.7, 11.5, 12.1)	77.0 D	H(9), H(7)	H(9b), H(7), H(9a)	H(14), H(9b), H(15)
9	H(9a) 1.40 (dd) (J 11.8, 12.1) H(9b) 2.41 (dd) (J 11.8, 3.7)	39.59 T	H(14), H(5)	H(9b), H(8) H(9a), H(8)	H(9b), H(7) H(14), H(9a) H(8)
10		40.91 S	H(14), H(9), H(2b), H(1), 1-O**H**		
11		139.54 S	H(7), H(6), H(8)		
12		170.02 S	H(13)		
13	H(13a) 5.91(dd) (J 3.1; 1.2) H(13b) 5.94 (dd) (J 3.2; 1.2)	117.63 T	H(7)	H(13b), H(7) H(13a), H(7)	
14	0.87 (s)	12.40 Q	H-9a,b; H-5		H-9b; H-6;H-8; H-2a; 1-OH
15	1.90 (br m*)	23.28	H(10)	H(3)	H(3)
1-O**H**	3.79 (d) (J 5.4)			H(1)	H(14)
6-O**H**	4.07 (d) (J 8.7)			H(6)	H(5)

* allylic coupling of ~1 Hz

4.5.4 Structure Elucidation of 1*α*,6*α*-dihydroxy-4*E*,9*Z*,11(13)-germacratrien-12,8*α*-olide (62)

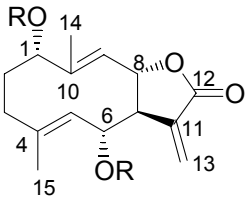

(62) R = H
(66) R = Ac

Compound **(62)** was obtained as white needles, mp 158 - 160 ºC, $[\alpha]_D$ –54.0 (*c* 0.50, MeOH). The high resolution EI-MS of **(62)** showed the molecular ion peak at *m/z* 264.1293 which established the molecular formula as $C_{15}H_{20}O_4$. Analysis of the ^1H, ^{13}C, HSQC, HMBC, COSY and NOESY data of **(62)** (see Table 4.8) revealed that it was a germacranolide with a 12,8-lactone ring, an exocyclic double bond conjugated with the lactone carbonyl group, two hydroxyl groups at C(1) and C(6), and two endocyclic double bonds at C(4) and C(9).

The presence of two hydroxyl groups was confirmed by the fragments at *m/z* 246 $[M - H_2O]^+$ and 228 $[M - H_2O - H_2O]^+$. The two one-proton doublet signals at δ_H 3.83 (J 4.1 Hz) and δ_H 4.14 (J 4.7 Hz) showed cross peaks in the COSY spectrum with H(1) (δ_H 4.39) and H(6) (δ_H 4.48), respectively, and were thus assigned as the 1-OH and 6-OH groups. These doublets were absent from the ^1H NMR spectrum (Table 4.9) of the diacetate derivative **(66)**.

The position of the 4,5-endocyclic double bond followed from the observed HMBC correlations between the methyl resonance, H(15) (δ_H 1.74) and the two signals at δ_C 133.15S and 131.31D assigned to C(4) and C(5), respectively, as well as the cross peaks in the COSY spectrum between H(15) and the methine proton H(5) (δ_H 4.93). Likewise, the position of the 9,10-endocyclic double bond followed from the correlations of H(14) (δ_H 1.76) and H(9) (δ_H 5.24) with C(9) (δ_C 126.46D) and C(10) (δ_C 142.87S). The observed multiplicities and broadening of the respective proton resonances is due to allylic coupling and further supported the assign-ments. The stereochemistry of the endocyclic double bonds was deduced from the observed NOESY correlations between the signals of H(9) and H(14) and by the

absence of an NOE between H(5) and H(15). The double bonds were therefore assigned as 4,5-(*E*) and 9,10-(*Z*).

The C(6) configuration and the trans fusion of the lactone ring was deduced from the observed proton-proton coupling constants and NOE correlations in the same way as for compounds **(59)**, **(60)** and **(61).** The assignment of the C(1) configuration was more difficult. The coupling constants of H(1) with the vicinal C(2) protons (J 10.5 and 4.8) indicate an antiperiplanar relationship between H(1) and one of the protons H(2a) or H(2b), *i.e.* an axial orientation of H(1). The conformation of germacrene derivatives, however, is often very difficult to determine due to the flexibility of medium sized rings.[13] An axial orientation of H(1) can be reached with either of the two possible configurations at C(1).

The NOESY spectrum of the acetylated derivative **(66)** in C_6D_6, however, showed a definite correlation between the H(1) and H(8) signals. Inspection of a molecular model revealed that this NOE could only be observed if the acetate group at C(1) was *α*-orientated *i.e.* C(1) has the *S* configuration . The alternative 1*R* configuration demands considerable transannular tension in order to bring H(1) and H(8) into close proximity.

Compound **(62)** was recrystallised to give trigonal crystals (detailed crystallographic data are tabulated in *Appendix (B)*). The X-ray crystal structure of **(62),** space group P 3_2, confirmed the *α*-orientation of both hydroxyl groups as well as the stereochemistry of the double bonds. The structure is illustrated in Figure 4.8 and shows that the molecule adopts a boat-chair conformation, with C(14) below and C(15) above the plane of the ring. This geometry is supported by the distinct NOE observed between H(6) and H(15).

The crystal structure revealed that there are four equivalent molecules in the asymmetric unit as well as one molecule of water. The water molecule and both the hydroxyl groups are each involved in two hydrogen bonds. The packing is such that there are empty channels running through the structure parallel to the *c* axis

[13] J.F. Sanz and J.A. Marco, *J. Nat. Prod.*, 1991, **54**, 591.

(Figure 4.9). The water molecule of each asymmetric unit lies on the edge of the channel.

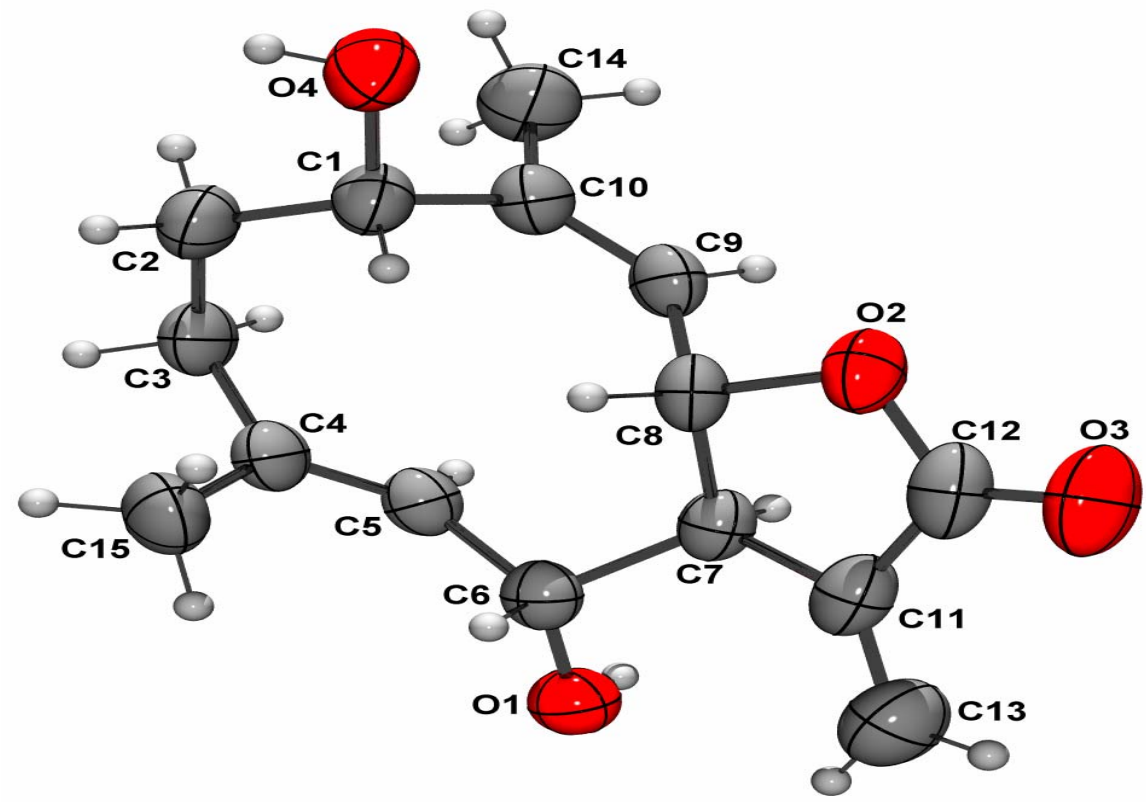

Figure 4.8 X-ray structure of **(62)**

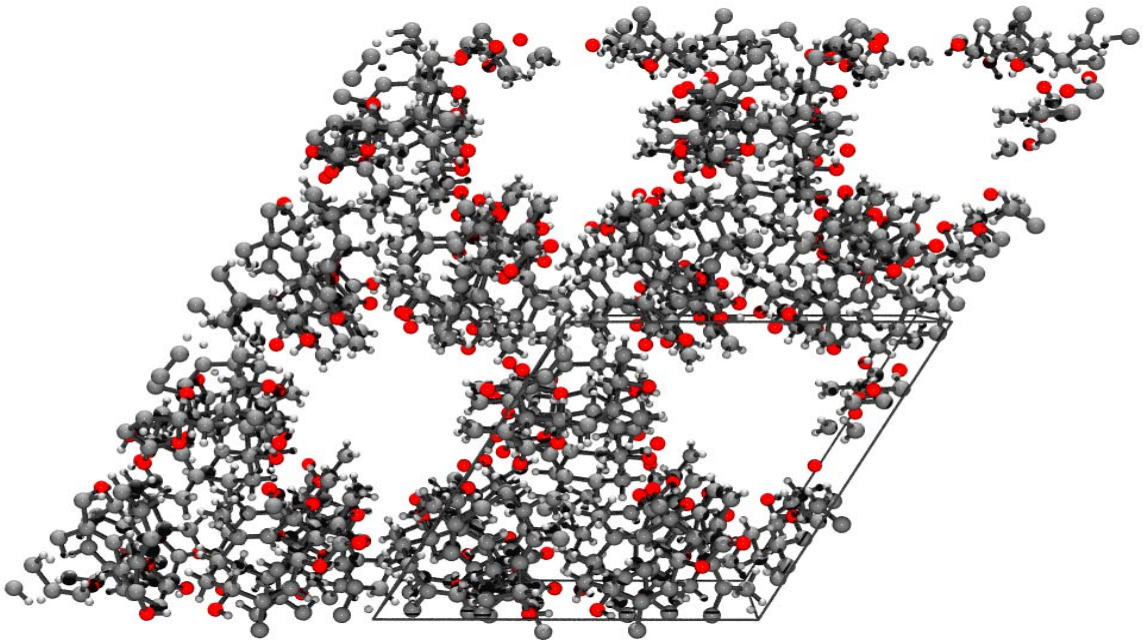

Figure 4.9 Packing of the molecules of **(62)**

To confirm that the channels are due to optimization of the H-bonds, an X-ray analysis was carried out on the diacetate derivative **(66)** which, as expected, did not show any channels. The crystals of **(66)**, space group P 2_1, were found to be monoclinic (Figure 4.10) (*Appendix (C)*).

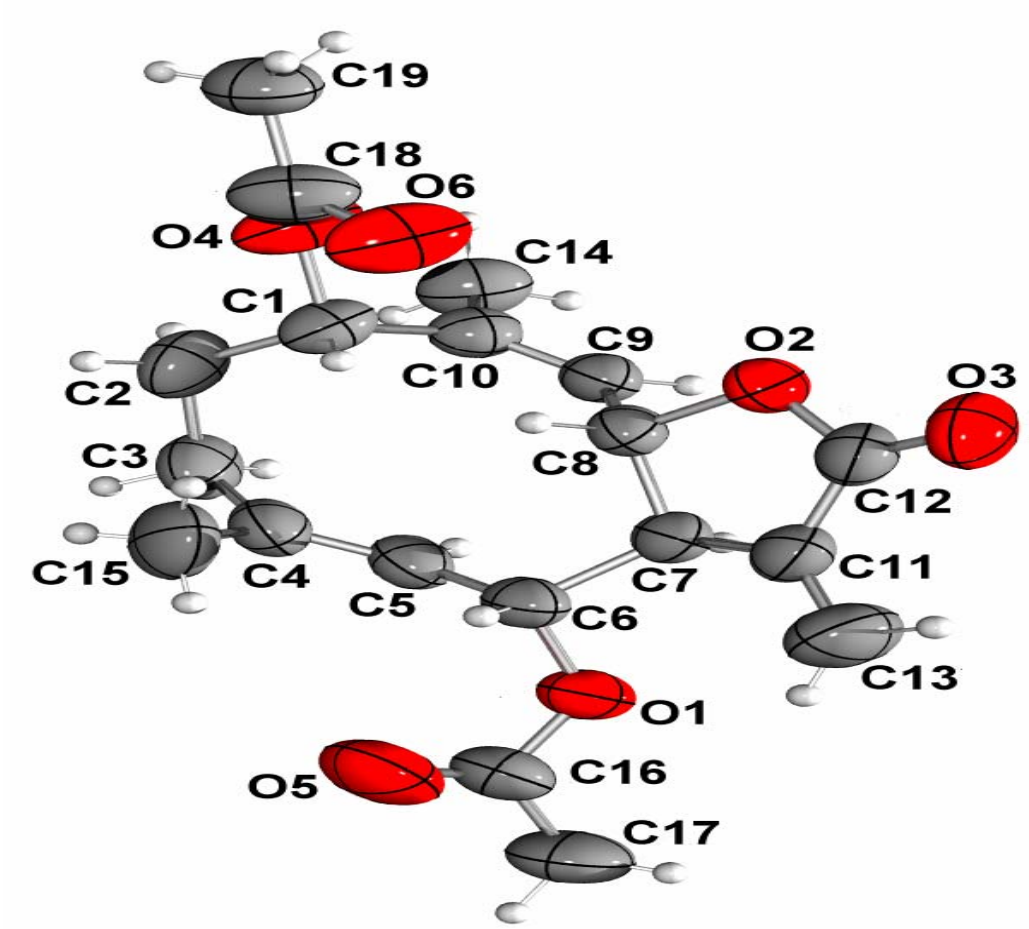

Figure 4.10 X-ray structure of **(66)**

The structure of **(62)** corresponds to tatridin A (also known as tavulin) which has been isolated from a number of plant species including *Artemisia tridentata* and *A. arbuscula* as well as *Tanacetum vulgare*.[14] The structure of **(62)** as 1*α*,6*α*-dihydroxy-4*E*,9*Z*,11(13)-germacratrien-12,8*α*-olide was confirmed by comparison of its ^{1}H, ^{13}C NMR and physical constants with published data for tatridin A.[13]

[14] A.I. Yunusov, G.P. Sidyakin and A.M. Nigmatullaev, *Khim. Prir. Soedin.*, 1979, **1**, 101.

Table 4.8 ^{1}H and ^{13}C NMR data (in acetone-d_6) for 1*α*,6*α*-dihydroxy-4*E*,9*Z*,11(13)-germacratrien-12,8*α*-olide **(62)**

Atom	^{1}H δ_H (J in Hz)	^{13}C δ_C	HMBC $^{13}C \leftrightarrow ^{1}H$	COSY $^{1}H \leftrightarrow ^{1}H$	NOESY $^{1}H \leftrightarrow ^{1}H$
1	4.39 (ddd) (J 4.1, 4.8, 10.5)	65.99 D	H(3), H(9),1-O**H**, H(2)	1-O**H**, H(2a), H(2b)	H(15), H(2)
2	H(2a) 1.67 (m) H(2b) 1.93 (m)	27.89 T	H(3), 1-O**H**, H(1)	H(1), H(2b), H(3a) H(1), H(2a), H(3)	H(2b) H(2a)
3	H(3a) 1.89 (ddd) (J 12.3; 12.4; 5.9) H(3b) 2.20 (m)	35.40 T	H(2), H(5), H(15)	H(3b), H(2a), H(2b) H(3a), H(2)	H(3b) H(3a), H(5)
4		133.15 S	H(3), H(6), H(15)		
5	4.93 (br d) (J 10.5)	131.31 D	H(15), H(3), H(7)	H(6), H(15)	H(7), H(3a)
6	4.48 (ddd) (J 4.7, 10.5, 8.8)	70.55 D	6-O**H**, H(7), H(8)	6-O**H**, H(5), H(7)	H(15)
7	2.75 (dddd) (J 3.5, 3.2, 8.8, 9.0)	52.60 D	H(9), H(6), 6-OH, H(8), H(13), H(5)	H(13b), H(13a), H(6), H(8)	H(9), H(5)
8	4.60 (dd) (J 9.0, 10.0)	74.4 D	H(7)	H(7), H(9)	H(15)
9	5.24 (br dq) (J 10.0, 1.4)	126.46 D	H(14), H(7), H(1), H(8)	H(8), H(14)	H(14), H(7)
10		142.87 S	H(14), H(8), H(2b), 1-O**H**		
11		139.76 S	H(7), H(6), H(13)		
12		170.02 S	H(13)		
13	H(13a) 5.94 (dd) (J 3.2; 1.7) H(13b) 6.03 (dd) (J 3.5, 1.7)	120.91 T	H(7)	H(7), H(13b) H(7), H(13a)	
14	1.76 (d) (J 1.4)	16.36 Q	H(9), H(1)	H(9)	H(9)
15	1.74 (br s)	14.84 Q	H(5), H(3)	H(5)	H(1), H(6), H(8)
1-O**H**	3.83 (d) (J 4.1)			H(1)	
6-O**H**	4.14 (d) (J 4.7)			H(6)	

Table 4.9 ^{1}H data (in $CDCl_3$) 1*α*,6*α*-diacetoxy-4*E*,9*Z*,11(13)-germacratrien-12,8*α*-olide **(66)**

Proton	δ_H (J in Hz)
H-1	5.44#
H-2a	1.67
H-2b/3a	1.8-2.0#
H-3b	2.29 (br m*)
H-5	4.87 (br d) (10.5)
H-6	5.41#
H-7	3.01 (br m*)
H-8	4.75 (dd) (J 9.8, 9.8)
H-9	5.36#
H-13a	5.71 (br dd*)
H-13b	6.25 (br dd*)
H-14	1.80 (br m*)
H-15	1.93 (s)
-O-COC**H**$_3$	2.00 (br s)
	2.06 (br s)

* broadened signals, all J's could not be determined
\# peaks obscured due to overlap

4.5.5 Structure Elucidation of 1*α*,6*α*-dihydroxy-4*E*,10(14),11(13)-germacratrien-12,8*α*-olide (63)

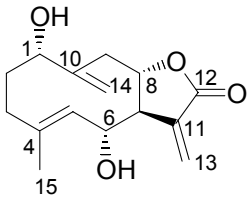

(63)

Compound **(63)** was isolated as colourless crystals, mp. 159 - 161 ºC, $[\alpha]_D$ +24.0 (*c* 0.50, MeOH). The high resolution EI-MS did not show a molecular ion peak for **(63)**, but a $[M - H_2O]^+$ fragment at *m/z* 246.1219 and a second fragment at *m/z* 228.1169 $[M - H_2O - H_2O]^+$ confirmed the presence of two hydroxyl groups and pointed to a $C_{15}H_{20}O_4$ molecular formula. The ^{1}H, ^{13}C, HSQC, HMBC, COSY and NOESY data of **(63)**, summarized in Table 4.10, suggested that it was a close analogue of compound **(62)**.

Subsequent analysis of the NMR data led to the deduction that **(63)** was also a germacranolide with a 12,8-lactone ring, an exocyclic double bond conjugated with

the lactone carbonyl, two hydroxyl groups at C(1) and C(6), and a 4,5-(*E*) endocyclic double bond. The C(4) (δ_C 134.80S) resonance was weak and broadened and was only detected when the ^{13}C spectrum was run with a delay of 3 seconds between pulses.

The only major difference between the structure of compound **(62)** and compound **(63)** was that the latter lacked a 9,10-endocyclic double bond but had a second exocyclic methylene group at C(10). The C(9) (δ_C 42.25T) protons resonating at δ_H 2.45 and δ_H 2.79, arbitrarily assigned as H(9a) and H(9b), respectively, were linked by HMBC correlations to the lactone carbon atom, C(8) (δ_C 79.66D) and the allylic carbons, C(10) (δ_C 148.62S) and C(14) (δ_C 113.77T). Cross peaks in the COSY spectrum indicated the geminal relationship between the C(9) protons (J = 14.2 Hz) as well as vicinal coupling between H(9) and H(8) (δ_H 4.60), with J = 9.6 and 2.3 Hz.

In addition, H(9b) shows allylic coupling (J~2 Hz) with the pair of broadened signals resonating at δ_H 5.06 and δ_H 5.10, corresponding to the exocyclic methylene protons, H(14a) and H(14b). This was supported by the observed multiplicities of the H(9a) (dd) and H(9b) (dddd) proton signals, which were analysed using the ^1H NMR spectrum of **(63)** in $CDCl_3$ (Table 4.11), where these signals appeared more defined and better resolved than in acetone-d_6. The coupling of only H(9b), and not H(9a), with the C(14) protons suggests that it is in the same plane as the π-system. Observed coupling constants and NOESY correlations with H(8) indicate that H(9b) is *β*-orientated, while H(9a) is *α*-orientated. NOE correlations between H(9b), H(14) and the methyl resonance at δ_H 1.70, H(15), indicate that in solution they are all on the same side of the cyclodecane ring *i.e*. they are *β*-orientated.

Contrary to this, the X-ray structure analysis of **(63)** showed that the methyl and methylene groups at C(4) and C(10) are *anti* (Figure 4.11). Apart from this, it was confirmed that the lactone ring was linked with the germacrane ring in a trans manner and that the 2 hydroxyl groups were *α*-orientated. The crystals were orthorhombic and the structure was found to have the P $2_12_12_1$ space group. The

10-membered ring adopts a boat-boat conformation. The hydroxyl groups are maintained in a pseudo-equatorial position, away from the inner part of the ring to minimize transannular interactions. Detailed crystallographic data for **(63)** are tabulated in *Appendix (D)*.

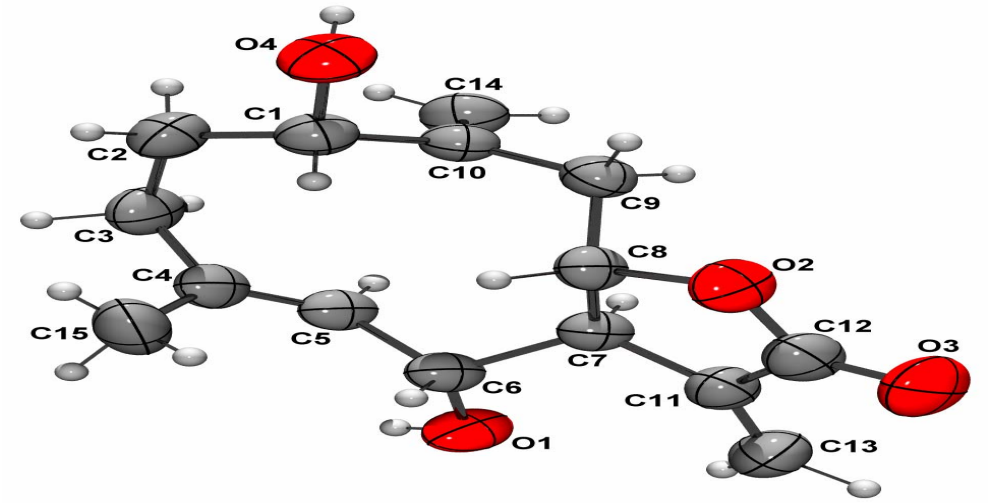

Figure 4.11 X-ray structure of **(63)**

Compound **(63)** was identified as tanachin, first isolated from *Tanacetum pseudoachillea*[15]. This compound has subsequently been isolated from a variety of plants in the *Asteraceae* family in Middle Asia.[12,13,16] The identification of **(63)** as 1*α*,6*α*-dihydroxy-4E,10(14),11(13)-germacratrien-12,8*α*-olide was confirmed by comparison of its ^{1}H, ^{13}C NMR and physical constants with published data for tanachin.[17]

Table 4.10 ^{1}H and ^{13}C NMR data (in acetone-d_6) for 1*α*,6*α*-dihydroxy-4*E*, 10(14),11(13)-germacratrien-12,8*α*-olide **(63)**

Atom	^{1}H δ_H (J in Hz)	^{13}C δ_C	HMBC $^{13}C\leftrightarrow{}^{1}H$	COSY $^{1}H\leftrightarrow{}^{1}H$	NOESY $^{1}H\leftrightarrow{}^{1}H$
1	3.90 (ddd) (J 6.2, 10.3, 4.4)	70.35 D	H(3), H(9), 1-O**H**, H(2), H(14)	1-O**H**, H(2a), H(2b)	H(15), H(9b), H(8), H(14)
2	2.03 (m)	31.89 T	H(3), 1-O**H**, H(1)	H(1), H(3)	
3	H(3a) 2.01 (m)	35.06 T	H(2), H(5), H(15)	H(3b), H(2)	

[15] A.I Yunusov, N.D. Abdullaev, S.Z. Kasymov and G.P. Sidyakin., *Khim. Prir. Soedin.*, 1976, **2**, 263.
[16] M.B. Izbosarov, Kh. T. Zairova, B. Kh. Abduazimov, V.M. Malikov, *Khim. Prir. Soedin*, 2000, **36**, 288.
[17] A.I.Yunusov, N.D. Adbullaev, Sh. Z. Kasymov, G.P. Sidyakin and M.R. Yagudaev, ., *Khim. Prir. Soedin.*, 1976, **4**, 462.

	H(3b) 2.24 (m)			H(3a), H(2)	H(5), H(14)
4		134.80 S	H(3), H(6), H(15), H(2)		
5	5.07 (br dd) (J 9.9, 1.4)	132.91 D	H(15), H(3), H(6), 6-O**H**	H(15), H(6)	H(9a), H(7)
6	4.31 (ddd) (J 4.4, 9.9, 9.5)	70.99 D	6-O**H**, H(7), H(5)	6-O**H**, H(5), H(7)	H(15), H(8)
7	2.82 (dddd) (J 2.8, 3.2, 6.6, 9.5)	52.82 D	H(9), H(6), 6-O**H**, H(8), H(13)	H(13a), H(13b), H(8), H(6)	H(13a), H(5), H(9a)
8	4.60 (br ddd) (J 6.6, 9.6, 2.3)	79.66 D	H(7), H(9), H(6)	H(7), H(9a), H(9b)	H(15), H(1), H(6), H(9b), H(14)
9	H(9a) 2.45 (dd) (J 9.6, 14.2) H(9b) 2.79 (dddd) (J 2.3, 14.2, 2.0; 2.0)	42.25 T	H(14), H(7), H(1)	H(8), H(9b) H(8), H(9a), H(14a), H(14b)	H(5), H(7) H(1), H(14), H(8), H(15)
10		148.62 S	H(14), 1-OH, H(1), H(9), H(2)		
11		139.27 S	H(7), H(6), H(13)		
12		170.11 S	H(7), H(13)		
13	H(13a) 6.12 (dd) (J 2.8, 1.4) H(13b) 6.16 (dd) (J 3.2; 1.4)	132.77 T	H(7)	H(7), H(13b) H(7), H(13a)	H(7)
14	H(14a) 5.06 (br d) (J 2.0) H(14b) 5.10 (br s)	113.77 T	H(9), H(1)	H(9b)	H(1), H(8), H(9b), H(15)
15	1.70 (d) (J 1.4)	14.84 Q	H(5), H(3)		H(1), H(6), H(8), H(14), H(9b)
1-O**H**	3.68 (d, 6.2)			H(1)	
6-O**H**	4.14 (d, 4.4)			H(6)	

Table 4.11 ^{1}H data (in $CDCl_3$) for 1*α*,6*α*-dihydroxy-4*E*,10(14),11(13)-germacratrien-12,8*α*-olide **(63)**

Proton	δ_H (J in Hz)
H-1	3.81 (ddd) (J 4.6, 10.3, 6.3)
H-2a/b	2.00 (m*)
H-3a	1.95 (m*)
H-3b	2.17 (m*)
H-5	5.00 (br dd) (J 9.8, 1.4)
H-6	4.19 (ddd) (4.3, 9.8, 9.6)
H-7	2.74 (dddd) (J 9.6, 6.6, 2.8, 3.2)
H-8	3.90 (br m*)
H-9a	2.31 (dd) (J 9.6, 14.2)
H-9b	2.82 (dddd) (14.2, 2.0, 1.9, 2.3)
H-13a	6.13 (dd) (1.4, 2.8)
H-13b	6.17 (dd) (1.4, 3.2)
H-14a	4.99 (br d) (J 1.8)
H-14b	5.04 (br s)
H-15	1.61 (d) (J 1.4)
1-OH	3.10 (d) (J 6.3)
6-OH	3.58 (d) (J 4.3)

* broadened signals, all J's could not be determined

4.5.6 Characterization of Compounds (59) – (63)

Compounds **(59)**, **(62)** and **(63)** were identified as germacranolides by their lactone and cyclodecane rings, as well as the exocyclic double bond conjugated with the lactone carbonyl. They were characterised as germacrane lactones with a linear structure due to the α,β-unsaturated lactone being fused to the C(8)-C(7) positions of the carbocyclic skeleton. Similarly, compounds **(60)** and **(61)** were identified as the linear germacranolide derivatives, known as eudesmanolides, distinguished by the cyclodecane ring being split into two six membered rings by a C(5)-C(10) bond. All the compounds were further characterized by the position and

stereochemistry of hydroxyl groups, double bonds and, in the case of **(59)**, the epoxide moeity on the cyclodecane ring.

The presence of certain broadened, unresolved signals in the ^{1}H and ^{13}C spectra is indicative of conformational equilibria in solution. In general the 7,8-germacranolides are known to be conformationally labile. It has been shown, however, that certain conformations are hindered because of steric repulsion between the *syn*-directed C(15) methyl group and the α-OH substituent at C(6) and that transition between the more favoured conformations is determined by the conformational mobility of the C(9)-C(10)-C(1)-C(2) section.[18] The presence of a hydroxyl group at C(1) in compounds **(62)** and **(63)** therefore renders the 10-membered rings less mobile than **(59)**, for instance.

Although compounds **(59)** – **(63)** are all known compounds, having been previously isolated from a variety of plant species, this is the first report of their isolation from *Oncosiphon piluliferum* and in fact the first report on any chemical constituents of this plant. The compounds identified, however, are all sesquiterpene lactones which are common components in the *Asteraceae* family. The bitter taste of *O. piluliferum* suggests that the sesquiterpene lactone content is relatively high, and thus it is evident that several other structurally related compounds occur in the dichloromethane extract.

4.5.7 Absolute Configurations of Compounds (59)–(63)

Due to the relatively high yield of **(63)**, Mosher's method could be applied to determine the absolute stereochemistry of this compound. This technique is a empirically derived chemical method used to determine the absolute configuration of organic compounds possessing a secondary hydroxyl group.[19,20,21]

---

[18] M.K. Makhmudov, B.K. Abuazimov, B. Tashkhodzhaev and B.T. Ibragimov, *Khim. Prir. Soedin.*, 1989, **2**, 198.
[19] J.A. Dale and H.S. Mosher, *J. Am. Chem. Soc.*, 1973, **95**, 512.
[20] I. Ohtani, T. Kusumi, Y. Kashman and H. Kakisawa, *J. Am. Chem. Soc.*, 1991, **113**, 4092.
[21] M.J. Rieser, Y. Hui, K. Rupprecht, J.F. Kozlowski, K.V. Wood, J.L. McLaughlin, P.R. Hanson, Z. Zhuang and T. R. Hoye, *J. Am. Chem. Soc.*, 1992, **114**, 10203.

4.5.7.1 Mosher Esters of Compound (63)

The Mosher acid, (*R*)-*α*-methoxy-*α*-trifluoromethylphenyl acetic acid, [(*R*)-MTPA] upon treatment with thionyl chloride is converted to the *S* acid chloride [(*S*)-MTPA-Cl]. The ester formation *of* this acid chloride with a chiral alcohol then leads to the formation of the (*R*)-MTPA ester. Similarly, the *S* acid gives rise to the *S* ester via the *R* acid chloride (Figure 4.12).[21]

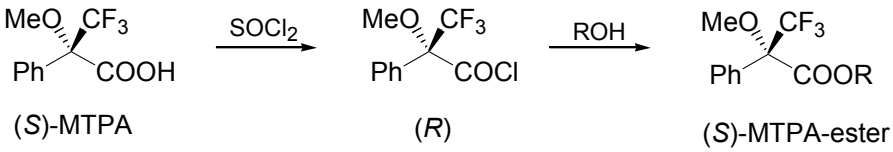

Figure 4.12 (*S*)-Mosher acid esterification of an alcohol

Since compound **(63)** has 2 secondary hydroxyl groups the (*R*)-MTPA esterification of compound **(63)** resulted in the isolation of three products, a diester and two monoesters, compounds **(67)**, **(68)** and **(69)**. Ester formation of compound **(63)** with (*S*)-MTPA produced the Mosher esters **(70)**, **(71)** and **(72)**.

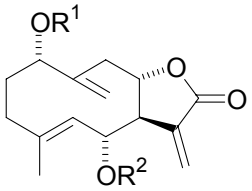

Compound	R^1	R^2
(67)	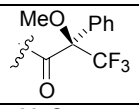	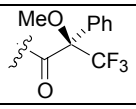
(68)	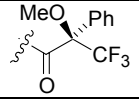	H
(69)	H	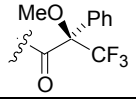
(70)	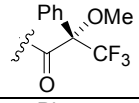	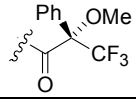
(71)	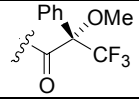	H
(72)	H	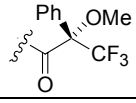

Figure 4.13 Mosher esters of compound **(63)**

4.5.7.2 Mosher's Method

Mosher's method is based on the hypothesis that MTPA ester groups exist in solution in a conformation in which the methine proton, ester carbonyl group and trifluoromethyl group lie in the same plane (Figure 4.14).

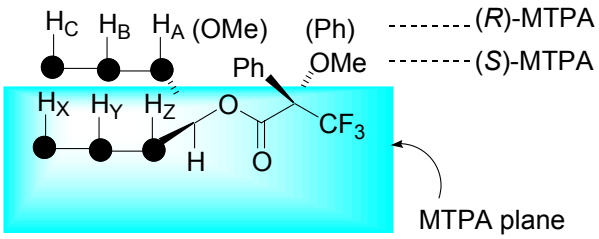

Figure 4.14 MTPA plane of an MTPA ester. $H_{A,B,C}$ and $H_{X,Y,Z}$ are on the right and left sides of the plane respectively.

Due to the diamagnetic effect of the phenyl group the $H_{A,B,C...}$ NMR signals of the (*R*)-MTPA ester should appear upfield relative to those of the (*S*)-MTPA ester. The reverse should hold true for $H_{X,Y,Z...}$. Therefore protons on the right side of the MTPA plane must have positive $\Delta\delta$ (δ_S - δ_R) values and protons on the left side of the plane must have negative values, as illustrated in Figure 4.15.[20]

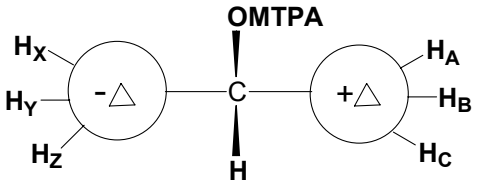

Figure 4.15 Model to determine of the absolute configuration of secondary alcohols.

4.5.7.3 Application of Mosher's Method – Absolute Stereochemistry of Compound (63)

Proton signals were assigned for each of the (R)- and (*S*)-MTPA esters of **(63)**. The COSY spectra were used to determine the approximate chemical shifts of those signals that were severely overlapped in the ^{1}H NMR spectra. $\Delta\delta$ values were obtained for the protons of the 1,6-di-*O*-MTPA derivatives, compounds **(67)** and **(70)**, the 1-*O*-MTPA derivatives, compounds **(68)** and **(71),** and the 6-*O*-MTPA derivatives, compounds **(69)** and **(72)**, of compound **(63)**. These values are summarized in Figure 4.16.

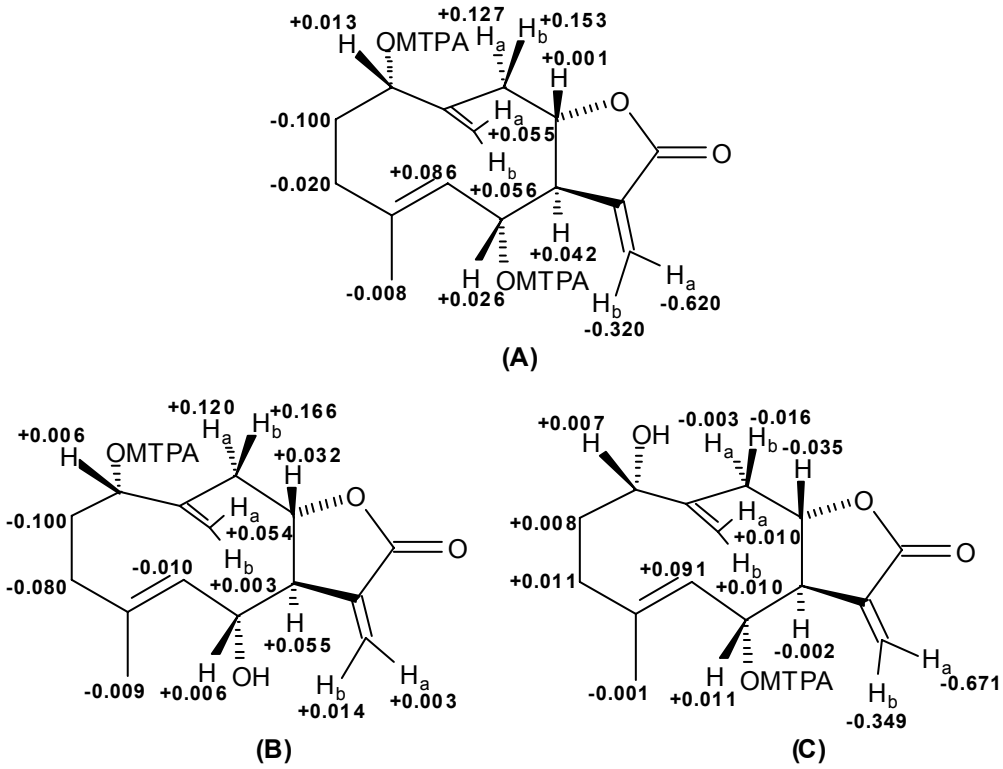

Figure 4.16 $\Delta\delta$ Values obtained for the 1,6-*O*-di-MTPA derivative **(A)**, the 1-*O*-MTPA derivative **(B)** and the 6-*O*-MTPA derivative **(C)** of compound **(63)**

Since the $\Delta\delta$ values for the H(2), H(3) and H(5) protons **(B)** are negative they are located on the left side of the MTPA plane at C(1) whereas the positive $\Delta\delta$ values for the H(14), H(9) and H(8) protons places them on the right side of the MTPA plane. Substitution of these two groups of protons into the model shown in Figures 4.14 and 4.15 and subsequent application of the Cahn-Ingold-Prelog sequence rules,[22] indicates that C(1) has the *S* configuration.

Similarly, it follows from **(C)** that the H(5), H(2) and H(3) protons are on the right side and H(7), H(8) and the H(13) protons are on the left side of the MTPA plane at C(6). The R configuration is thus assigned to C(6).

From **(A)** it can be noted that for the diesters, the $\Delta\delta$ values for the protons on either side of the MTPA plane at C(1) support the findings of **(B)**, but at C(6) the positive and negative $\Delta\delta$ values are irregularly dispersed on the left and right sides

[22] R.T. Morrison and R.N. Boyd, 'Organic Chemistry', 6th edition, Prentice Hall International, New York, 1992

of the MTPA plane. This may be due to changes in the conformation of the diester due to steric congestion around the C(6) stereogenic centre.

The absolute configuration of the other stereogenic centres, C(7) and C(8) of **(63)** followed from the established relative stereochemistry and application of the Cahn-Ingold-Prelog sequence rules, and compound **(63)** is thus (1*S*,6*R*,7*S*,8*S*)-1,6-dihydroxy-4*E*,10(14),11(13)-germacratrien-12,8-olide.

4.5.7.4 Biosynthesis of Compounds (59) – (62)

In recognizing that compounds **(59)** – **(63)** are all structurally related and have the same relative stereochemistry at C(6), C(7) and C(8) it is evident that these secondary metabolites are formed from a common biogenetic precursor. Thus the absolute stereochemistry of the other compounds can be deduced from that of **(63)**. Figure 4.17 outlines the proposed biosynthesis of **(59)** – **(63)** based on literature precedent and summarises the deduced absolute configurations.

Although the possibility cannot be ruled out, it seems unlikely that costinolide **(25)** is the biogenetic precursor of compounds **(59)** – **(63)**, as this would require not only hydroxylation of costinolide at C(8), but also the shifting of the lactone ring from C(6)-C(7) to C(7)-C(8). It appears more likely that hydroxylation occurs at C(8) of **(39),** the immediate precursor of costinolide, to give the 6,8-dihydroxy-germacratrien-12-oic acid **(74)**. The manner in which the C(6) and C(8) oxygen atoms are introduced is not known, but sufficient evidence suggests that direct oxidation of C-H to C-OH is a common biological process.[23] The less sterically hindered C(7)-C(8) lactone closure of **(74)** yields the basic sesquiterpene lactone precursor known as deacetyllaurenobiolide **(75)**. This compound is reported to have been isolated from *Tanacetum densum* concurrently with compounds **(61)** and **(63)**.[12]

[23] TA Geissman, 'The Biogenesis of Sesquiterpene Lactones of the Compositae', University of California Press, California, 1973.

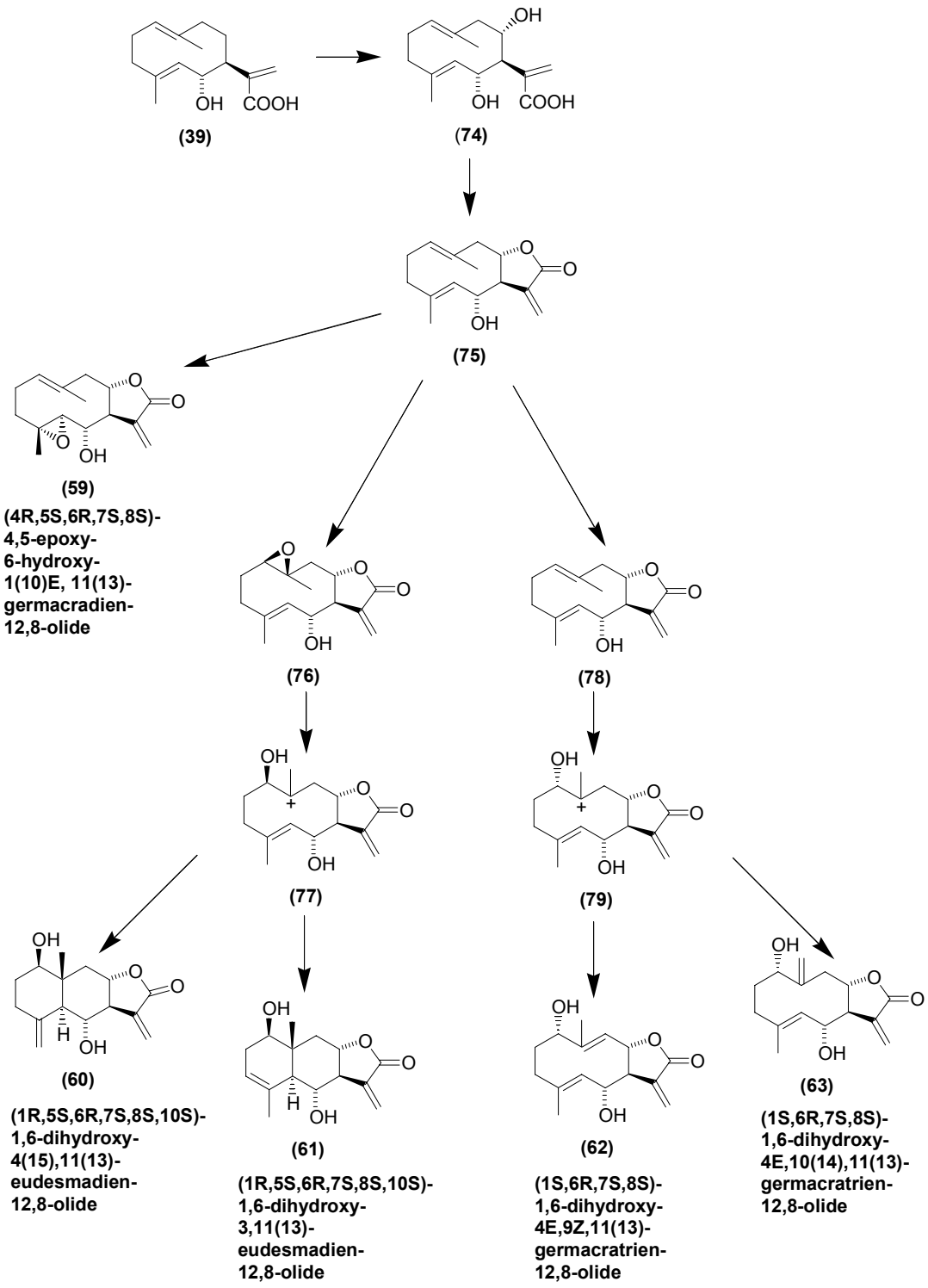

Figure 4.17 Postulated biosynthesis of compounds **(59)**, **(60)**, **(61)**, **(62)** and **(63)**

Compound **(59)** would result from the selective epoxidation of the 4,5-double bond of **(75)** from below the plane of the ring. As epoxidation is considered an important

means of introducing oxygen into natural organic compounds,[24] it is probable that the 1-OH group in compounds **(60)**, **(61)**, **(62)** and **(63)** arises from the selective epoxidation of the 1,10-double bond of **(75)**. The opposite configurations of the 1-OH groups in the eudesmanolides, **(60)** and **(61**), and the germacranolides, **(62)** and **(63)**, suggests that the epoxidation of this allylic system can occur from either face in **(75)**. Epoxidation from above the plane of the ring yields **(76)**, which upon acid-catalysed epoxide opening gives the 1β-OH intermediate cation **(77)**. Subsequent ring closure would yield the eudesmanolides **(60)** and **(61)**. Similarly epoxidation from below the plane of the ring of **(75)** yields **(78)**, which can be converted to germacranolides **(62)** or **(63)** *via* the 1*α*-OH intermediate cation **(79)**.

4.6 $NaBH_4$ Reduction of Compound (63)

Compounds **(59)**-**(63)** were all found to possess an α-methylene-γ-lactone functional group. Since it has been established that this moiety is typically responsible for the biological activity of sesquiterpene lactones,[25] an attempt was made to determine what effect the reduction of the C(11)-C(13) exocyclic double bond would have on the antiplasmodial activity and cytotoxicity of these compounds. The relatively high yield of **(63)** provided additional material to attempt the reduction of the C(11)-C(13) exocyclic double bond with $NaBH_4$ in methanol. Although the yield of the reaction was low (34%) adequate product **(73)** was recovered for characterization by NMR and bioassaying. No additional physical data could be obtained on the compound due to its instability.

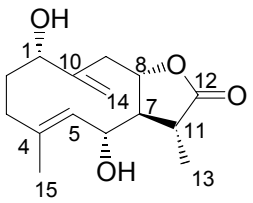

(73)

Compound **(73)** was recovered as a pale yellow gum. The ^{1}H NMR data of **(73)**, summarized in Table 4.12, clearly indicated that the *α*-methylene lactone function

[24] T.A. Geissman, *Phytochemistry*, 1970, **9**, 2377.
[25] E. Rodriguez, G.H.N. Towers and J.C. Mitchell, *Phytochemistry*, 1976, **15**, 1573.

of **(63)** had been reduced to give the 11,13-dihydro derivative and that the reaction yielded only one of the two possible stereoisomers.

The pair of doublets corresponding to those of the C(13) methylene group in **(63)** were absent from the ^{1}H NMR spectrum of **(73)** and were replaced by a methyl signal resonating at δ_H 1.39 (d, J 7.2 Hz). There was also an additional proton signal at δ_H 2.63 identified as H(11). The assignment of H(11) was supported by the observed multiplicity of this resonance which appeared as a dq due to vicinal coupling with H(7) (J 9.1 Hz) and the methyl protons, H(13) (J 7.2 Hz).

The stereochemistry at C(11) followed from the magnitude of the coupling constant between H(7) and H(11) (J 9.1Hz), which suggested an antiperiplanar relationship between them. This was confirmed by the strong NOE correlation observed between H(13) and H(7) in the NOESY spectrum of **(73)**.

The reduction of **(63)** with $NaBH_4$ in methanol therefore yielded (1*S*,6*R*,7*S*,8*S*, *11*R)-1,6-dihydroxy-11,13-dihydro-4*E*,10(14),11(13)-germacratrien-12,8-olide. The fact that the reduction resulted in only one of the possible stereoisomers was in accordance with previous reports on the reduction of related sesquiterpene lactones with $NaBH_4$.[9,26] The anion **(80)** is protonated from the less-hindered side of the enolate double bond to form the thermodynamically more stable stereo-isomer *ie*. where the new methyl group is less hindered.

[26] M.A. Irwin, K.H. Lee, R.F. Simpson and T.A. Geissman , *Phytochemistry*, 1969, **8**, 2009.

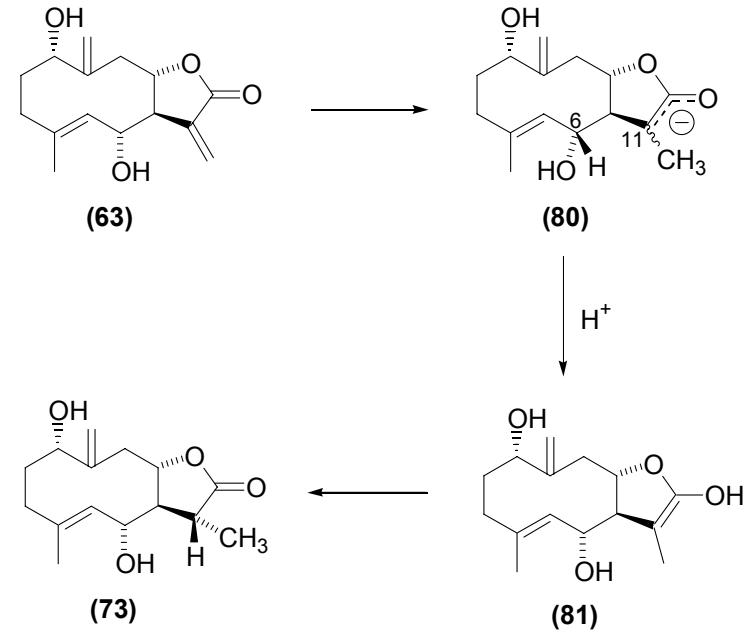

(1S,6R,7S,8S,11R)-1,6-dihydroxy-11,13-dihydro-4E,10(14)-germacradien-12,8-olide

Figure 4.19 $NaBH_4$ reduction of compound **(63).**

Table 4.12 ^1H data (in $CDCl_3$) for (1*S*,6*R*,7*S*,8*S*,*11*R)-1,6-dihydroxy-11,13-dihydro- 4*E*,10(14)-germacradien-12,8-olide **(73)**

Proton	**δ_H (J in Hz)**
H(1)	3.92 (dd) (J 4.9, 9.7)
H(2)	2.00 (m)
H(3a)	1.90 (ddd) (J 5.5, 5.7, 13.5)
H(3b)	2.06 (ddd) (J 5.5, 5.1, 8.8)
H(5)	5.10 (br d) (J 10.1)
H(6)	4.26 (dd) (J 10.1, 9.8)
H(7)	2.26 (ddd) (J 5.5, 9.1, 9.8)
H(8)	3.89 (ddd) (J 2.5, 8.3, 5.5)
H(9a)	2.41 (dd) (J 15.3, 8.3)
H(9b)	2.80 (dddd) (J 2.3, 2.2, 2.5, 15.3)
H(11)	2.63 (dq) (J 7.2, 9.1)
H(13)	1.39 (d)

	(J 7.2)
H(14a)	5.03 (br d) (J 2.2)
H(14b)	5.07 (br dd) (J 2.2, ~1)
H(15)	1.65 (d) (J 1.3)

4.7 *In vitro* Antiplasmodial Activity and Cytotoxicity of Compounds from *O.piluliferum*

Compounds **(60)**, **(61)**, **(62)**, **(63)**, **(64)** and **(73)** were tested for *in vitro* antiplasmodial against the D10 and K1 *P. falciparum* strains using the pLDH assay. The corresponding IC_{50} and RI values of chloroquine and the 6 compounds are listed in Table 4.13

Table 4.13 *In vitro* antiplasmodial activity of chloroquine, compounds **(60)** - **(64)** and compound **(73)**

Tested sample	**D10 IC_{50} (μg/ml)**	**K1 IC_{50} (μg/ml)**	**RI***
Chloroquine	11.1×10^{-3}	181.76×10^{-3}	15.36
Compound **(64)**	0.5	1.6	3.2
Compound **(60)**	4.4	4.2	1.0
Compound **(61)**	2.6	2.3	0.9
Compound **(62)**	0.4	1.0	2.5
Compound **(63)**	0.5	1.8	3.6
Compound **(73)**	70.0	ND	ND

* RI = K_1 IC_{50} / D_{10} IC_{50}

ND = Not determined

Compound **(73)** can be considered completely inactive. The germacranolides **(64)**, **(62)** and **(63)** showed equipotent antiplasmodial activity and were found to be significantly more active than the eudesmanolides **(60)** and **(61).** This is most likely due to the flexibility and conformational features of the 10-membered ring as opposed to the bi-cyclohexane ring system but the effect of other structural

features cannot be ruled out. For instance, the presence of a 4,15-exocyclic methylene group, such as that in **(60)**, has been reported to decrease antiplasmodial activity in structurally related eudesmanolides.[27] This might explain why **(60)** was the least active of the isolated compounds and why it had a higher IC_{50} than **(61)** when these two compounds differ only in the position of one double bond.

No significant conclusions could be drawn from the structure-activity relationship between the three germacranolides. In the case of compounds **(62)** and **(63)** the difference in antiplasmodial activity was minimal yet they also differ in the position of one double bond. While in compound **(62)**, C-10 has an exocyclic double bond; in compound **(63)** there is a C(9)-C(10) endocyclic double bond. Compound **(64)**, which has a 4,5-epoxide moiety, was equipotent to compounds **(62)** and **(63)** which both have a double bond in this position.

There are no previous reports of compounds **(59)** and **(60)** being investigated for any biological activity. Compounds **(61)**, **(62)** and **(63)** have been found to show antibacterial activity.[12,16] This is the first report of any of the compounds having antiplasmodial activity.

The *in vitro* cytotoxicity of the compounds against CHO cells was determined using the MTT assay. The corresponding IC_{50} and SI values of chloroquine and the 6 compounds are listed in Table 4.14

Table 4.14 *In vitro* cytotoxicity of chloroquine, compounds **(60)** - **(64)** and compound **(73)**

Tested sample	**CHO IC_{50} (μg/ml)**	**SI***
Chloroquine	18.5	1666.7
Compound **(64)**	2.2	4.4
Compound **(60)**	10.1	2.3
Compound **(61)**	4.0	1.5

[27] G. Lang, C.M. Passreiter, C.W. Wright, N.H. Filipowicz, J. Addae-Kyereme, B.E. Medinilla and J. Castillo, *Z. Naturforsch.*, 2002, **57c**, 282.

Compound **(62)**	6.0	15.0
Compound **(63)**	6.4	12.8
Compound **(73)**	>100	>1.4

* SI = cytotoxicity CHO IC_{50}/antiplasmodial D_{10} IC_{50}

All compounds, except compound **(73)**, also showed significant toxicity to CHO cells at similar concentrations and this is emphasized by their low SI values – only **(62)** and **(63)** can be considered hits based on the criteria discussed in Chapter 3.[28] The data suggests that the observed antiplasmodial activity might be due to general toxicity. The antiplasmodial and cytotoxicity assay results of compound **(73)** clearly show that the C(11)-C(13) exocyclic double bond of **(63)** is primarily responsible for both the antiplasmodial activity and toxicity to CHO cells as both are significantly decreased when this double bond is reduced. This result is in accordance with previous findings that the presence of an α-methylene-γ-lactone functional group is an active centre for cytotoxicity[29] and antiplasmodial activity.[30,31] Since compounds **(64)**, **(60)**, **(61)**, **(62)** and **(63)** all possess an α-methylene-γ-lactone moiety, one would expect that they would all show equipotent antiplasmodial activity and toxicity to CHO cells, which is clearly not the case. The fact that there are significant differences in the IC_{50} values of each compound in the two assays as well as between the various compounds suggests that there is more than just the cytotoxic effect of the α-methylene-γ-lactone group coming into play.

4.8 Conclusion and Research Prospects

Although *Oncosiphon piluliferum* is reported to have been used medicinally, it was shown here to contain structurally related sesquiterpene lactones with significant toxicity. The compounds **(59)**, **(60)**, and **(61)** did show antiplasmodial activity but their potential for development of antimalarial drugs is limited due to inherent cytotoxicity and lack of selectivity. This is often the case with antimalarial compounds identified from plants.[32] Although their activity and SI values cannot be

[28] R. Pink, A. Hudson, M. Mouriès and M. Bendig, *Nature Rev. Drug Discov.*, 2005, **4**, 727.
[29] A.K. Picman, *Biochem. Syst. Ecol.*, 1986, **14**, 255.
[30] G. Francois, C.M. Passreiter, H.J. Woerdenbag and M. Van Looveren, *Planta Med.*, 1996, 62, 126.
[31] J.D. Phillipson and C.W. Wright, *J. Ethnopharmacol.*, 1991, **32**, 155.
[32] S. Schwikkard and F.R. van Heerden, *Nat. Prod. Rep.*, 2002, **19**, 675.

compared to that of chloroquine, **(62)** and **(63)** can be considered as hits that could be subjected to more detailed analysis, involving accurate IC_{50} determinations against whole parasites, measurement of general cytotoxicity and *in vivo* assessment in animal models.

These compounds could also be used as models to generate lead compounds with enhanced antiplasmodial activity and reduced cytoxicity. One such medicinal chemistry approach would be to investigate how the addition of known biologically active moieties to the C(11)-C(13) exocyclic double bond (the cytotoxic component) would affect the antiplasmodial activity. Further structure-activity relationship studies would also help draw a conclusion as to whether the antiplasmodial activity observed for sesquiterpene lactones such as **(59)**, **(60)**, **(61)**, **(62)** and **(63)** is indeed biological activity or just the result of general cytotoxicity.

CHAPTER 5

Experimental

5.1 Plant Material

Vernonia staehelinoides plant material was collected in April 1999 from Perseverence Farm in the Magaliesburg region of Gauteng. The collection was undertaken by Errol Nienaber, a plant collector contracted by the CSIR. Voucher specimen (EN00323) containing flowers and aerial parts of the plant was identified and retained at the National Herbarium (Pretoria).

The initial sample of *Oncospihon piluliferum* plant material was also collected by Errol Nienaber in October 1999 from Dwarsvlei Farm near Middelburg in the Eastern Cape. The recollection of *O. piluliferum* plant material from the original collection site was conducted by Jean Meyer of the South African National Botanical Institute (SANBI) in November 2002. Voucher specimen (EN00579) containing flowers and aerial parts of the plant was identified and retained at the National Herbarium.

5.2. Extract Preparation

Plant material was dried in an oven at 30 – 60 °C. Dried material was then ground to a coarse powder using a hammer mill. Powdered plant material was sequentially extracted with cold dichloromethane, dichloromethane/methanol (1:1) and purified water.

For each extraction procedure the plant material was steeped in sufficient solvent for 4 - 5 h at room temperature, with occasional stirring. The solvent was subsequently drained and the plant material was air-dried before extraction with the next solvent. Organic extracts were concentrated by rotary vacuum evaporation below 45 ºC and then further dried in vacuo at ambient temperature for 24 h. The aqueous extract of *V. staehelinoides* was concentrated by freeze-drying. All extracts were stored at -20 ºC and the yields of the extracts were recorded in terms of starting plant material.

5.3 *In Vitro* Antiplasmodial Activity

The *in vitro* antiplasmodial assays were conducted by the Pharmacology Department at the University of Cape Town. The chloroquine sensitive (D10) and chloroquine-resistant (K1) strains of *Plasmodium falciparum* were continuously cultured according to the methods described by Trager and Jensen[1]. The parasites were maintained at a 5% haematocrit with RPMI 1640 (Biowhittaker) medium supplemented with Albumax II (lipid rich bovine serum albumin) (GibcoBRL) (25 g/L), hypoxanthine (44 mg/L), HEPES (N-[2-Hydroxyethyl]-piperazine-N'-[2-Ethansulphonic acid]) (Sigma-Aldrich) (6 g/L), sodium hydrogen carbonate (Sigma-Aldrich) (2.1 g/L) and gentamycin (Sigma-Aldrich) (50 mg/L). The cultures were incubated at 37 ºC in an atmosphere of 93% N_2, 4% CO_2 and 3% O_2.

Parasite viability was measured using parasite lactate dehydrogenase (pLDH) activity.[2] This enzymatic assay differentiates between pLDH and host LDH activity by using 3-acetylpyridine adenine dinucleotide (APAD). The pLDH uses APAD as a coenzyme in the conversion of pyruvate to lactate and reduces it to APADH. The formation of APADH can be measured by the subsequent reduction of a yellow nitroblue tetrazolium (NBT) salt to a blue formazan product, the absorbance of which can be monitored on a microplate reader.

The *in vitro* assays were performed as described by Clarkson *et al*.[3] Microtitration techniques were used to measure the activity of a large number of samples over a wide range of concentrations. The microtitre plates (Greiner) consisted of 96 wells arranged in a matrix of eight rows (A to H) and 12 coloumns (1 to 12). Rows A to H in column 1 contained unparasitised RBC (blank), column 2 served as a parasite control (parasitised RBC in the trophozoite stage, adjusted to a 2% parasitaemia and 2% haemotocrit, and no drug) and columns 3 to 12 contained parasites and varying concentrations of the drug. A solution of chloroquine diphosphate (Sigma) in Millipore water served as a positive control in all experiments. The initial concentration of chloroquine was 1000 ng/ml. All tests were performed in duplicate

---

[1] W. Trager and J.B. Jensen, *Science*, 1976, **193**, 673.
[2] M.T. Makler J.M. Ries, J.A. Williams, J.E. Bancroft, R.C. Piper, B.L. Gibbins and D.J. Hinrichs, *Am. J. Trop. Med. Hyg.*, 1993, **48**, 739.
[3] C. Clarkson, W.E. Campbell and P. Smith, *Planta Med*., 2003, **8**, 720.

and no attempt was made to determine 50% inhibitory concentration (IC_{50}) values in excess of 100 µg/ml.

Crude plant extracts received from the CSIR were stored at -20 ºC prior to testing and stock solutions were made up a day before the experiment and stored at -20 ºC. Crude extracts were first dissolved in methanol or DMSO, depending on their solubility, sonicated for 10 minutes and then diluted in Millipore water to give a 2 mg/ml solution. This was further diluted in RPMI 1640 medium to give 200 µg/ml stock solutions. The highest concentration of solvent that the parasites were exposed to was 0.5%, which was shown to have no measurable effect on parasite viability.[4] Extracts were tested in nine serial twofold dilutions (final concentration range: 100 -0.2 µg/ml) in the 96-well microtitre plates. Fractions and pure compounds were dissolved in 10% methanol and were further diluted in complete medium on the day of the experiment. The starting concentration for a full dose-response was 100 µg/ml, which was diluted 2-fold in complete medium to give ten concentrations, with the lowest concentration being 0.195 µg/ml. The microtitre test plates were placed in a desiccator cabinet, flushed with a gas mixture consisting of 93% N_2, 4% CO_2 and 3% O_2, sealed and incubated at 37 ºC for 48 h.

The pLDH activity was measured using a 1.96 mM NBT (Sigma) and 0.24 mM phenazine ethosulphate (PES) (Sigma) solution in Millipore water, and the Malstat reagent containing triton (1ml/L), APAD (0.33 g/L) and TRIS buffer (3.3 g/L) in Millipore water. Malstat reagent (100 µl) and NBT/PES (25µl) solution were added to all the wells of another 96-well microtitre plate. The test plate was removed from the desiccator after the 48 h incubation period and the parasites were re-suspended in each well and then transferred (15 µl) with a multi-channel dispenser to the corresponding wells in the plate containing the Malstat and NBT/PES solution. This plate was placed in a 7520 Microplate Reader (Cambridge Technology), blanked on the wells in column 1 and the absorbance of the blue formazan salt was measured at λ 620 nm. Since the amount of formazan produced is proportional to parasite viability, the percentage parasite survival in each well was calculated using the formula:

[4] C. Clarkson V.J. Maharaj, N.R. Crouch, O.M. Grace, P. Pillay, M.G. Matsabisa, N. Bhagwandhin, P.J. Smith, P.I. Folb., *J. Ethnopharmacol.*, 2004, **92**, 177.

$$\% \text{ Parasite Viability} = \frac{A_{\lambda 620} \text{ test well (PRBC + drug)}}{A_{\lambda 620} \text{ parasite control well (PRBC + no drug)}} \times 100$$

Dose response curves were constructed using non-linear dose-response curve fitting analyses with GraphPad Prism v.4.00 software. The concentration of the drug that inhibits 50% of the parasites (IC_{50} values) was established from the dose response curves using GraphPad Prism.

5.4 Bioassay-guided Fractionation, Targeted Purification and Selected Derivatisations of Active Compounds

The fractionation process involved column and thin layer chromatographic techniques. Different sized columns, ranging from 1.5 – 6 cm in diameter, were used depending on the amount of sample and the purification stage. Silica gel column chromatography was conducted using Silica gel 60 (0.063 - 0.2 mm) and flash silica gel chromatography was carried out using 35 - 75 micron flash silica gel (Merck Art).

Thin layer chromatography was carried out on 0.20 mm pre-coated (SIL-25 UV_{254}) glass-backed plates. The plates were first viewed under UV, developed using a vanillin : concentrated H_2SO_4 (1 g : 100 ml) spray reagent and then heated.

5.4.1 Bioassay-guided Fractionation of P01009A

(i) Fractionation of P01009A

The crude dichloromethane extract (1.5 g) was fractionated on a silica gel column (87 x 2.5 cm) using a gradient eluent of increasing polarity (ethyl acetate-hexane 1:9→ ethyl acetate-hexane 3:2). The column was stripped with ethyl acetate. A total of 6 pooled fractions (1A - 1F) were generated. These fractions were bio-assayed against *P. falciparum* D10.

(ii) Further Purification of Fraction 1D

Fraction 1D (70 mg) was chromatographed on a silica gel column (50 x 1.5 cm). Silica gel was eluted with dichloromethane. Polarity was gradually increased by addition of methanol in 1% increments to methanol-dichloromethane (1:9). Column was stripped with methanol. Eight fractions were generated (2A - 2F) and bioassay

results revealed that two of these showed improved antiplasmodial activity, *ie*. 2C (2.6 mg) and 2D (1.3 mg).

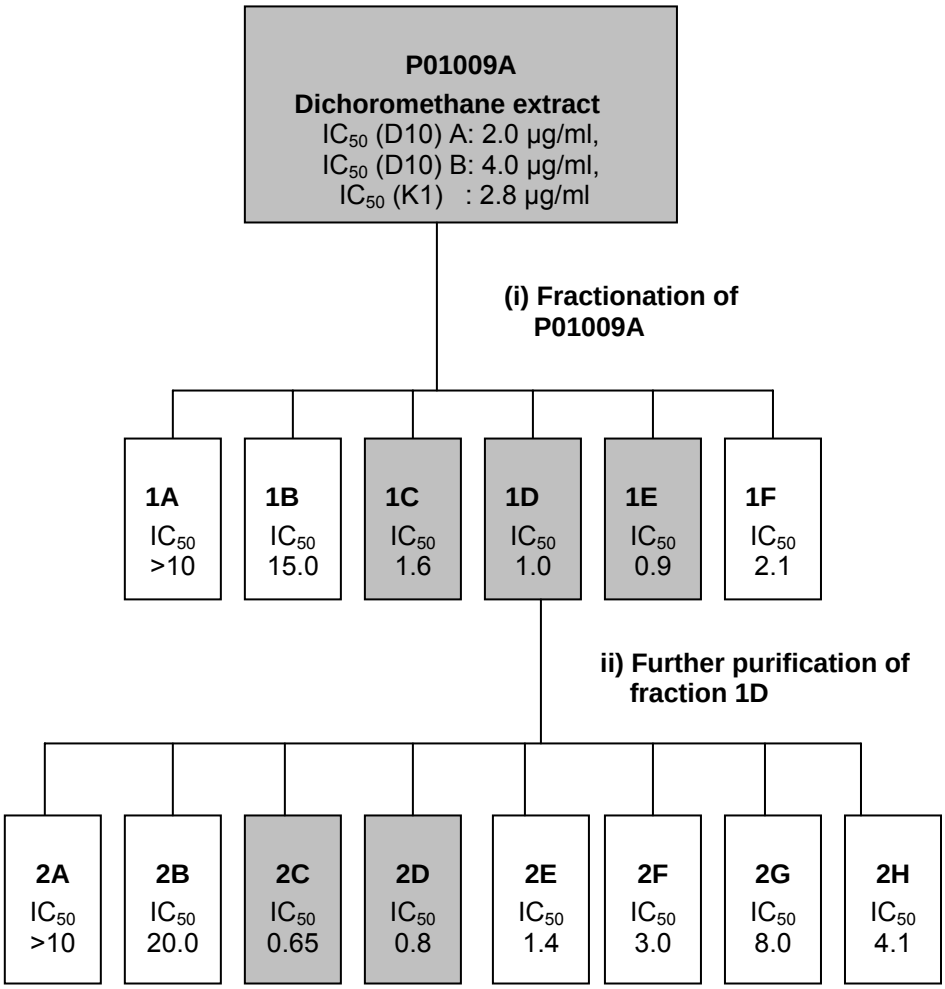

Figure 5.1 Fractionation of dichloromethane extract of *V. staehelinoides.* IC_{50} values are in µg/ml

5.4.2 Bioassay-guided Fractionation of P01009B

(i) Fractionation of P01009B

The crude 1:1 dichloromethane/methanol extract (2 g) was subjected to silica gel column chromatography (92 x 2.5 cm) using a gradient eluent of increasing polarity (ethyl acetate-hexane 1:9→ ethyl acetate-hexane 3:2). Column was stripped with ethyl acetate. A total of 7 pooled fractions (3A - 3G) were generated. These fractions were bio-assayed against *P. falciparum* D10.

(ii) Purification of Fraction 3E

Fraction 3E (107 mg) was subjected to flash silica gel chromatography. Flash silica gel (15 g) was eluted with ethyl acetate-hexane (1:4). Ten pooled fractions were generated (4A - 4J). These fractions were bio-assayed against *P. falciparum* D10**.**

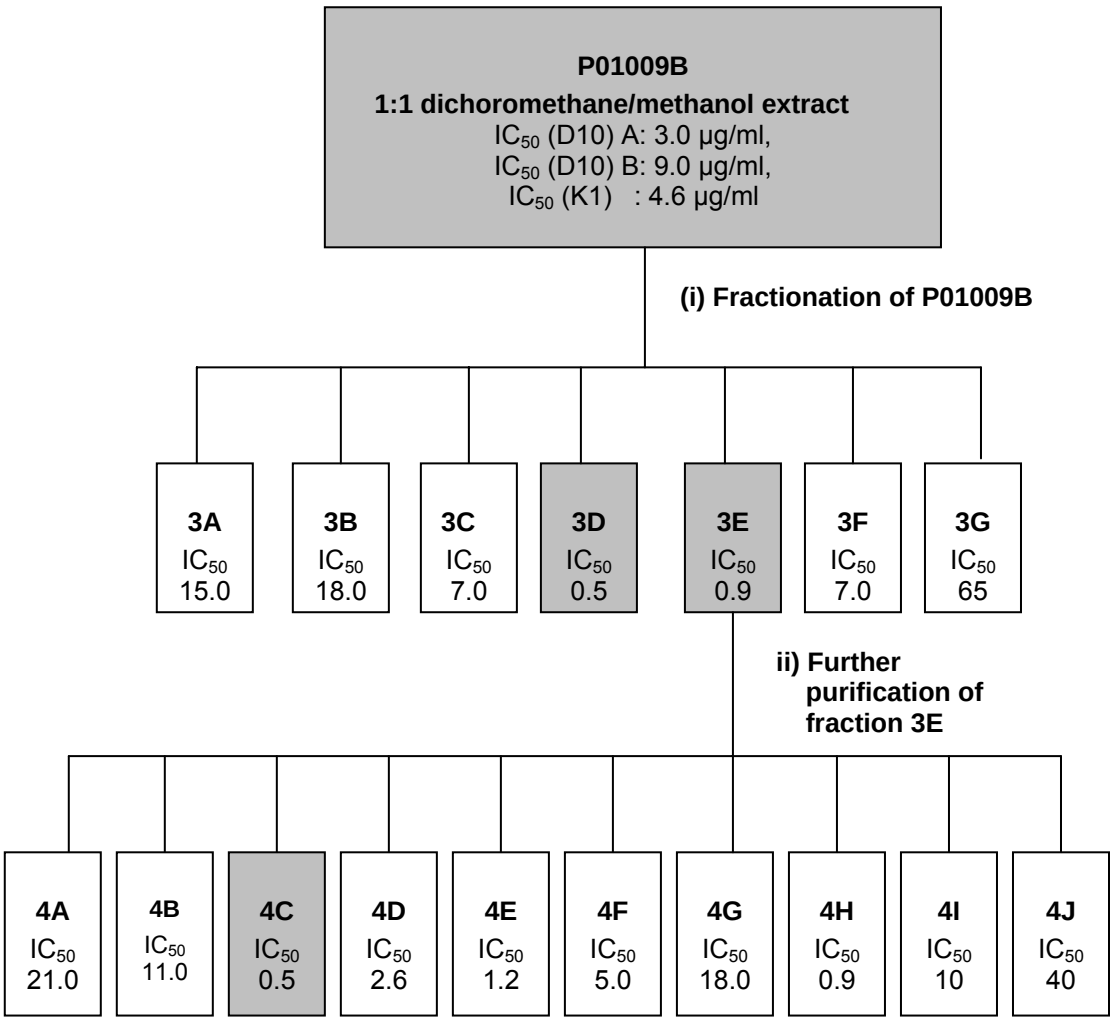

Figure 5.2 Fractionation of the dichloromethane/methanol (1:1) extract of *V. staehelinoides.* IC_{50} values are in µg/ml

5.4.3 Targeted Purification of Active Compounds from P01009A

(i) Liquid-liquid Partitioning of P01009A

Crude extract (2 g) was dissolved in methanol-water (9:1) (200 ml), and extracted with hexane (3 x 100 ml) (Figure 5.3). The combined hexane layers were evaporated under reduced pressure to yield 5A, the hexane-soluble fraction (0.4 g). The methanol from the methanol/water layer was evaporated off under reduced pressure. An additional 30 ml of water was added to the remaining water layer,

which was subsequently extracted with dichloromethane (3 x 100 ml). The combined dichloromethane layers were evaporated under reduced pressure to yield 5B, the dichloromethane-soluble fraction (1.4 g). The water layer was freeze-dried to yield 5C, the aqueous fraction (0.1 g).

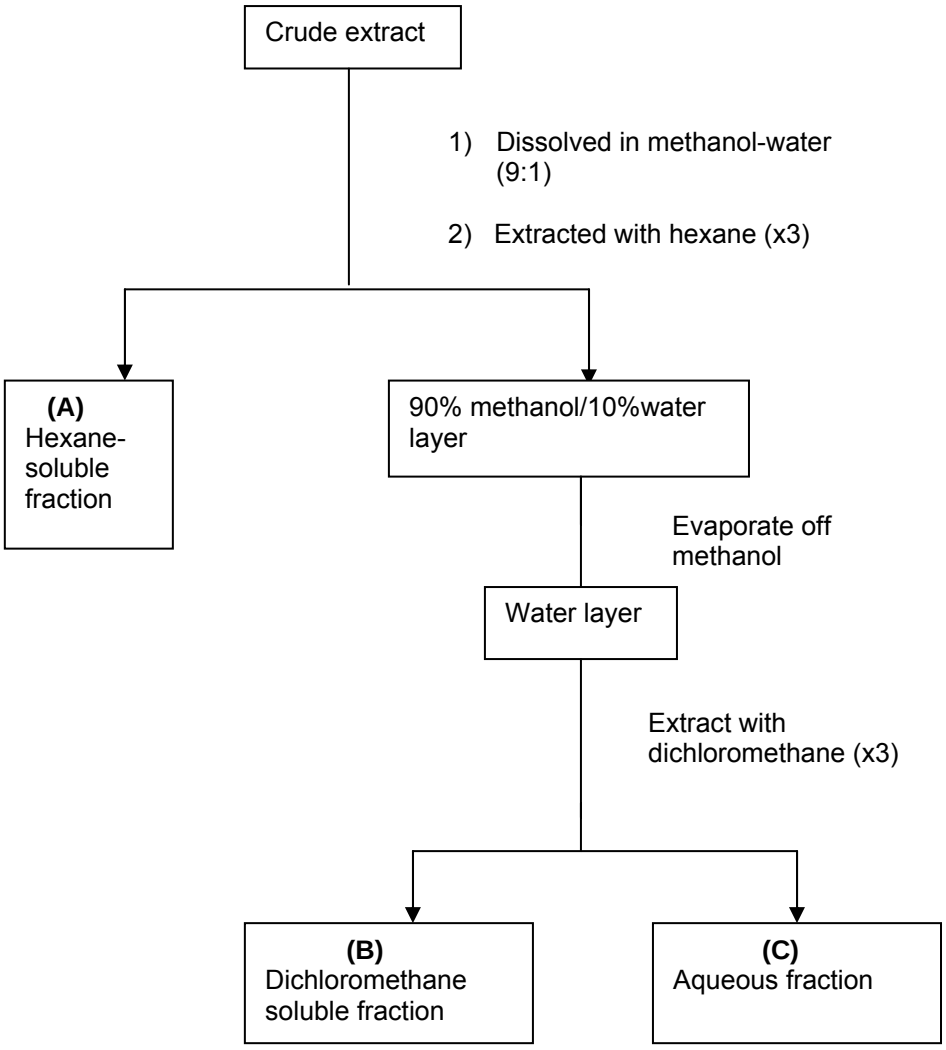

Figure 5.3 Liquid/liquid partitioning method

(ii) Flash Silica Gel Chromatography of the Dichloromethane-soluble Fraction (A)

The dichloromethane-soluble fraction from liquid/liquid partitioning of P01009A was subjected to flash silica gel chromatography using ethyl acetate-hexane-dichloromethane (1:5.75:5.75) to yield 4 pooled fractions (6A - 6D). Target compounds were concentrated in fractions 6A and 6C.

(iii) Purification of Compound (50)

Target compound **(50)** was concentrated in fraction 6A; easily discernable by TLC analysis (dark orange colour when sprayed with vanillin). Fraction 6A was purified by flash silica gel chromatography with acetone-hexane-dichloromethane (7:46.5:46.5). All fractions containing **(50)** were pooled and further purified by flash silica gel chromatography with acetone-hexane-dichloromethane (6:47:47), to yield semi-purified **(50)**. Further purification by flash silica gel chromatography using acetone-hexane-dichloromethane (3:48.5:48.5) yielded compound **(50)** as a colourless gum (7.7 mg); R_f 0.29 (acetone:hexane:dichloromethane 1:4.5:4.5); $[\alpha]_D$ –77.4 (*c* 0.31, $CHCl_3$)

^1H and ^{13}C NMR data : Listed in Table 3.3 (Chapter 3)

EI-MS : *m/z* 316 $[M– C_3H_5COOH]^+$. Exact mass: Calculated for $C_{17}H_{16}O_6$, 316.0947; Found, 316.0868

(iv) Purification of Compound (51)

Target compound **(51)** was concentrated in fraction 6C; easily discernable by TLC analysis (dark brown colour when sprayed with vanillin). Flash silica gel chromatography of fraction 5C with acetone-hexane-dichloromethane(1:4.5:4.5) yielded **(51)** in a semi-purified state. Further purification by flash silica gel chromatography, using acetone-hexane-dichloromethane (7:46.5:46.5), yielded a colourless gum **(51)** (11.2 mg); R_f 0.23 (acetone:hexane:dichloromethane 1:4.5:4.5); $[\alpha]_D$ -209.8 (*c* 0.51, $CHCl_3$)

^1H and ^{13}C NMR data : Listed in Table 3.4 (Chapter 3)

EI-MS : *m/z* 316 $[M– C_7H_{10}O_4]^+$. Exact mass: Calculated for $C_{17}H_{16}O_6$, 316.0947; Found, 316.0885

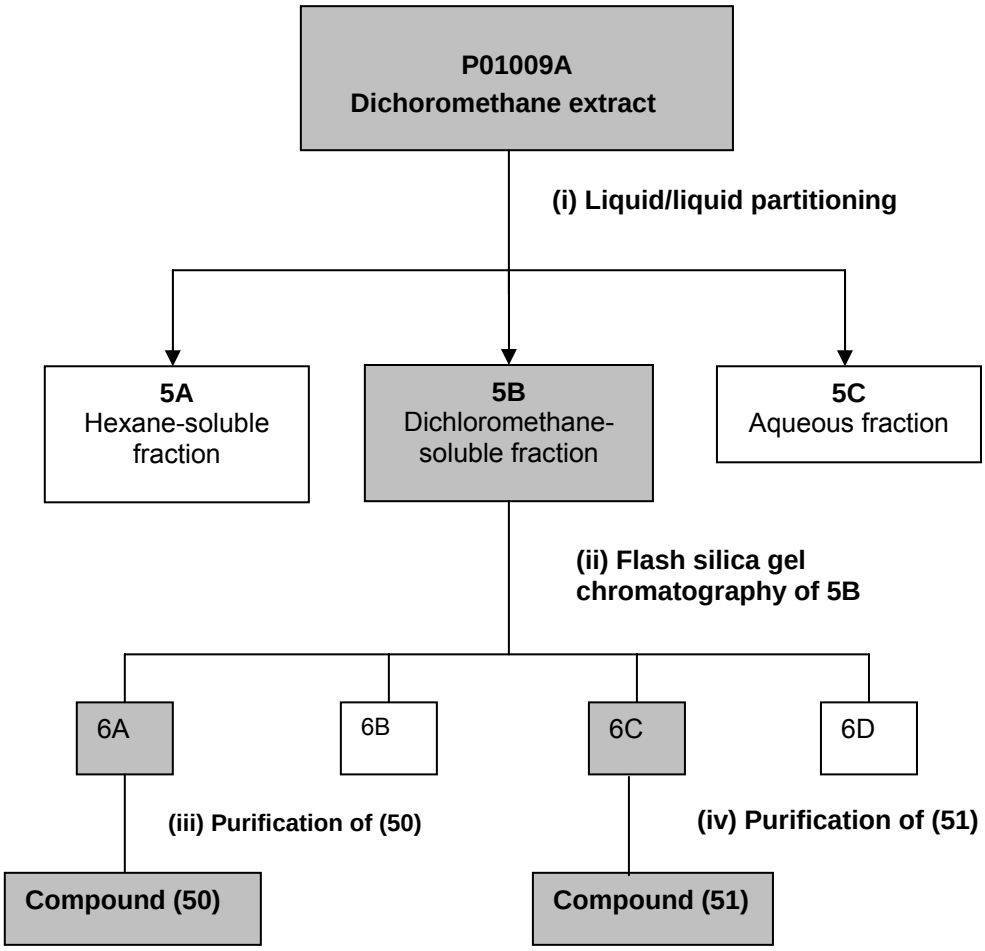

Figure 5.4 Targeted purification of compounds **(50)** and **(51)** from P01009A

5.4.4 Bioassay-guided Fractionation of P01609A

(i) Primary Fractionation of P01609A

The crude dichloromethane extract (15 g) was subjected to silica gel column chromatography using a gradient eluent of increasing polarity (ethyl acetate-hexane (1:20)→ ethyl acetate-hexane (3:2)→100% ethyl acetate) to yield a total of 32 pooled fractions. These fractions were bio-assayed against *P. falciparum* D10. Solubility problems were encountered with the first twelve fractions and the bio-assay results of these were subsequently disregarded. The remaining 20 fractions were assigned as 7A - 7T.

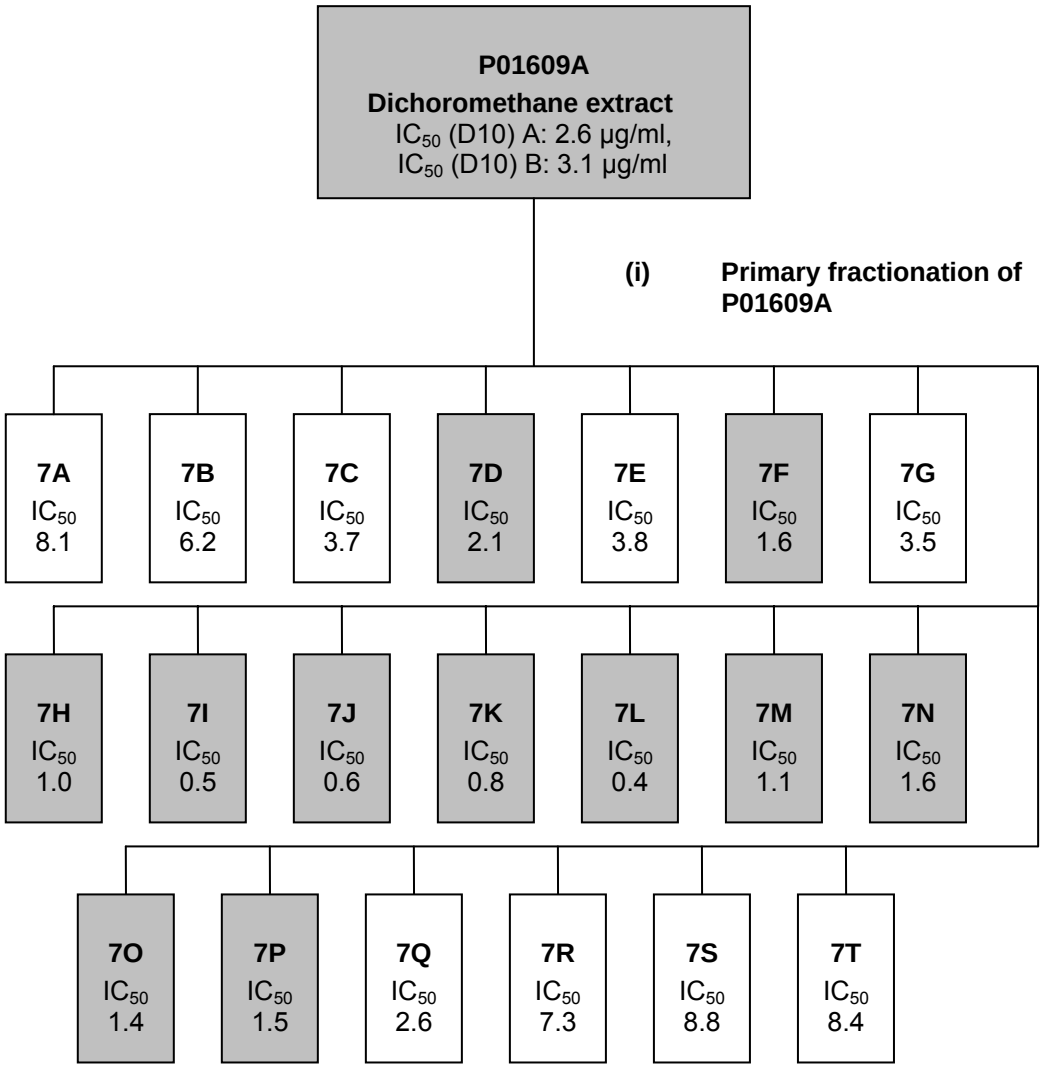

Figure 5.5 Summary of IC_{50} values of the primary fractions generated from silica gel column chromatography of P01609A. IC_{50} values are in µg/ml

(ii) Further Fractionation of 7I

Fraction 7I (840 mg) was chromatographed on a silica gel column (2.5 x 40 cm). The silica gel was eluted with acetone-hexane-dichloromethane (1:2:2). A total of 8 pooled fractions (8A - 8H) were generated and these were bio-assayed against *P. falciparum* D10 (Figure 5.6).

(iii) Further Fractionation of 8D

Fraction 8D (200 mg) was subjected to flash silica gel chromatography, using 13 g of flash silica gel and acetone-dichloromethane (1:99). Two major fractions were generated (9A + 9B), with 9B being a semi-pure compound which was easily discernible on TLC by its dark pink colour when sprayed with vanillin.

(iv) Further Purification of 9B

Approximately 45 mg of 9B was subjected to successive flash silica gel purifications; first using ethyl acetate-hexane-dichloromethane (1:4.5:4.5) and then decreasing the polarity of the eluent slightly to ethyl acetate-hexane-dichloromethane (1:11.5:11.5). This yielded 16 mg of compound **(59)**, which decomposed during NMR analysis.

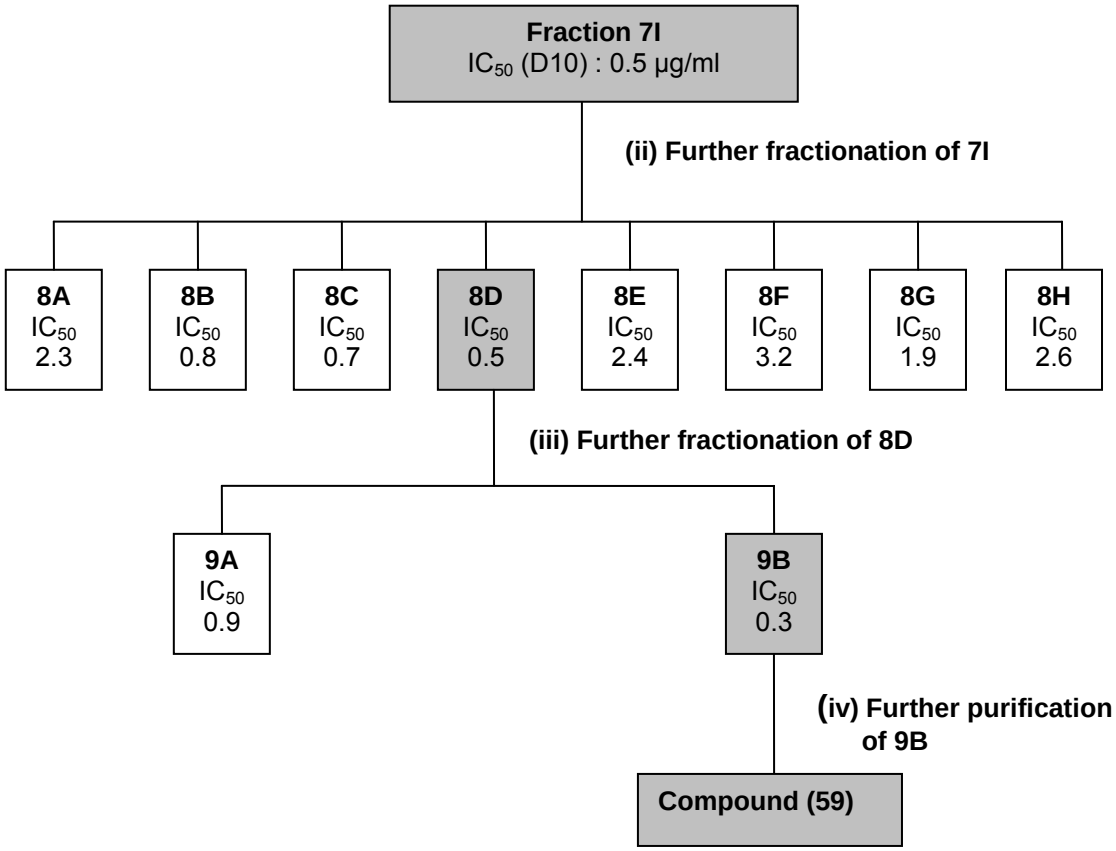

Figure 5.6 Further purification of fraction 7I. IC_{50} values are in µg/ml

(v) Further Fractionation of 7M

Fraction 7M (450 mg) was chromatographed on a silica gel column (Figure 5.7). Silica gel was eluted with acetone-hexane-dichloromethane (1:1.5:1.5). Four pooled fractions were generated (10A - 10D). Major fraction 10C showed crystalline properties.

(vi) Crystallisation of 10C

Fraction 10C (132 mg) was first decolourised with charcoal and then crystallised from ethyl acetate/hexane. The crystals were filtered and submitted for assaying.

(vii) Further Purification of 11A

Successive flash silica gel purifications of 11A (80 mg), first using methanol-dichloromethane (1:49) and then methanol-dichloromethane (1:99), yielded fraction 12A (18 mg) and colourless crystals of **(60)** (12 mg); mp. 278 – 280 ºC {Lit.[5] : 280 ºC}; R_f 0.27 (methanol-dichloromethane 1:24); $[\alpha]_D$ +2.0 (*c* 0.49, MeOH)

^1H and ^{13}C NMR data : Listed in Table 4.6 (Chapter 4)

EI-MS : *m/z* 264 $[M]^+$. Exact mass: Calculated for $C_{15}H_{20}O_4$, 264.1362;
Found, 264.1347

Crystallographic data : *Appendix (A)*

(viii) Further Purification of Fraction 7O

Successive purifications of 7O (335 mg) by silica gel column chromatography (Figure 5.8), first using acetone-hexane-dichloromethane (6:7:7), and then ethyl acetate-hexane (2:3) yielded colourless crystals of **(63)** (20mg); mp. 159 – 161 ºC {Lit.[6]: 158-159 ºC}; R_f 0.35 (acetone:hexane:dichloromethane 3:3.5:3.5); $[\alpha]_D$ +24.0 (*c* 0.50, MeOH) {Lit.[6]: $[\alpha]_D^{23}$ +34.8 (*c* 1.84, MeOH)}

^1H and ^{13}C NMR data : Listed in Table 4.10 (Chapter 4)

EI-MS : *m/z* 246 $[M - H_2O]^+$. Exact mass: Calculated for $C_{15}H_{18}O_3$, 246.1256;
Found, 246.1219

Crystallographic data: *Appendix (D)*

[5] M.L Cardona, I. Fernández, B. Garcia and J. R. Pedro, *J. Nat. Prod.*, 1990, **53**, 1042
[6] A.I Yunusov, N.D. Abdullaev, S.Z. Kasymov and G.P. Sidyakin., *Khim. Prir. Soedin.*, 1976, **2**, 263.

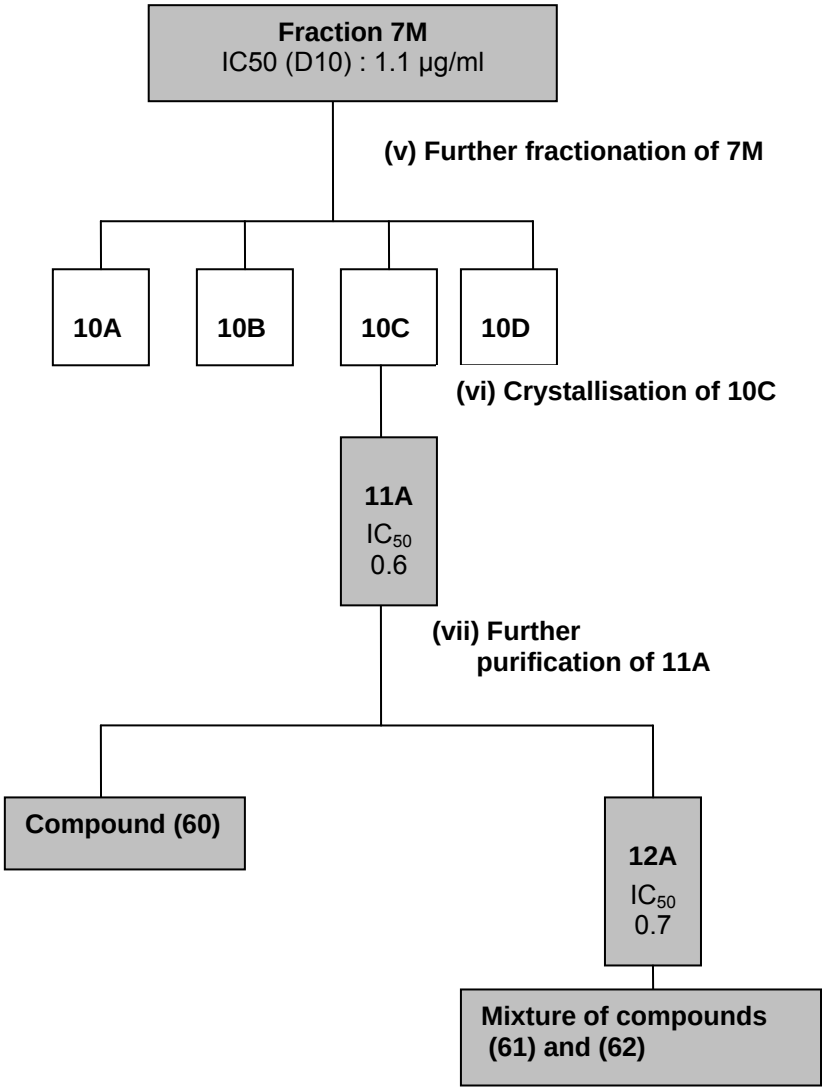

Figure 5.7 Further purification of fraction 7M. IC_{50} values are in µg/ml

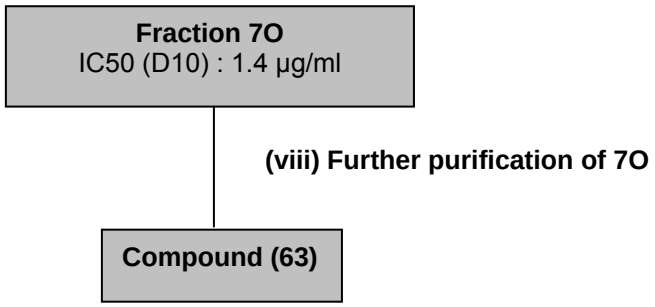

Figure 5.8 Further purification of fraction 7O. IC_{50} values are in µg/ml

5.4.5 Targeted Purification and Selected Derivatisations of Active Compounds from P01069A

(ix) Liquid-liquid Partitioning of P01609A

57 g of the crude extract was subjected to liquid/liquid partitioning as illustrated in Figure 5.3. The combined chloromethane layers were evaporated under reduced pressure to yield 13B, the dichloromethane-soluble fraction (25 g).

(x) Fractionation of 13B

24 g of 13B was chromatographed on a silica gel column (7 x 57 cm). The silica gel was eluted with acetone-hexane-dichloromethane (1:2:2). A total of 8 pooled fractions were generated (14A – 14H).

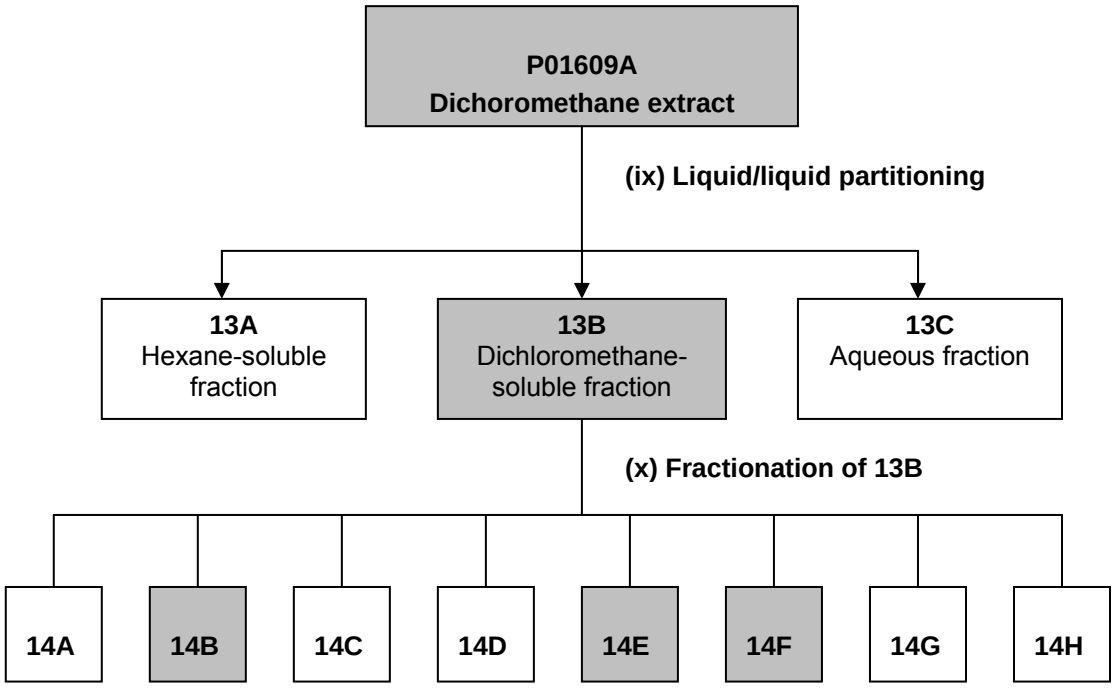

Figure 5.9 Fractionation of PO1609A.

(xi) Targeted Isolation of Compound (59)

8.7 g of 14B was subjected to a series of successive flash silica gel purifications, first using ethyl acetate-hexane-dichloromethane (1:24.5:24.5), then ethyl acetate-hexane-dichloromethane (2:9:9) followed by ethyl acetate-hexane-dichloromethane (4:23:23). Compound **(59)** was concentrated in sub-fraction 14B5 (98 mg) (Figure 5.10). 25 mg of 14B5 was purified on a preparative silica

plate to yield the colourless gum **(59)** (18 mg); R_f 0.26 (ethyl acteate-hexane 2:3); $[\alpha]_D$ and MS data not obtained due to decomposition of compound.

^{1}H NMR data : listed in Table 4.4 (Chapter 4)

(xii) Acetylation of Compound (59)

Acetic anhydride (0.5 ml, 5 mmol) was added to 14B5 (30 mg, 0.11 mmol) in 3 ml of anhydrous pyridine. The mixture was stirred at room temperature for 15 h. Chloroform (50 ml) was added to the reaction and the organic layer was washed with saturated citric acid (4 x 100 ml), saturated sodium hydrogen carbonate solution (100 ml) and water (100 ml). The chloroform layer was dried over calcium chloride and evaporated to dryness under reduced pressure. Flash silica gel chromatography of the crude product using acetone-hexane-dichloromethane (1:9.5:9.5) yielded the yellow gum **(64)** (16mg**,** 48%); R_f 0.41 (acetone-hexane-dichloromethane 1:4.5:4.5); $[\alpha]_D$ +41.2 (*c* 0.34, $CHCl_3$)

^{1}H NMR and ^{13}C NMR data : Listed in Table 4.5 (Chapter 4)

EI-MS : *m/z* 264 $[M - (CH_2=C=O)]^+$ Exact mass: Calculated for $C_{15}H_{20}O_4$ 264.1362; Found, 264.1313

(xiii) Benzoylation of Compound (59)

28mg (0.106 mmol) of 14B5 was dissolved in 5 ml of chloroform. *p*-nitrobenzoylchloride (20 mg, 0.107 mmol) and DMAP (20.9 mg, 0.171 mmol) was added and the reaction mixture was stirred at room temperature. The reaction was monitored on TLC and after 24 h only a minor trace of product was observed and the starting material was still concentrated. The reaction mixture was heated (60 ºC) under reflux conditions but no improvement in the product yield was observed. Excess *p*-nitrobenzoylchloride and DMAP were added and a marked improvement in the product yield was subsequently observed. The reaction was quenched once a large quantity of salt began to precipitate out of solution and no more improvement in product yield was observed. Chloroform (50 ml) was added to the reaction mixture and the salt was filtered off. The chloroform solution was washed with 0.1 M HCl (100 ml) and water (100 ml), dried over calcium chloride. The crude

product (48 mg) was subjected to flash silica gel chromatography using acetone-hexane-dichloromethane (1:19.5:19.5) to yield the white crystals **(65)** (6 mg, 14%).

^{1}H NMR data: Listed in Table 4.4 (Chapter 4)

Various solvents, combinations of solvents and other crystallisation techniques were attempted to produce crystals of **(65)** suitable for X-ray crystallography. Compound eventually showed evidence of decomposition and turned yellowish so no additional physical data was obtained on **(65)**.

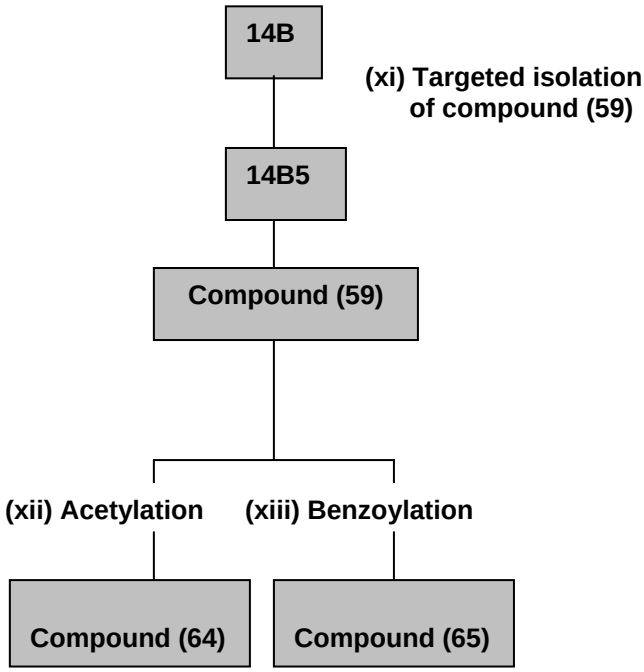

Figure 5.10 Isolation and derivatisation of **(59)**.

(xiv) Targeted isolation of compounds (60), (61) and (62)

520 mg of fraction 14E was subjected to flash silica gel chromatography using acetone:hexane:dichloromethane (1:2:2), to yield 4 sub-fractions (14E1 – 14E4). Sub-fraction 14E2 crystallised on standing to yield coarse white crystals (80 mg), which were subjected to flash silica gel chromatography using methanol-dichloromethane (1:49) to yield 42 mg of compound **(60)** (recrystallised from ethyl acetate) and white crystals of **(61)** (6 mg); mp. 234 - 236 ºC; R_f 0.21 (methanol-dichloromethane 1:24); $[\alpha]_D$ –38.5 (*c* 0.39, MeOH).

^{1}H NMR and ^{13}C NMR data : Listed in Table 4.7 (Chapter 4)

EI-MS : *m*/z 264 $[M]^{+}$ Exact mass: Calculated for $C_{15}H_{20}O_4$, 264.1362; Found, 264.1261

Sub-fractions 14E3 and 14 E4 were combined and crystallised from ethyl acetate/hexane to yield white needle-like crystals of compound **(62)** (104 mg); mp. 158 – 160 ºC {Lit. [7] :160 - 161 ºC}; R_f 0.26 (methanol-dichloromethane 1:24); $[\alpha]_D$ –54.0 (*c* 0.50, MeOH) {Lit. : $[\alpha]_D^{25}$ –32.0 (*c* 1.0, MeOH)}

^{1}H NMR and ^{13}C NMR data : Listed in Table 4.7 (Chapter 4)

EI-MS : *m/z* 264 $[M]^{+}$ Exact mass: Calculated for $C_{15}H_{20}O_4$, 264.1362; Found, 264.1293

40 mg of **(62)** was recrystallized from acetone in a hexane-saturated atmosphere to yield dense cubic crystals, suitable for X-ray analysis.

Crystallographic data: *Appendix (B)*

(xv) Acetylation of Compound (62)

Acetic anhydride (0.1 ml, 0.96 mmol) was added to compound **(62)** (30 mg, 0.12 mmol) in 0.5 ml of anhydrous pyridine. The mixture was stirred at room temperature for 24 h. Chloroform (50 ml) was added to the reaction and the organic layer was washed with saturated citric acid (3 x 100 ml), saturated sodium hydrogen carbonate solution (100 ml) and water (100 ml). The chloroform layer was dried over calcium chloride and evaporated to dryness under reduced pressure. The crude product was subjected to flash silica gel chromatography using acetone-hexane-dichloromethane (1:4.5:4.5) to yield white needle-like crystals of **(66)** (19 mg, 50%) mp. 203 – 205 ºC; R_f 0.33 (methanol:dichloromethane 1:24). No additional physical data was obtained due to

[7] A.I. Yunusov, G.P. Sidyakin and A.M. Nigmatullaev, *Khim. Prir. Soedin.*, 1979, **1**, 101.

poor recovery of product from attempts at recrystallisation to produce better quality crystals for X-ray analysis.

^{1}H NMR data : Listed in Table 4.9 (Chapter 4)

Crystallographic data : *Appendix (C)*

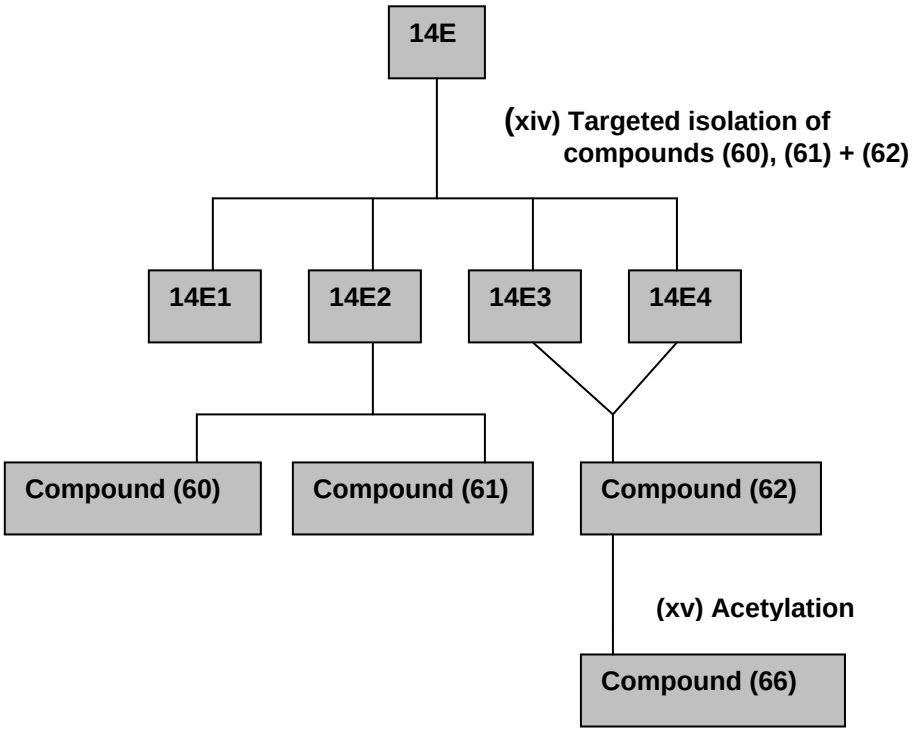

Figure 5.11 Isolation and derivatisation of **(60)**,**(61)** and **(62)**.

(xvi) Targeted Isolation of Compound (63)

730 mg of 14F was subjected to flash silica gel chromatography using acetone-hexane-dichloromethane (6:7:7). 170 mg of **(63)** was subsequently recovered (Figure 5.12). Crystals were formed at the bottom of test tubes during chromatography and these were recovered for X-ray analysis.

(xvii) (*R*)-Mosher Esterification

Oxalyl chloride (0.065 ml, 0.75 mmol) was added to a solution of *R*(+)-*α*-methoxy-*α*-trifluoromethylphenyl acetic acid (98.5 : 1.5) (58.9 mg, 0.25 mmol) and DMF (19 µl, 0.25 mmol) in anhydrous hexane (6 ml). The mixture was stirred at room temperature for 1 h. The solution was then filtered through a small cotton wool

plug to filter off the white DMFCl precipitate formed. The filtrate was evaporated under reduced pressure to yield (*S*)-MTPA-Cl (59.0 mg, 0.23 mmol).

A solution of compound **(63)** (33.2 mg, 0.13 mmol) in dichloromethane (4 ml), triethylamine (0.3 ml, 0.25 mmol) and a spatula tip of DMAP was added to a solution of the acid chloride in dichloromethane. The reaction was quenched after 48 h with water and the organic layer was washed with 0.1 M HCl and saturated $NaHCO_3$ solution. The organic solution was dried over Na_2SO_4, filtered and evaporated. The crude product (57 mg) was subjected to flash silica gel chromatography using acetone-hexane-dichloromethane (1:4.5:4.5). 20.1 mg of the diester **(67)**; R_f 0.85 (acetone-hexane-dichloromethane 3:8.5:8.5), 16.1 mg of one monoester **(68)**; R_f 0.55 (acetone-hexane-dichloromethane 3:8.5:8.5), and 5.1 mg of the other monoester **(69)**; R_f 0.31 (acetone-hexane-dichloromethane 3:8.5:8.5) were recovered. Relative $\Delta\delta$ values were determined from ^{1}H and COSY NMR data. Products showed signs of deterioration and thus no additional physical data were obtained on these.

(xviii) (*S*)-Mosher Esterification

Oxalyl chloride (0.065 ml, 0.75mmol) was added to a solution of of *S*(-)-*α*-methoxy-*α*-trifluoromethylphenyl acetic acid (98.5 : 1.5) (58.3 mg, 0.25 mmol) and DMF (19 µl, 0.25 mmol) in anhydrous hexane (6 ml). The mixture was stirred at room temperature for 1 h. The solution was then filtered through a small cotton wool plug to filter off the white DMFCl precipitate formed. The filtrate was evaporated under reduced pressure to yield 52.2 mg (0.20mmol) of (*R*)-MTPA-Cl.

A solution of **(63)** (33.4 mg, 0.13 mmol) in dichloromethane (4 ml), triethylamine (0.3 ml, 0.25 mmol) and a spatula tip of DMAP was added to a solution of the acid chloride in dichloromethane. The reaction was quenched after 48 h with water and the organic layer was washed with 0.1 M HCl and saturated $NaHCO_3$ solution. The organic solution was dried over Na_2SO_4, filtered and evaporated. The crude product (52 mg) was subjected to flash silica gel chromatography using acetone-hexane-dichloromethane (1:4.5:4.5). 9.8 mg of the diester **(70)**; R_f 0.57 (acetone-hexane-dichloromethane 1:4.5:4.5), 22.4 mg of one monoester **(71)**; R_f 0.19 (acetone-hexane-dichloromethane 1:4.5:4.5), and 1.7 mg of the other monoester

(72); R_f 0.10 (acetone-hexane-dichloromethane 1:4.5:4.5), were recovered. Relative $\Delta\delta$ values were determined from ^{1}H and COSY NMR data. Products showed signs of deterioration and thus no additional physical data were obtained on these.

(ixx) $NaBH_4$ Reduction of Compound (63)

15 mg (0.06 mmol) of **(63)** was dissolved in anhydrous methanol (10 ml). The solution was cooled to 0 ºC, and $NaBH_4$ (78 mg, 2 mmol) was added. The mixture was stirred at 0 ºC for 10 min, after which 20% acetic acid (10 ml) was added. The solution was diluted further with water (20 ml) and extracted twice with chloroform (50 ml). The crude product was subjected to flash silica gel chromatography using acetone-hexane-dichloromethane (1:8.5:8.5) which yielded a pale yellow gum, **(73)** (5 mg, 34%); R_f 0.25 (acetone-hexane-dichloromethane 1:4.4:4.5). No additional physical data could be obtained on the compound due to its instability.

^{1}H NMR data : listed in Table 4.12

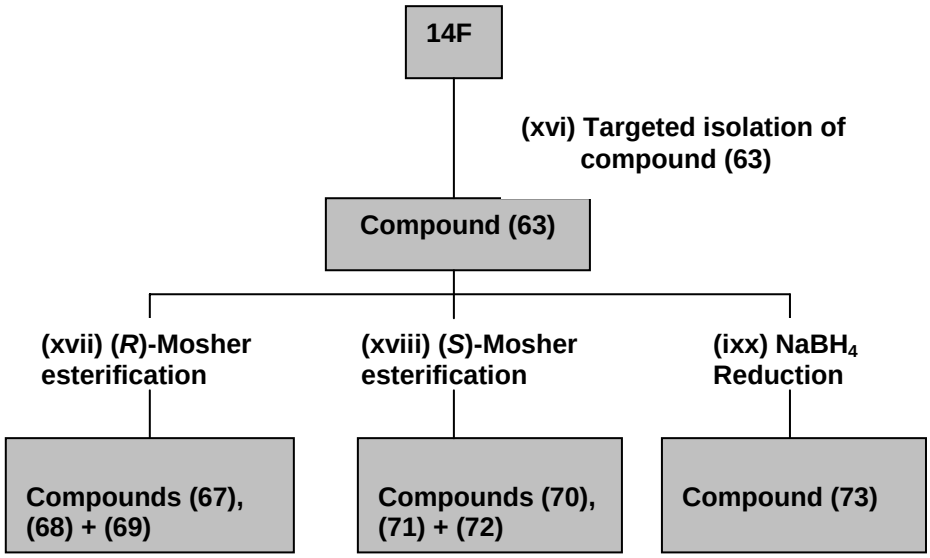

Figure 5.12 Isolation and derivatisation of **(63)**.

5.5 Nuclear Magnetic Resonance (NMR) Spectroscopy

NMR spectroscopy was carried out on a Varian 400 MHz Unity spectrometer by Sue Rhodes and Madelyn Bekker of the Analytical Function at Bio/Chemtek (now Biosciences), CSIR. All the spectra were recorded at room temperature in either deuteriated acetone, deuteriated chloroform, or deuteriated benzene. The chemical shifts were all recorded in ppm relative to TMS.

5.6 Mass Spectrometry

High resolution mass spectra were recorded on a VG 70SEQ HRMS instrument, in the positive EI mode with a resolution of 7500 at 8kV. The mass spectrometry was performed by Dr. T van der Merwe at the University of the Witwatersrand.

5.7 X-ray Crystallography

X-ray crystallography experiments were conducted by Dr Dave Liles at the University of Pretoria on a Bruker (Siemens) P4 4-circle diffractometer fitted with a Bruker SMART 1000 CCD area detector using Mo-K_α X-radiation and a graphite-crystal monochromator. Data reduction was conducted using Bruker SAINT software (2001) and structure solution and refinement was accomplished using Bruker SHELXTL (2001).

5.8 Optical Rotations

Optical rotations were measured in chloroform or methanol at room temperature on a Perkin-Elmer 241 polarimeter at 589 nm (Na D-line) using a 1 dm cell.

5.9 Melting Point Determinations

Melting points were determined using a Reichert hot stage apparatus and are uncorrected.

5.10 *In Vitro* Cytotoxicity Assay

Compounds were tested for *in vitro* cytotoxicity against a Chinese Hamster Ovarian (CHO) cell line using the 3-(4,5-dimethylthiazol-2-yl)-2,5-

diphenyltetrazolium bromide (MTT) assay.[8] This colorimetric assay is based on the ability of viable cells to metabolise a yellow water-soluble tetrazolium salt into a water-insoluble purple formazan product. The amount of formazan produced can be measured spectrophotometrically and is proportional to the metabolic activity and number of cells in the test plate. This assay was conducted by the UCT Pharmacology Department. The CHO cells were cultured in Dulbecos Modified Eagles Medium (DMEM) : Hams F-12 medium (1:1) supplemented with 10% heat inactivated fetal calf serum (FCS) and gentamycin (0.04 µg/ml). The medium reagents were obtained from Highveld Biological, South Africa.

Samples were dissolved in methanol:water (1:9). Stock solutions (2 mg/ml) were prepared and were stored at -20 ºC until use. The highest concentration of methanol to which the cells were exposed had no measurable effect on the cell viability. Emetine was used as the positive control in all cases. The initial concentration of emetine was 100 µg/ml, which was serially diluted in complete medium with 10-fold dilutions to give 6 concentrations, the lowest being 0.001 µg/ml. The same dilution technique was applied to all test samples with an initial concentration of 100 µg/ml to give 5 concentrations, with the lowest concentration being 0.01 µg/ml.

In the initial stage of the experiments, the cells were adjusted to a concentration of 10^5 / ml and 100 µl of this cell suspension were seeded in all wells except in column 1 (blank) in a 96 well culture plate (Costar). The plates were incubated at 37 ºC for 24 h in a humidified 5% CO_2-air atmosphere. After the incubation period, the medium was carefully aspirated out of the wells and 100 µl of the different test substances (drug solutions) were added in quadruplicate to columns 3 through to 9. A further 100 µl of culture medium was then added to all of the wells containing cells and drugs (columns 3 to 9), and 200 µl of medium was dispensed to the wells in column 1 (blank) and column 2 (cells and no drug). The microplate was then incubated at 37 ºC for 48 h.

After the 48 h incubation period, 25 µl of sterile MTT (5 mg/ml in PBS) was added to each well and incubation was continued for 4 h at 37 ºC. The plates were then

[8] T. Mosmann, *Journal of Immunological Methods*,1983, **65**, 55.

centrifuged at 2050 rpm for 10 min and the supernatant was carefully aspirated from the wells, ensuring that the formazan crystals were not disturbed. The formazan crystals were dissolved in DMSO (100 µl) and the plate was gently shaken for 5 min on a microtitre plate shaker. The plate was blanked on the wells in column 1 and the absorbance of the crystals was measured at λ 540 nm on a Microtitre Plate Reader (Cambridge Technologies). The cell viability was calculated in each well using the formula :

$$\% \text{ Cell Viability} = \frac{A_{\lambda 540} \text{ test well (cells + drug)}}{A_{\lambda 540} \text{ cell control well (cells + no drug)}} \times 100$$

The concentration of drug that inhibits 50% of the cells (IC_{50} values) for these samples were obtained from dose-response curves, using a non-linear dose-response curve fitting analyses via GraphPad Prism v.2.01 software.

Appendix (A)

Table A1. Crystal data and structure refinement for Compound **(60)**

Empirical formula	$C_{15}\ H_{20}\ O_4$	
Formula weight	264.31	
Temperature	293(2) K	
Wavelength	0.71073 Å	
Crystal system	Orthorhombic	
Space group	P 2_1 2_1 2_1	
Unit cell dimensions	a = 8.4056(5) Å	a= 90º.
	b = 12.1568(7) Å	b= 90º.
	c = 13.6101(8) Å	g = 90º.
Volume	1390.75(14) $Å^3$	
Z	4	
Density (calculated)	1.262 Mg/m^3	
Absorption coefficient	0.091 mm^{-1}	
F(000)	568	
Crystal size	0.48 x 0.28 x 0.20 mm^3	
Theta range for data collection	2.85 to 26.54º.	
Index ranges	-10<=h<=4, -14<=k<=13, -16<=l<=14	
Reflections collected	7595	
Independent reflections	1575 [R(int) = 0.0284]	
Completeness to theta = 25.00º	99.9 %	
Absorption correction	Semi-empirical from equivalents	
Max. and min. transmission	0.980 and 0.886	
Refinement method	Full-matrix least-squares on F^2	
Data / restraints / parameters	1575 / 0 / 172	
Goodness-of-fit on F^2	1.088	
Final R indices [I>2sigma(I)]	R1 = 0.0320, wR2 = 0.0892	
R indices (all data)	R1 = 0.0345, wR2 = 0.0929	

Extinction coefficient	0
Largest diff. peak and hole	0.175 and -0.161 e.Å^{-3}

Table A2. Atomic coordinates (x 10^4) and equivalent isotropic displacement Parameters. (Å^{2}x 10^3) for Compound **(60).** U(eq) is defined as one third of the trace of the orthogonalized U^{ij} tensor.

	x	y	z	U(eq)
O(1)	12211(2)	7570(1)	8349(1)	49(1)
O(2)	9411(2)	5125(1)	10447(1)	47(1)
O(3)	11302(2)	4848(1)	11570(1)	60(1)
O(4)	5113(2)	6516(1)	7931(1)	47(1)
C(1)	6570(2)	7080(2)	7752(1)	40(1)
C(2)	6629(2)	7526(2)	6707(2)	50(1)
C(3)	8167(3)	8162(2)	6522(2)	55(1)
C(4)	9620(2)	7526(2)	6837(1)	42(1)
C(5)	9520(2)	7146(1)	7896(1)	35(1)
C(6)	11082(2)	6697(1)	8337(1)	35(1)
C(7)	10731(2)	6346(1)	9384(1)	35(1)
C(8)	9388(2)	5512(2)	9420(1)	36(1)
C(9)	7837(2)	5997(2)	9100(1)	39(1)
C(10)	8035(2)	6375(1)	8016(1)	35(1)
C(11)	11915(2)	5800(2)	10046(1)	38(1)
C(12)	10916(2)	5206(2)	10778(1)	43(1)
C(13)	13481(2)	5730(2)	10047(2)	50(1)
C(14)	8155(2)	5359(2)	7345(1)	44(1)
C(15)	10805(3)	7327(2)	6235(2)	64(1)

Table A3. Bond lengths [Å] and angles [º] for Compound **(60)**

O(1)-C(6)	1.423(2)	C(9)-H(9A)	0.9700
O(1)-H(1O)	0.8200	C(9)-H(9B)	0.9700
O(2)-C(12)	1.346(2)	C(10)-C(14)	1.539(2)
O(2)-C(8)	1.474(2)	C(11)-C(13)	1.319(3)
O(3)-C(12)	1.207(2)	C(11)-C(12)	1.489(3)
O(4)-C(1)	1.424(2)	C(13)-H(13A)	0.9300
O(4)-H(4O)	0.8200	C(13)-H(13B)	0.9300
C(1)-C(2)	1.523(3)	C(14)-H(14A)	0.9600
C(1)-C(10)	1.544(2)	C(14)-H(14B)	0.9600
C(1)-H(1)	0.9800	C(14)-H(14C)	0.9600
C(2)-C(3)	1.527(3)	C(15)-H(15A)	0.9300
C(2)-H(2A)	0.9700	C(15)-H(15B)	0.9300
C(2)-H(2B)	0.9700		
C(3)-C(4)	1.508(3)	C(6)-O(1)-H(1O)	109.5
C(3)-H(3A)	0.9700	C(12)-O(2)-C(8)	107.83(13)
C(3)-H(3B)	0.9700	C(1)-O(4)-H(4O)	109.5
C(4)-C(15)	1.312(3)	O(4)-C(1)-C(2)	111.03(15)
C(4)-C(5)	1.515(2)	O(4)-C(1)-C(10)	112.23(14)
C(5)-C(6)	1.543(2)	C(2)-C(1)-C(10)	112.93(15)
C(5)-C(10)	1.571(2)	O(4)-C(1)-H(1)	106.7
C(5)-H(5)	0.9800	C(2)-C(1)-H(1)	106.7
C(6)-C(7)	1.516(2)	C(10)-C(1)-H(1)	106.7
C(6)-H(6)	0.9800	C(1)-C(2)-C(3)	111.20(16)
C(7)-C(11)	1.498(2)	C(1)-C(2)-H(2A)	109.4
C(7)-C(8)	1.518(2)	C(3)-C(2)-H(2A)	109.4
C(7)-H(7)	0.9800	C(1)-C(2)-H(2B)	109.4
C(8)-C(9)	1.496(2)	C(3)-C(2)-H(2B)	109.4
C(8)-H(8)	0.9800	H(2A)-C(2)-H(2B)	108.0
C(9)-C(10)	1.553(2)	C(4)-C(3)-C(2)	112.31(16)

C(4)-C(3)-H(3A)	109.1	C(7)-C(8)-H(8)	108.9
C(2)-C(3)-H(3A)	109.1	C(8)-C(9)-C(10)	107.44(13)
C(4)-C(3)-H(3B)	109.1	C(8)-C(9)-H(9A)	110.2
C(2)-C(3)-H(3B)	109.1	C(10)-C(9)-H(9A)	110.2
H(3A)-C(3)-H(3B)	107.9	C(8)-C(9)-H(9B)	110.2
C(15)-C(4)-C(3)	122.06(19)	C(10)-C(9)-H(9B)	110.2
C(15)-C(4)-C(5)	125.44(19)	H(9A)-C(9)-H(9B)	108.5
C(3)-C(4)-C(5)	112.49(16)	C(14)-C(10)-C(1)	111.05(14)
C(4)-C(5)-C(6)	115.51(15)	C(14)-C(10)-C(9)	109.49(14)
C(4)-C(5)-C(10)	108.96(15)	C(1)-C(10)-C(9)	107.46(14)
C(6)-C(5)-C(10)	115.11(13)	C(14)-C(10)-C(5)	111.42(14)
C(4)-C(5)-H(5)	105.4	C(1)-C(10)-C(5)	106.13(13)
C(6)-C(5)-H(5)	105.4	C(9)-C(10)-C(5)	111.18(14)
C(10)-C(5)-H(5)	105.4	C(13)-C(11)-C(12)	122.04(18)
O(1)-C(6)-C(7)	109.20(14)	C(13)-C(11)-C(7)	133.81(18)
O(1)-C(6)-C(5)	107.95(13)	C(12)-C(11)-C(7)	104.05(15)
C(7)-C(6)-C(5)	107.41(13)	O(3)-C(12)-O(2)	121.70(18)
O(1)-C(6)-H(6)	110.7	O(3)-C(12)-C(11)	128.35(18)
C(7)-C(6)-H(6)	110.7	O(2)-C(12)-C(11)	109.94(15)
C(5)-C(6)-H(6)	110.7	C(11)-C(13)-H(13A)	120.0
C(11)-C(7)-C(6)	124.10(15)	C(11)-C(13)-H(13B)	120.0
C(11)-C(7)-C(8)	100.26(14)	H(13A)-C(13)-H(13B)	120.0
C(6)-C(7)-C(8)	111.36(14)	C(10)-C(14)-H(14A)	109.5
C(11)-C(7)-H(7)	106.6	C(10)-C(14)-H(14B)	109.5
C(6)-C(7)-H(7)	106.6	H(14A)-C(14)-H(14B)	109.5
C(8)-C(7)-H(7)	106.6	C(10)-C(14)-H(14C)	109.5
O(2)-C(8)-C(9)	114.41(14)	H(14A)-C(14)-H(14C)	109.5
O(2)-C(8)-C(7)	103.56(13)	H(14B)-C(14)-H(14C)	109.5
C(9)-C(8)-C(7)	112.04(14)	C(4)-C(15)-H(15A)	120.0
O(2)-C(8)-H(8)	108.9	C(4)-C(15)-H(15B)	120.0
C(9)-C(8)-H(8)	108.9	H(15A)-C(15)-H(15B)	120.0

Symmetry transformations used to generate equivalent atoms:

Table A4. Anisotropic displacement parameters ($Å^2 x\ 10^3$) Compound **(60)**
The anisotropic displacement factor exponent takes the form:
$-2p^2[\ h^2a^{*2}U^{11} + ... + 2\ h\ k\ a^*\ b^*\ U^{12}\ ]$

	U^{11}	U^{22}	U^{33}	U^{23}	U^{13}	U^{12}
O(1)	33(1)	44(1)	68(1)	8(1)	3(1)	-8(1)
O(2)	37(1)	60(1)	43(1)	15(1)	2(1)	-5(1)
O(3)	55(1)	77(1)	47(1)	21(1)	-5(1)	-4(1)
O(4)	30(1)	63(1)	47(1)	-5(1)	0(1)	-2(1)
C(1)	32(1)	43(1)	46(1)	-3(1)	-2(1)	1(1)
C(2)	41(1)	56(1)	53(1)	10(1)	-8(1)	2(1)
C(3)	52(1)	57(1)	56(1)	19(1)	-6(1)	-2(1)
C(4)	42(1)	42(1)	43(1)	7(1)	1(1)	-4(1)
C(5)	32(1)	34(1)	40(1)	0(1)	3(1)	-1(1)
C(6)	30(1)	35(1)	41(1)	2(1)	4(1)	-2(1)
C(7)	31(1)	37(1)	37(1)	-1(1)	2(1)	-1(1)
C(8)	33(1)	41(1)	33(1)	3(1)	2(1)	-3(1)
C(9)	30(1)	47(1)	41(1)	1(1)	4(1)	-3(1)
C(10)	30(1)	36(1)	38(1)	-1(1)	2(1)	-1(1)
C(11)	37(1)	40(1)	37(1)	0(1)	-2(1)	-2(1)
C(12)	41(1)	47(1)	42(1)	4(1)	-1(1)	0(1)
C(13)	39(1)	61(1)	51(1)	7(1)	-5(1)	-1(1)
C(14)	45(1)	41(1)	46(1)	-6(1)	-1(1)	0(1)
C(15)	69(2)	76(2)	47(1)	14(1)	12(1)	11(1)

Table A5. Hydrogen coordinates (x 10^4) and isotropic displacement parameters ($Å^2$x 10^3) for Compound **(60)**

	x	y	z	U(eq)
H(1O)	13088	7332	8192	58
H(4O)	4945	6079	7484	56
H(1)	6584	7719	8192	49
H(2A)	5726	8008	6598	60
H(2B)	6554	6920	6245	60
H(3A)	8250	8330	5827	66
H(3B)	8130	8852	6877	66
H(5)	9272	7808	8277	42
H(6)	11480	6076	7950	42
H(7)	10352	7002	9730	42
H(8)	9652	4894	8987	43
H(9A)	7561	6618	9513	47
H(9B)	6997	5452	9149	47
H(13A)	13995	5300	10515	60
H(13B)	14072	6111	9580	60
H(14A)	9095	4949	7507	66
H(14B)	8208	5592	6671	66
H(14C)	7235	4903	7437	66
H(15A)	10764	7582	5591	77
H(15B)	11685	6932	6452	77

Table A6. Torsion angles [º] for Compound **(60)**

O(4)-C(1)-C(2)-C(3)	178.31(16)	O(4)-C(1)-C(10)-C(5)	-173.72(15)
C(10)-C(1)-C(2)-C(3)	-54.6(2)	C(2)-C(1)-C(10)-C(5)	59.84(19)
C(1)-C(2)-C(3)-C(4)	49.6(2)	C(8)-C(9)-C(10)-C(14)	70.54(18)
C(2)-C(3)-C(4)-C(15)	125.2(2)	C(8)-C(9)-C(10)-C(1)	-168.74(14)
C(2)-C(3)-C(4)-C(5)	-54.0(2)	C(8)-C(9)-C(10)-C(5)	-53.00(19)
C(15)-C(4)-C(5)-C(6)	12.6(3)	C(4)-C(5)-C(10)-C(14)	59.78(18)
C(3)-C(4)-C(5)-C(6)	-168.24(16)	C(6)-C(5)-C(10)-C(14)	-71.82(19)
C(15)-C(4)-C(5)-C(10)	-118.7(2)	C(4)-C(5)-C(10)-C(1)	-61.23(17)
C(3)-C(4)-C(5)-C(10)	60.4(2)	C(6)-C(5)-C(10)-C(1)	167.17(14)
C(4)-C(5)-C(6)-O(1)	63.38(19)	C(4)-C(5)-C(10)-C(9)	-177.79(14)
C(10)-C(5)-C(6)-O(1)	-168.22(14)	C(6)-C(5)-C(10)-C(9)	50.62(19)
C(4)-C(5)-C(6)-C(7)	-178.99(14)	C(6)-C(7)-C(11)-C(13)	19.5(3)
C(10)-C(5)-C(6)-C(7)	-50.58(19)	C(8)-C(7)-C(11)-C(13)	144.2(2)
O(1)-C(6)-C(7)-C(11)	-67.1(2)	C(6)-C(7)-C(11)-C(12)	-156.89(16)
C(5)-C(6)-C(7)-C(11)	176.07(16)	C(8)-C(7)-C(11)-C(12)	-32.16(17)
O(1)-C(6)-C(7)-C(8)	173.17(13)	C(8)-O(2)-C(12)-O(3)	-173.07(19)
C(5)-C(6)-C(7)-C(8)	56.35(18)	C(8)-O(2)-C(12)-C(11)	8.3(2)
C(12)-O(2)-C(8)-C(9)	-151.44(17)	C(13)-C(11)-C(12)-O(3)	20.7(4)
C(12)-O(2)-C(8)-C(7)	-29.20(19)	C(7)-C(11)-C(12)-O(3)	-162.4(2)
C(11)-C(7)-C(8)-O(2)	37.20(16)	C(13)-C(11)-C(12)-O(2)	-160.8(2)
C(6)-C(7)-C(8)-O(2)	170.25(14)	C(7)-C(11)-C(12)-O(2)	16.1(2)
C(11)-C(7)-C(8)-C(9)	161.00(14)		
C(6)-C(7)-C(8)-C(9)	-65.95(19)		
O(2)-C(8)-C(9)-C(10)	179.04(14)		
C(7)-C(8)-C(9)-C(10)	61.56(18)		
O(4)-C(1)-C(10)-C(14)	65.03(19)		
C(2)-C(1)-C(10)-C(14)	-61.4(2)		
O(4)-C(1)-C(10)-C(9)	-54.70(18)		
C(2)-C(1)-C(10)-C(9)	178.87(15)		

Symmetry transformations used to generate equivalent atoms:

Table A7. Hydrogen bonds for Compound **(60)** [Å and º].

D-H...A	d(D-H)	d(H...A)	d(D...A)	<(DHA)
O(1)-H(1O)...O(4)#1	0.82	2.00	2.8139(19)	170.1
O(4)-H(4O)...O(3)#2	0.82	1.98	2.756(2)	157.9

Symmetry transformations used to generate equivalent atoms:

#1 x+1,y,z #2 -x+3/2,-y+1,z-1/2

Appendix (B)

Table B1. Crystal data and structure refinement for Compound **(62)**.

Empirical formula	$C_{60}\ H_{82}\ O_{17}$	
Formula weight	1075.25	
Temperature	293(2) K	
Wavelength	0.71073 Å	
Crystal system	Trigonal	
Space group	P 3_2	
Unit cell dimensions	a = 15.8884(8) Å	a= 90º.
	b = 15.8884(8) Å	b= 90º.
	c = 22.0221(15) Å	g = 120º.
Volume	4814.5(5) $Å^3$	
Z	3	
Density (calculated)	1.110 Mg/m^3	
Absorption coefficient	0.081 mm^{-1}	
F(000)	1730	
Crystal size	0.48 x 0.32 x 0.20 mm^3	
Theta range for data collection	2.37 to 26.51º.	
Index ranges	-18<=h<=19, -18<=k<=15, -13<=l<=27	
Reflections collected	26394	
Independent reflections	9762 [R(int) = 0.0333]	
Completeness to theta = 25.00º	99.9 %	
Absorption correction	Semi-empirical from equivalents	
Max. and min. transmission	0.984 and 0.927	
Refinement method	Full-matrix least-squares on F^2	
Data / restraints / parameters	9762 / 1 / 710	
Goodness-of-fit on F^2	1.082	
Final R indices [I>2sigma(I)]	R1 = 0.0495, wR2 = 0.1412	
R indices (all data)	R1 = 0.0658, wR2 = 0.1531	

Largest diff. peak and hole 0.574 and -0.267 e.Å^{-3}

Table B2. Atomic coordinates (x 10^4) and equivalent isotropic displacement parameters (Å^{2}x 10^3) for Compound **(62)**. U(eq) is defined as one third of the trace of the orthogonalized U^{ij} tensor.

	x	y	z	U(eq)
O(1)	7547(2)	1049(2)	3074(1)	57(1)
O(2)	4820(2)	-826(2)	1768(1)	58(1)
O(3)	5457(2)	-1566(2)	1246(1)	80(1)
O(4)	3388(2)	1096(2)	1950(1)	75(1)
C(1)	4229(2)	1276(2)	2285(2)	51(1)
C(2)	4586(3)	2194(2)	2669(2)	57(1)
C(3)	5386(3)	2386(2)	3129(2)	55(1)
C(4)	6173(2)	2241(2)	2864(1)	48(1)
C(5)	6280(2)	1492(2)	3039(1)	47(1)
C(6)	6804(2)	1073(2)	2716(1)	47(1)
C(7)	6048(2)	41(2)	2509(1)	46(1)
C(8)	5160(2)	-8(2)	2193(1)	47(1)
C(9)	4328(2)	-191(2)	2592(2)	49(1)
C(10)	3919(2)	364(2)	2656(1)	49(1)
C(11)	6374(3)	-433(2)	2049(2)	55(1)
C(12)	5542(3)	-1005(2)	1643(2)	59(1)
C(13)	7215(3)	-384(3)	1978(2)	75(1)
C(14)	3103(3)	99(3)	3101(2)	71(1)
C(15)	6756(3)	2931(2)	2363(2)	66(1)
O(5)	2684(2)	3447(2)	2605(1)	56(1)
O(6)	5221(2)	4427(2)	4057(1)	57(1)
O(7)	4632(2)	3003(2)	4525(1)	73(1)
O(8)	6457(2)	7916(2)	3831(1)	67(1)
C(16)	5702(2)	7116(2)	3496(2)	51(1)

C(17)	5323(3)	7601(2)	3063(2)	57(1)
C(18)	4585(3)	6953(2)	2582(2)	55(1)
C(19)	3814(2)	6004(2)	2846(1)	48(1)
C(20)	3794(2)	5189(2)	2685(1)	46(1)
C(21)	3291(2)	4240(2)	3009(1)	46(1)
C(22)	4069(2)	4031(2)	3256(1)	45(1)
C(23)	4884(2)	4894(2)	3613(1)	46(1)
C(24)	5749(2)	5594(2)	3255(2)	50(1)
C(25)	6120(2)	6545(2)	3191(2)	53(1)
C(26)	3731(3)	3215(2)	3711(1)	52(1)
C(27)	4535(3)	3492(2)	4142(2)	54(1)
C(28)	2889(3)	2399(3)	3764(2)	69(1)
C(29)	7010(3)	7130(3)	2803(2)	79(1)
C(30)	3166(3)	6069(3)	3314(2)	64(1)
O(9)	3197(2)	2668(2)	1587(1)	58(1)
O(10)	3755(2)	4768(2)	-116(1)	64(1)
O(11)	2319(2)	3889(3)	-560(1)	93(1)
O(12)	7164(2)	6471(2)	-71(1)	61(1)
C(31)	6557(2)	5756(2)	365(1)	50(1)
C(32)	7181(2)	5578(3)	821(2)	55(1)
C(33)	6644(3)	4929(3)	1368(2)	59(1)
C(34)	5712(2)	4034(2)	1195(1)	49(1)
C(35)	4875(2)	3938(2)	1383(1)	48(1)
C(36)	3891(2)	3272(2)	1134(2)	50(1)
C(37)	3534(2)	3897(2)	808(2)	50(1)
C(38)	4314(2)	4654(2)	380(1)	49(1)
C(39)	4967(3)	5628(3)	637(2)	54(1)
C(40)	5937(2)	6124(2)	646(2)	52(1)
C(41)	2679(3)	3375(3)	390(2)	60(1)
C(42)	2848(3)	3994(3)	-143(2)	64(1)
C(43)	1913(4)	2519(4)	432(3)	98(2)

C(44)	6481(3)	7107(3)	941(2)	82(1)
C(45)	5805(3)	3331(3)	780(2)	64(1)
O(13)	291(2)	6975(2)	708(1)	54(1)
O(14)	-1037(2)	5045(2)	2476(1)	57(1)
O(15)	-1675(2)	5876(3)	2891(1)	89(1)
O(16)	968(2)	3571(2)	2497(1)	57(1)
C(46)	915(2)	4205(2)	2052(1)	47(1)
C(47)	1730(2)	4410(3)	1597(2)	53(1)
C(48)	1795(2)	5011(3)	1032(1)	54(1)
C(49)	1685(2)	5882(2)	1182(1)	48(1)
C(50)	903(2)	5896(2)	982(1)	47(1)
C(51)	512(2)	6523(2)	1198(1)	47(1)
C(52)	-427(2)	5884(2)	1540(1)	46(1)
C(53)	-352(2)	5185(2)	1989(1)	47(1)
C(54)	-618(2)	4193(2)	1758(1)	49(1)
C(55)	-94(2)	3753(2)	1778(1)	49(1)
C(56)	-779(2)	6407(3)	1944(2)	54(1)
C(57)	-1213(2)	5796(3)	2485(2)	59(1)
C(58)	-704(4)	7255(3)	1888(2)	86(1)
C(59)	-492(3)	2735(3)	1540(2)	72(1)
C(60)	2450(2)	6644(3)	1587(2)	61(1)
O(1S)	6981(4)	7830(4)	4988(2)	132(2)

Table B3. Bond lengths [Å] and angles [º] for Compound **(62)**.

O(1)-C(6)	1.435(4)	O(4)-C(1)	1.424(4)
O(1)-H(1)	0.8200	O(4)-H(4)	0.8200
O(2)-C(12)	1.341(4)	C(1)-C(10)	1.516(4)
O(2)-C(8)	1.467(4)	C(1)-C(2)	1.528(5)
O(3)-C(12)	1.207(4)	C(1)-H(1A)	0.9800

C(2)-C(3)	1.532(5)	O(5)-H(5)	0.8200
C(2)-H(2A)	0.9700	O(6)-C(27)	1.346(4)
C(2)-H(2B)	0.9700	O(6)-C(23)	1.480(4)
C(3)-C(4)	1.498(5)	O(7)-C(27)	1.209(4)
C(3)-H(3A)	0.9700	O(8)-C(16)	1.441(4)
C(3)-H(3B)	0.9700	O(8)-H(8)	0.8200
C(4)-C(5)	1.340(4)	C(16)-C(25)	1.522(5)
C(4)-C(15)	1.505(5)	C(16)-C(17)	1.526(5)
C(5)-C(6)	1.482(4)	C(16)-H(16A)	0.9800
C(5)-H(5A)	0.9300	C(17)-C(18)	1.533(5)
C(6)-C(7)	1.539(4)	C(17)-H(17A)	0.9700
C(6)-H(6)	0.9800	C(17)-H(17B)	0.9700
C(7)-C(11)	1.502(4)	C(18)-C(19)	1.504(5)
C(7)-C(8)	1.540(4)	C(18)-H(18A)	0.9700
C(7)-H(7A)	0.9800	C(18)-H(18B)	0.9700
C(8)-C(9)	1.489(5)	C(19)-C(20)	1.328(4)
C(8)-H(8A)	0.9800	C(19)-C(30)	1.496(5)
C(9)-C(10)	1.339(4)	C(20)-C(21)	1.488(4)
C(9)-H(9A)	0.9300	C(20)-H(20)	0.9300
C(10)-C(14)	1.507(5)	C(21)-C(22)	1.530(4)
C(11)-C(13)	1.308(5)	C(21)-H(21)	0.9800
C(11)-C(12)	1.474(5)	C(22)-C(26)	1.509(4)
C(13)-H(13A)	0.9300	C(22)-C(23)	1.548(4)
C(13)-H(13B)	0.9300	C(22)-H(22)	0.9800
C(14)-H(14A)	0.9600	C(23)-C(24)	1.490(5)
C(14)-H(14B)	0.9600	C(23)-H(23)	0.9800
C(14)-H(14C)	0.9600	C(24)-C(25)	1.327(5)
C(15)-H(15A)	0.9600	C(24)-H(24)	0.9300
C(15)-H(15B)	0.9600	C(25)-C(29)	1.509(5)
C(15)-H(15C)	0.9600	C(26)-C(28)	1.323(5)
O(5)-C(21)	1.446(4)	C(26)-C(27)	1.470(5)

C(28)-H(28A)	0.9300	C(37)-C(38)	1.543(5)
C(28)-H(28B)	0.9300	C(37)-H(37)	0.9800
C(29)-H(29A)	0.9600	C(38)-C(39)	1.478(5)
C(29)-H(29B)	0.9600	C(38)-H(38)	0.9800
C(29)-H(29C)	0.9600	C(39)-C(40)	1.335(5)
C(30)-H(30A)	0.9600	C(39)-H(39)	0.9300
C(30)-H(30B)	0.9600	C(40)-C(44)	1.502(5)
C(30)-H(30C)	0.9600	C(41)-C(43)	1.297(6)
O(9)-C(36)	1.440(4)	C(41)-C(42)	1.468(5)
O(9)-H(9)	0.8200	C(43)-H(43A)	0.9300
O(10)-C(42)	1.349(5)	C(43)-H(43B)	0.9300
O(10)-C(38)	1.475(4)	C(44)-H(44A)	0.9600
O(11)-C(42)	1.200(4)	C(44)-H(44B)	0.9600
O(12)-C(31)	1.432(4)	C(44)-H(44C)	0.9600
O(12)-H(12)	0.8200	C(45)-H(45A)	0.9600
C(31)-C(40)	1.508(5)	C(45)-H(45B)	0.9600
C(31)-C(32)	1.533(4)	C(45)-H(45C)	0.9600
C(31)-H(31)	0.9800	O(13)-C(51)	1.434(4)
C(32)-C(33)	1.538(5)	O(13)-H(13)	0.8200
C(32)-H(32A)	0.9700	O(14)-C(57)	1.356(4)
C(32)-H(32B)	0.9700	O(14)-C(53)	1.464(4)
C(33)-C(34)	1.502(5)	O(15)-C(57)	1.201(4)
C(33)-H(33A)	0.9700	O(16)-C(46)	1.438(4)
C(33)-H(33B)	0.9700	O(16)-H(16)	0.8200
C(34)-C(35)	1.326(4)	C(46)-C(55)	1.515(4)
C(34)-C(45)	1.507(5)	C(46)-C(47)	1.536(4)
C(35)-C(36)	1.487(5)	C(46)-H(46)	0.9800
C(35)-H(35)	0.9300	C(47)-C(48)	1.539(5)
C(36)-C(37)	1.545(4)	C(47)-H(47A)	0.9700
C(36)-H(36)	0.9800	C(47)-H(47B)	0.9700
C(37)-C(41)	1.501(5)	C(48)-C(49)	1.515(5)

C(48)-H(48A)	0.9700	O(4)-C(1)-C(2)	110.0(3)
C(48)-H(48B)	0.9700	C(10)-C(1)-C(2)	113.7(3)
C(49)-C(50)	1.328(4)	O(4)-C(1)-H(1A)	109.2
C(49)-C(60)	1.505(5)	C(10)-C(1)-H(1A)	109.2
C(50)-C(51)	1.492(5)	C(2)-C(1)-H(1A)	109.2
C(50)-H(50)	0.9300	C(1)-C(2)-C(3)	115.6(3)
C(51)-C(52)	1.519(4)	C(1)-C(2)-H(2A)	108.4
C(51)-H(51)	0.9800	C(3)-C(2)-H(2A)	108.4
C(52)-C(56)	1.503(5)	C(1)-C(2)-H(2B)	108.4
C(52)-C(53)	1.536(4)	C(3)-C(2)-H(2B)	108.4
C(52)-H(52)	0.9800	H(2A)-C(2)-H(2B)	107.4
C(53)-C(54)	1.502(5)	C(4)-C(3)-C(2)	112.6(3)
C(53)-H(53)	0.9800	C(4)-C(3)-H(3A)	109.1
C(54)-C(55)	1.329(5)	C(2)-C(3)-H(3A)	109.1
C(54)-H(54)	0.9300	C(4)-C(3)-H(3B)	109.1
C(55)-C(59)	1.506(5)	C(2)-C(3)-H(3B)	109.1
C(56)-C(58)	1.298(6)	H(3A)-C(3)-H(3B)	107.8
C(56)-C(57)	1.472(5)	C(5)-C(4)-C(3)	120.8(3)
C(58)-H(58A)	0.9300	C(5)-C(4)-C(15)	123.5(3)
C(58)-H(58B)	0.9300	C(3)-C(4)-C(15)	115.5(3)
C(59)-H(59A)	0.9600	C(4)-C(5)-C(6)	127.6(3)
C(59)-H(59B)	0.9600	C(4)-C(5)-H(5A)	116.2
C(59)-H(59C)	0.9600	C(6)-C(5)-H(5A)	116.2
C(60)-H(60A)	0.9600	O(1)-C(6)-C(5)	113.7(3)
C(60)-H(60B)	0.9600	O(1)-C(6)-C(7)	110.4(2)
C(60)-H(60C)	0.9600	C(5)-C(6)-C(7)	107.8(2)
		O(1)-C(6)-H(6)	108.2
C(6)-O(1)-H(1)	109.5	C(5)-C(6)-H(6)	108.2
C(12)-O(2)-C(8)	110.1(3)	C(7)-C(6)-H(6)	108.2
C(1)-O(4)-H(4)	109.5	C(11)-C(7)-C(6)	116.9(3)
O(4)-C(1)-C(10)	105.3(3)	C(11)-C(7)-C(8)	102.0(3)

C(6)-C(7)-C(8)	113.3(2)	C(4)-C(15)-H(15A)	109.5
C(11)-C(7)-H(7A)	108.1	C(4)-C(15)-H(15B)	109.5
C(6)-C(7)-H(7A)	108.1	H(15A)-C(15)-H(15B)	109.5
C(8)-C(7)-H(7A)	108.1	C(4)-C(15)-H(15C)	109.5
O(2)-C(8)-C(9)	107.8(2)	H(15A)-C(15)-H(15C)	109.5
O(2)-C(8)-C(7)	104.8(2)	H(15B)-C(15)-H(15C)	109.5
C(9)-C(8)-C(7)	116.4(3)	C(21)-O(5)-H(5)	109.5
O(2)-C(8)-H(8A)	109.2	C(27)-O(6)-C(23)	110.4(2)
C(9)-C(8)-H(8A)	109.2	C(16)-O(8)-H(8)	109.5
C(7)-C(8)-H(8A)	109.2	O(8)-C(16)-C(25)	109.5(3)
C(10)-C(9)-C(8)	127.5(3)	O(8)-C(16)-C(17)	103.8(2)
C(10)-C(9)-H(9A)	116.3	C(25)-C(16)-C(17)	115.2(3)
C(8)-C(9)-H(9A)	116.3	O(8)-C(16)-H(16A)	109.4
C(9)-C(10)-C(14)	121.1(3)	C(25)-C(16)-H(16A)	109.4
C(9)-C(10)-C(1)	122.7(3)	C(17)-C(16)-H(16A)	109.4
C(14)-C(10)-C(1)	116.1(3)	C(16)-C(17)-C(18)	117.0(3)
C(13)-C(11)-C(12)	122.7(3)	C(16)-C(17)-H(17A)	108.0
C(13)-C(11)-C(7)	130.5(4)	C(18)-C(17)-H(17A)	108.0
C(12)-C(11)-C(7)	106.8(3)	C(16)-C(17)-H(17B)	108.0
O(3)-C(12)-O(2)	120.9(4)	C(18)-C(17)-H(17B)	108.0
O(3)-C(12)-C(11)	128.9(4)	H(17A)-C(17)-H(17B)	107.3
O(2)-C(12)-C(11)	110.1(3)	C(19)-C(18)-C(17)	111.8(3)
C(11)-C(13)-H(13A)	120.0	C(19)-C(18)-H(18A)	109.3
C(11)-C(13)-H(13B)	120.0	C(17)-C(18)-H(18A)	109.3
H(13A)-C(13)-H(13B)	120.0	C(19)-C(18)-H(18B)	109.3
C(10)-C(14)-H(14A)	109.5	C(17)-C(18)-H(18B)	109.3
C(10)-C(14)-H(14B)	109.5	H(18A)-C(18)-H(18B)	107.9
H(14A)-C(14)-H(14B)	109.5	C(20)-C(19)-C(30)	124.6(3)
C(10)-C(14)-H(14C)	109.5	C(20)-C(19)-C(18)	119.0(3)
H(14A)-C(14)-H(14C)	109.5	C(30)-C(19)-C(18)	116.2(3)
H(14B)-C(14)-H(14C)	109.5	C(19)-C(20)-C(21)	126.9(3)

C(19)-C(20)-H(20)	116.5	O(6)-C(27)-C(26)	110.1(3)
C(21)-C(20)-H(20)	116.5	C(26)-C(28)-H(28A)	120.0
O(5)-C(21)-C(20)	112.0(2)	C(26)-C(28)-H(28B)	120.0
O(5)-C(21)-C(22)	106.9(2)	H(28A)-C(28)-H(28B)	120.0
C(20)-C(21)-C(22)	107.9(3)	C(25)-C(29)-H(29A)	109.5
O(5)-C(21)-H(21)	110.0	C(25)-C(29)-H(29B)	109.5
C(20)-C(21)-H(21)	110.0	H(29A)-C(29)-H(29B)	109.5
C(22)-C(21)-H(21)	110.0	C(25)-C(29)-H(29C)	109.5
C(26)-C(22)-C(21)	116.4(3)	H(29A)-C(29)-H(29C)	109.5
C(26)-C(22)-C(23)	101.8(2)	H(29B)-C(29)-H(29C)	109.5
C(21)-C(22)-C(23)	113.4(2)	C(19)-C(30)-H(30A)	109.5
C(26)-C(22)-H(22)	108.3	C(19)-C(30)-H(30B)	109.5
C(21)-C(22)-H(22)	108.3	H(30A)-C(30)-H(30B)	109.5
C(23)-C(22)-H(22)	108.3	C(19)-C(30)-H(30C)	109.5
O(6)-C(23)-C(24)	107.1(2)	H(30A)-C(30)-H(30C)	109.5
O(6)-C(23)-C(22)	104.1(2)	H(30B)-C(30)-H(30C)	109.5
C(24)-C(23)-C(22)	116.3(3)	C(36)-O(9)-H(9)	109.5
O(6)-C(23)-H(23)	109.7	C(42)-O(10)-C(38)	110.9(3)
C(24)-C(23)-H(23)	109.7	C(31)-O(12)-H(12)	109.5
C(22)-C(23)-H(23)	109.7	O(12)-C(31)-C(40)	106.2(3)
C(25)-C(24)-C(23)	128.7(3)	O(12)-C(31)-C(32)	110.1(2)
C(25)-C(24)-H(24)	115.7	C(40)-C(31)-C(32)	114.3(3)
C(23)-C(24)-H(24)	115.7	O(12)-C(31)-H(31)	108.7
C(24)-C(25)-C(29)	120.5(3)	C(40)-C(31)-H(31)	108.7
C(24)-C(25)-C(16)	123.7(3)	C(32)-C(31)-H(31)	108.7
C(29)-C(25)-C(16)	115.8(3)	C(31)-C(32)-C(33)	116.3(3)
C(28)-C(26)-C(27)	122.6(3)	C(31)-C(32)-H(32A)	108.2
C(28)-C(26)-C(22)	130.6(3)	C(33)-C(32)-H(32A)	108.2
C(27)-C(26)-C(22)	106.8(3)	C(31)-C(32)-H(32B)	108.2
O(7)-C(27)-O(6)	120.9(3)	C(33)-C(32)-H(32B)	108.2
O(7)-C(27)-C(26)	129.0(3)	H(32A)-C(32)-H(32B)	107.4

C(34)-C(33)-C(32)	112.9(3)	C(40)-C(39)-H(39)	115.7
C(34)-C(33)-H(33A)	109.0	C(38)-C(39)-H(39)	115.7
C(32)-C(33)-H(33A)	109.0	C(39)-C(40)-C(44)	121.0(3)
C(34)-C(33)-H(33B)	109.0	C(39)-C(40)-C(31)	123.3(3)
C(32)-C(33)-H(33B)	109.0	C(44)-C(40)-C(31)	115.7(3)
H(33A)-C(33)-H(33B)	107.8	C(43)-C(41)-C(42)	121.3(4)
C(35)-C(34)-C(33)	119.1(3)	C(43)-C(41)-C(37)	130.7(4)
C(35)-C(34)-C(45)	124.7(3)	C(42)-C(41)-C(37)	107.9(3)
C(33)-C(34)-C(45)	116.1(3)	O(11)-C(42)-O(10)	121.1(4)
C(34)-C(35)-C(36)	127.2(3)	O(11)-C(42)-C(41)	129.7(4)
C(34)-C(35)-H(35)	116.4	O(10)-C(42)-C(41)	109.2(3)
C(36)-C(35)-H(35)	116.4	C(41)-C(43)-H(43A)	120.0
O(9)-C(36)-C(35)	113.7(3)	C(41)-C(43)-H(43B)	120.0
O(9)-C(36)-C(37)	110.2(2)	H(43A)-C(43)-H(43B)	120.0
C(35)-C(36)-C(37)	107.9(3)	C(40)-C(44)-H(44A)	109.5
O(9)-C(36)-H(36)	108.3	C(40)-C(44)-H(44B)	109.5
C(35)-C(36)-H(36)	108.3	H(44A)-C(44)-H(44B)	109.5
C(37)-C(36)-H(36)	108.3	C(40)-C(44)-H(44C)	109.5
C(41)-C(37)-C(38)	102.0(3)	H(44A)-C(44)-H(44C)	109.5
C(41)-C(37)-C(36)	116.8(3)	H(44B)-C(44)-H(44C)	109.5
C(38)-C(37)-C(36)	112.0(2)	C(34)-C(45)-H(45A)	109.5
C(41)-C(37)-H(37)	108.5	C(34)-C(45)-H(45B)	109.5
C(38)-C(37)-H(37)	108.5	H(45A)-C(45)-H(45B)	109.5
C(36)-C(37)-H(37)	108.5	C(34)-C(45)-H(45C)	109.5
O(10)-C(38)-C(39)	107.8(3)	H(45A)-C(45)-H(45C)	109.5
O(10)-C(38)-C(37)	104.4(2)	H(45B)-C(45)-H(45C)	109.5
C(39)-C(38)-C(37)	116.8(3)	C(51)-O(13)-H(13)	109.5
O(10)-C(38)-H(38)	109.2	C(57)-O(14)-C(53)	110.0(2)
C(39)-C(38)-H(38)	109.2	C(46)-O(16)-H(16)	109.5
C(37)-C(38)-H(38)	109.2	O(16)-C(46)-C(55)	110.9(2)
C(40)-C(39)-C(38)	128.5(3)	O(16)-C(46)-C(47)	104.8(2)

C(55)-C(46)-C(47)	114.9(3)	C(56)-C(52)-H(52)	108.5
O(16)-C(46)-H(46)	108.7	C(51)-C(52)-H(52)	108.5
C(55)-C(46)-H(46)	108.7	C(53)-C(52)-H(52)	108.5
C(47)-C(46)-H(46)	108.7	O(14)-C(53)-C(54)	106.9(2)
C(46)-C(47)-C(48)	116.5(3)	O(14)-C(53)-C(52)	105.1(2)
C(46)-C(47)-H(47A)	108.2	C(54)-C(53)-C(52)	117.3(3)
C(48)-C(47)-H(47A)	108.2	O(14)-C(53)-H(53)	109.1
C(46)-C(47)-H(47B)	108.2	C(54)-C(53)-H(53)	109.1
C(48)-C(47)-H(47B)	108.2	C(52)-C(53)-H(53)	109.1
H(47A)-C(47)-H(47B)	107.3	C(55)-C(54)-C(53)	128.3(3)
C(49)-C(48)-C(47)	112.8(3)	C(55)-C(54)-H(54)	115.9
C(49)-C(48)-H(48A)	109.0	C(53)-C(54)-H(54)	115.9
C(47)-C(48)-H(48A)	109.0	C(54)-C(55)-C(59)	121.1(3)
C(49)-C(48)-H(48B)	109.0	C(54)-C(55)-C(46)	123.8(3)
C(47)-C(48)-H(48B)	109.0	C(59)-C(55)-C(46)	115.1(3)
H(48A)-C(48)-H(48B)	107.8	C(58)-C(56)-C(57)	122.1(4)
C(50)-C(49)-C(60)	124.7(3)	C(58)-C(56)-C(52)	130.5(3)
C(50)-C(49)-C(48)	118.6(3)	C(57)-C(56)-C(52)	107.2(3)
C(60)-C(49)-C(48)	116.6(3)	O(15)-C(57)-O(14)	120.6(3)
C(49)-C(50)-C(51)	127.6(3)	O(15)-C(57)-C(56)	130.0(4)
C(49)-C(50)-H(50)	116.2	O(14)-C(57)-C(56)	109.5(3)
C(51)-C(50)-H(50)	116.2	C(56)-C(58)-H(58A)	120.0
O(13)-C(51)-C(50)	112.4(2)	C(56)-C(58)-H(58B)	120.0
O(13)-C(51)-C(52)	107.7(2)	H(58A)-C(58)-H(58B)	120.0
C(50)-C(51)-C(52)	108.1(2)	C(55)-C(59)-H(59A)	109.5
O(13)-C(51)-H(51)	109.5	C(55)-C(59)-H(59B)	109.5
C(50)-C(51)-H(51)	109.5	H(59A)-C(59)-H(59B)	109.5
C(52)-C(51)-H(51)	109.5	C(55)-C(59)-H(59C)	109.5
C(56)-C(52)-C(51)	115.9(3)	H(59A)-C(59)-H(59C)	109.5
C(56)-C(52)-C(53)	101.7(2)	H(59B)-C(59)-H(59C)	109.5
C(51)-C(52)-C(53)	113.4(2)	C(49)-C(60)-H(60A)	109.5

C(49)-C(60)-H(60B) 109.5	H(60A)-C(60)-H(60C)109.5
H(60A)-C(60)-H(60B)109.5	H(60B)-C(60)-H(60C)109.5
C(49)-C(60)-H(60C) 109.5	

Symmetry transformations used to generate equivalent atoms:

Table B4. Anisotropic displacement parameters ($Å^2 x\ 10^3$) for Compound **(62)**. The anisotropic displacement factor exponent takes the form: $-2p^2[\ h^2a^{*2}U^{11} + ... + 2\ h\ k\ a^*\ b^*\ U^{12}\ ]$

	U^{11}	U^{22}	U^{33}	U^{23}	U^{13}	U^{12}
O(1)	54(1)	57(1)	60(1)	3(1)	0(1)	28(1)
O(2)	76(2)	50(1)	55(1)	-13(1)	-10(1)	37(1)
O(3)	121(2)	69(2)	62(2)	-17(1)	0(2)	57(2)
O(4)	83(2)	55(1)	92(2)	-7(1)	-31(2)	39(1)
C(1)	59(2)	44(2)	53(2)	-1(1)	-4(2)	29(2)
C(2)	66(2)	48(2)	65(2)	-3(2)	2(2)	34(2)
C(3)	66(2)	45(2)	57(2)	-11(2)	-2(2)	29(2)
C(4)	55(2)	40(2)	46(2)	-6(1)	-2(1)	21(1)
C(5)	52(2)	42(2)	41(2)	0(1)	0(1)	19(1)
C(6)	54(2)	42(2)	42(2)	5(1)	4(1)	23(1)
C(7)	59(2)	42(2)	41(2)	3(1)	5(1)	29(1)
C(8)	63(2)	35(1)	43(2)	-2(1)	0(1)	25(1)
C(9)	58(2)	36(2)	49(2)	5(1)	1(1)	20(1)
C(10)	55(2)	44(2)	47(2)	-1(1)	1(1)	23(1)
C(11)	76(2)	51(2)	49(2)	5(1)	9(2)	40(2)
C(12)	93(3)	47(2)	45(2)	2(2)	5(2)	40(2)
C(13)	86(3)	81(3)	73(3)	-2(2)	9(2)	52(2)
C(14)	72(2)	70(2)	71(2)	9(2)	17(2)	36(2)
C(15)	68(2)	43(2)	80(3)	9(2)	10(2)	22(2)
O(5)	61(1)	50(1)	59(1)	-6(1)	-7(1)	30(1)

O(6)	72(2)	55(1)	52(1)	1(1)	-8(1)	37(1)
O(7)	105(2)	76(2)	55(1)	15(1)	-1(1)	57(2)
O(8)	83(2)	51(1)	67(2)	-9(1)	-17(1)	34(1)
C(16)	55(2)	42(2)	55(2)	-2(1)	-2(2)	25(1)
C(17)	68(2)	45(2)	64(2)	2(2)	1(2)	32(2)
C(18)	67(2)	49(2)	54(2)	9(2)	-2(2)	33(2)
C(19)	56(2)	53(2)	45(2)	3(1)	-4(1)	35(2)
C(20)	54(2)	48(2)	42(2)	-1(1)	-1(1)	29(1)
C(21)	56(2)	47(2)	41(2)	-2(1)	-1(1)	29(1)
C(22)	54(2)	41(2)	43(2)	-1(1)	3(1)	27(1)
C(23)	58(2)	47(2)	44(2)	2(1)	1(1)	35(2)
C(24)	57(2)	48(2)	54(2)	-1(1)	3(2)	33(2)
C(25)	52(2)	54(2)	54(2)	-1(2)	1(1)	28(2)
C(26)	70(2)	48(2)	45(2)	2(1)	5(2)	36(2)
C(27)	79(2)	56(2)	42(2)	1(2)	3(2)	45(2)
C(28)	78(3)	57(2)	66(2)	14(2)	8(2)	29(2)
C(29)	68(2)	69(2)	97(3)	11(2)	28(2)	31(2)
C(30)	66(2)	68(2)	73(2)	-4(2)	8(2)	44(2)
O(9)	60(1)	58(1)	57(1)	10(1)	7(1)	31(1)
O(10)	56(1)	94(2)	52(1)	18(1)	4(1)	46(1)
O(11)	69(2)	138(3)	71(2)	19(2)	-12(2)	52(2)
O(12)	55(1)	77(2)	58(1)	22(1)	9(1)	38(1)
C(31)	53(2)	60(2)	43(2)	6(1)	1(1)	33(2)
C(32)	51(2)	66(2)	52(2)	8(2)	-2(2)	31(2)
C(33)	59(2)	72(2)	47(2)	8(2)	-4(2)	34(2)
C(34)	56(2)	59(2)	39(2)	9(1)	1(1)	35(2)
C(35)	57(2)	60(2)	38(2)	5(1)	2(1)	37(2)
C(36)	58(2)	53(2)	48(2)	6(1)	4(1)	33(2)
C(37)	48(2)	61(2)	50(2)	5(2)	5(1)	35(2)
C(38)	51(2)	67(2)	44(2)	8(2)	3(1)	41(2)
C(39)	65(2)	64(2)	52(2)	11(2)	11(2)	46(2)

C(40)	59(2)	57(2)	48(2)	5(1)	3(2)	36(2)
C(41)	54(2)	72(2)	61(2)	3(2)	1(2)	36(2)
C(42)	55(2)	93(3)	56(2)	10(2)	2(2)	45(2)
C(43)	80(3)	86(3)	106(4)	12(3)	-28(3)	25(3)
C(44)	92(3)	67(2)	90(3)	-16(2)	3(2)	42(2)
C(45)	67(2)	76(2)	67(2)	-1(2)	4(2)	50(2)
O(13)	44(1)	60(1)	51(1)	13(1)	0(1)	22(1)
O(14)	52(1)	77(2)	49(1)	14(1)	13(1)	37(1)
O(15)	106(2)	119(2)	73(2)	21(2)	35(2)	79(2)
O(16)	54(1)	75(2)	50(1)	16(1)	10(1)	38(1)
C(46)	45(2)	52(2)	44(2)	4(1)	1(1)	24(1)
C(47)	50(2)	65(2)	49(2)	6(2)	7(1)	33(2)
C(48)	56(2)	70(2)	42(2)	7(2)	10(1)	36(2)
C(49)	43(2)	63(2)	36(2)	8(1)	7(1)	23(1)
C(50)	42(2)	57(2)	34(1)	3(1)	1(1)	20(1)
C(51)	40(2)	53(2)	42(2)	5(1)	-3(1)	19(1)
C(52)	35(1)	54(2)	44(2)	0(1)	-2(1)	19(1)
C(53)	36(1)	63(2)	41(2)	4(1)	1(1)	24(1)
C(54)	39(2)	54(2)	47(2)	5(1)	-1(1)	17(1)
C(55)	47(2)	51(2)	42(2)	2(1)	3(1)	19(1)
C(56)	47(2)	64(2)	57(2)	4(2)	4(2)	32(2)
C(57)	55(2)	80(2)	51(2)	7(2)	8(2)	40(2)
C(58)	105(3)	83(3)	85(3)	15(2)	31(3)	58(3)
C(59)	70(2)	62(2)	76(3)	-9(2)	-10(2)	28(2)
C(60)	44(2)	70(2)	63(2)	0(2)	-7(2)	24(2)
O(1S)	179(4)	162(4)	101(3)	33(3)	-3(3)	121(3)

Table B5. Hydrogen coordinates (x 10^4) and isotropic displacement parameters ($Å^2$x 10^3) for Compound **(62)**.

	x	y	z	U(eq)
H(1)	7299	696	3369	85
H(4)	3417	1614	1870	112
H(1A)	4743	1365	2002	61
H(2A)	4036	2151	2887	69
H(2B)	4827	2748	2398	69
H(3A)	5669	3048	3277	66
H(3B)	5099	1953	3473	66
H(5A)	5992	1201	3406	56
H(6)	7109	1467	2354	56
H(7A)	5818	-377	2869	55
H(8A)	5368	592	1963	56
H(9A)	4062	-757	2823	59
H(13A)	7306	-717	1661	91
H(13B)	7723	-14	2244	91
H(14A)	2814	-576	3205	107
H(14B)	2622	216	2920	107
H(14C)	3355	488	3460	107
H(15A)	7372	2960	2329	99
H(15B)	6858	3567	2453	99
H(15C)	6408	2707	1986	99
H(5)	2182	3456	2535	84
H(8)	6560	7715	4149	100
H(16A)	5181	6688	3775	61
H(17A)	5876	8123	2855	69
H(17B)	5026	7894	3305	69
H(18A)	4280	7293	2405	66
H(18B)	4922	6824	2260	66

H(20)	4130	5213	2334	55
H(21)	2901	4271	3343	56
H(22)	4366	3884	2913	54
H(23)	4612	5244	3828	55
H(24)	6073	5328	3049	60
H(28A)	2789	1974	4082	83
H(28B)	2398	2250	3482	83
H(29A)	7317	6754	2722	119
H(29B)	7456	7714	3014	119
H(29C)	6822	7296	2427	119
H(30A)	2650	5428	3411	96
H(30B)	2897	6448	3157	96
H(30C)	3537	6374	3673	96
H(9)	3205	3008	1870	86
H(12)	7667	6453	-116	92
H(31)	6132	5146	152	60
H(32A)	7683	6203	972	66
H(32B)	7504	5286	605	66
H(33A)	7066	4736	1567	70
H(33B)	6502	5302	1657	70
H(35)	4908	4330	1706	58
H(36)	3946	2848	833	60
H(37)	3375	4242	1116	60
H(38)	4706	4388	215	59
H(39)	4661	5935	815	65
H(43A)	1458	2287	120	118
H(43B)	1820	2138	773	118
H(44A)	6027	7282	1099	123
H(44B)	6891	7579	646	123
H(44C)	6873	7086	1266	123
H(45A)	5230	2704	810	96

H(45B)	6361	3281	897	96
H(45C)	5884	3560	369	96
H(13)	798	7411	563	81
H(16)	549	3436	2756	86
H(46)	1064	4816	2250	56
H(47A)	1647	3793	1462	63
H(47B)	2345	4748	1810	63
H(48A)	2417	5233	836	65
H(48B)	1290	4597	748	65
H(50)	560	5464	670	56
H(51)	983	7024	1472	56
H(52)	-938	5500	1244	55
H(53)	308	5497	2157	56
H(54)	-1227	3842	1578	59
H(58A)	-928	7495	2195	103
H(58B)	-426	7623	1540	103
H(59A)	-1143	2494	1396	107
H(59B)	-494	2323	1859	107
H(59C)	-92	2740	1211	107
H(60A)	2398	7220	1577	91
H(60B)	3082	6794	1447	91
H(60C)	2357	6402	1996	91

Table B6. Torsion angles [º] for Compound **(62)**.

O(4)-C(1)-C(2)-C(3)	170.6(3)	C(2)-C(3)-C(4)-C(15)	64.5(4)
C(10)-C(1)-C(2)-C(3)	52.8(4)	C(3)-C(4)-C(5)-C(6)	160.9(3)
C(1)-C(2)-C(3)-C(4)	45.1(4)	C(15)-C(4)-C(5)-C(6)	-13.7(5)
C(2)-C(3)-C(4)-C(5)	-110.5(3)	C(4)-C(5)-C(6)-O(1)	124.1(3)

C(4)-C(5)-C(6)-C(7)	-113.0(3)	C(16)-C(17)-C(18)-C(19)	44.8(4)
O(1)-C(6)-C(7)-C(11)	-69.2(3)	C(17)-C(18)-C(19)-C(20)	-111.4(3)
C(5)-C(6)-C(7)-C(11)	166.0(3)	C(17)-C(18)-C(19)-C(30)	64.0(4)
O(1)-C(6)-C(7)-C(8)	172.6(2)	C(30)-C(19)-C(20)-C(21)	-13.2(5)
C(5)-C(6)-C(7)-C(8)	47.8(3)	C(18)-C(19)-C(20)-C(21)	161.8(3)
C(12)-O(2)-C(8)-C(9)	-146.3(3)	C(19)-C(20)-C(21)-O(5)	129.1(3)
C(12)-O(2)-C(8)-C(7)	-21.8(3)	C(19)-C(20)-C(21)-C(22)	-113.5(3)
C(11)-C(7)-C(8)-O(2)	24.5(3)	O(5)-C(21)-C(22)-C(26)	-72.0(3)
C(6)-C(7)-C(8)-O(2)	151.0(2)	C(20)-C(21)-C(22)-C(26)	167.4(3)
C(11)-C(7)-C(8)-C(9)	143.4(3)	O(5)-C(21)-C(22)-C(23)	170.4(2)
C(6)-C(7)-C(8)-C(9)	-90.1(3)	C(20)-C(21)-C(22)-C(23)	49.8(3)
O(2)-C(8)-C(9)-C(10)	-120.2(3)	C(27)-O(6)-C(23)-C(24)	-144.6(3)
C(7)-C(8)-C(9)-C(10)	122.6(4)	C(27)-O(6)-C(23)-C(22)	-20.8(3)
C(8)-C(9)-C(10)-C(14)	-177.4(3)	C(26)-C(22)-C(23)-O(6)	25.5(3)
C(8)-C(9)-C(10)-C(1)	3.6(5)	C(21)-C(22)-C(23)-O(6)	151.3(2)
O(4)-C(1)-C(10)-C(9)	118.4(3)	C(26)-C(22)-C(23)-C(24)	143.0(3)
C(2)-C(1)-C(10)-C(9)	-121.1(3)	C(21)-C(22)-C(23)-C(24)	-91.2(3)
O(4)-C(1)-C(10)-C(14)	-60.7(4)	O(6)-C(23)-C(24)-C(25)	-121.7(4)
C(2)-C(1)-C(10)-C(14)	59.9(4)	C(22)-C(23)-C(24)-C(25)	122.5(4)
C(6)-C(7)-C(11)-C(13)	35.3(5)	C(23)-C(24)-C(25)-C(29)	-179.9(4)
C(8)-C(7)-C(11)-C(13)	159.5(4)	C(23)-C(24)-C(25)-C(16)	0.6(6)
C(6)-C(7)-C(11)-C(12)	-143.7(3)	O(8)-C(16)-C(25)-C(24)	126.4(3)
C(8)-C(7)-C(11)-C(12)	-19.5(3)	C(17)-C(16)-C(25)-C(24)	-117.1(4)
C(8)-O(2)-C(12)-O(3)	-170.5(3)	O(8)-C(16)-C(25)-C(29)	-53.1(4)
C(8)-O(2)-C(12)-C(11)	9.4(3)	C(17)-C(16)-C(25)-C(29)	63.3(4)
C(13)-C(11)-C(12)-O(3)	8.1(6)	C(21)-C(22)-C(26)-C(28)	32.2(5)
C(7)-C(11)-C(12)-O(3)	-172.8(3)	C(23)-C(22)-C(26)-C(28)	156.0(4)
C(13)-C(11)-C(12)-O(2)	-171.8(3)	C(21)-C(22)-C(26)-C(27)	-146.1(3)
C(7)-C(11)-C(12)-O(2)	7.3(3)	C(23)-C(22)-C(26)-C(27)	-22.2(3)
O(8)-C(16)-C(17)-C(18)	172.8(3)	C(23)-O(6)-C(27)-O(7)	-173.6(3)
C(25)-C(16)-C(17)-C(18)	53.1(4)	C(23)-O(6)-C(27)-C(26)	6.7(3)

C(28)-C(26)-C(27)-O(7)	12.7(6)	C(38)-C(37)-C(41)-C(43)	158.6(5)
C(22)-C(26)-C(27)-O(7)	-168.9(3)	C(36)-C(37)-C(41)-C(43)	36.1(6)
C(28)-C(26)-C(27)-O(6)	-167.7(3)	C(38)-C(37)-C(41)-C(42)	-18.6(3)
C(22)-C(26)-C(27)-O(6)	10.7(3)	C(36)-C(37)-C(41)-C(42)	-141.1(3)
O(12)-C(31)-C(32)-C(33)	172.1(3)	C(38)-O(10)-C(42)-O(11)	-170.6(4)
C(40)-C(31)-C(32)-C(33)	52.7(4)	C(38)-O(10)-C(42)-C(41)	8.8(4)
C(31)-C(32)-C(33)-C(34)	44.7(4)	C(43)-C(41)-C(42)-O(11)	9.0(7)
C(32)-C(33)-C(34)-C(35)	-113.6(3)	C(37)-C(41)-C(42)-O(11)	-173.6(4)
C(32)-C(33)-C(34)-C(45)	62.9(4)	C(43)-C(41)-C(42)-O(10)	-170.5(4)
C(33)-C(34)-C(35)-C(36)	161.9(3)	C(37)-C(41)-C(42)-O(10)	7.0(4)
C(45)-C(34)-C(35)-C(36)	-14.2(5)	O(16)-C(46)-C(47)-C(48)	175.0(3)
C(34)-C(35)-C(36)-O(9)	127.1(3)	C(55)-C(46)-C(47)-C(48)	53.1(4)
C(34)-C(35)-C(36)-C(37)	-110.3(3)	C(46)-C(47)-C(48)-C(49)	44.4(4)
O(9)-C(36)-C(37)-C(41)	-70.6(4)	C(47)-C(48)-C(49)-C(50)	-113.2(3)
C(35)-C(36)-C(37)-C(41)	164.8(3)	C(47)-C(48)-C(49)-C(60)	62.7(4)
O(9)-C(36)-C(37)-C(38)	172.3(3)	C(60)-C(49)-C(50)-C(51)	-12.9(5)
C(35)-C(36)-C(37)-C(38)	47.7(3)	C(48)-C(49)-C(50)-C(51)	162.6(3)
C(42)-O(10)-C(38)-C(39)	-145.4(3)	C(49)-C(50)-C(51)-O(13)	132.0(3)
C(42)-O(10)-C(38)-C(37)	-20.6(3)	C(49)-C(50)-C(51)-C(52)	-109.3(3)
C(41)-C(37)-C(38)-O(10)	23.0(3)	O(13)-C(51)-C(52)-C(56)	-75.5(3)
C(36)-C(37)-C(38)-O(10)	148.6(3)	C(50)-C(51)-C(52)-C(56)	162.9(3)
C(41)-C(37)-C(38)-C(39)	141.8(3)	O(13)-C(51)-C(52)-C(53)	167.4(3)
C(36)-C(37)-C(38)-C(39)	-92.5(3)	C(50)-C(51)-C(52)-C(53)	45.7(3)
O(10)-C(38)-C(39)-C(40)	-116.9(4)	C(57)-O(14)-C(53)-C(54)	-147.2(3)
C(37)-C(38)-C(39)-C(40)	126.0(4)	C(57)-O(14)-C(53)-C(52)	-21.9(3)
C(38)-C(39)-C(40)-C(44)	-178.8(4)	C(56)-C(52)-C(53)-O(14)	25.0(3)
C(38)-C(39)-C(40)-C(31)	1.7(5)	C(51)-C(52)-C(53)-O(14)	150.1(3)
O(12)-C(31)-C(40)-C(39)	122.1(3)	C(56)-C(52)-C(53)-C(54)	143.5(3)
C(32)-C(31)-C(40)-C(39)	-116.3(4)	C(51)-C(52)-C(53)-C(54)	-91.3(3)
O(12)-C(31)-C(40)-C(44)	-57.5(4)	O(14)-C(53)-C(54)-C(55)	-116.0(3)
C(32)-C(31)-C(40)-C(44)	64.1(4)	C(52)-C(53)-C(54)-C(55)	126.4(3)

C(53)-C(54)-C(55)-C(59)	178.1(3)	C(51)-C(52)-C(56)-C(57)	-143.6(3)
C(53)-C(54)-C(55)-C(46)	-0.1(5)	C(53)-C(52)-C(56)-C(57)	-20.2(3)
O(16)-C(46)-C(55)-C(54)	126.7(3)	C(53)-O(14)-C(57)-O(15)	-172.0(3)
C(47)-C(46)-C(55)-C(54)	-114.7(4)	C(53)-O(14)-C(57)-C(56)	9.0(4)
O(16)-C(46)-C(55)-C(59)	-51.6(4)	C(58)-C(56)-C(57)-O(15)	12.4(7)
C(47)-C(46)-C(55)-C(59)	67.0(4)	C(52)-C(56)-C(57)-O(15)	-170.9(4)
C(51)-C(52)-C(56)-C(58)	32.7(6)	C(58)-C(56)-C(57)-O(14)	-168.7(4)
C(53)-C(52)-C(56)-C(58)	156.2(4)	C(52)-C(56)-C(57)-O(14)	8.0(4)

Symmetry transformations used to generate equivalent atoms:

Table B7. Hydrogen bonds for Compound **(62)** [Å and º].

D-H...A	d(D-H)	d(H...A)	d(D...A)	<(DHA)
O(1)-H(1)...O(13)#1	0.82	2.02	2.835(3)	173.6
O(4)-H(4)...O(9)	0.82	1.98	2.780(3)	166.8
O(5)-H(5)...O(16)	0.82	2.03	2.840(3)	170.7
O(8)-H(8)...O(1S)	0.82	1.94	2.705(5)	154.4
O(9)-H(9)...O(5)	0.82	2.09	2.869(3)	158.3
O(12)-H(12)...O(1)#2	0.82	2.03	2.849(3)	175.9
O(13)-H(13)...O(8)#3	0.82	1.94	2.726(3)	161.4
O(16)-H(16)...O(12)#4	0.82	2.04	2.843(3)	166.4

Symmetry transformations used to generate equivalent atoms:

#1 -x+y,-x,z+1/3 #2 -y+1,x-y,z-1/3 #3 -y+1,x-y+1,z-1/3 #4 -x+y,-x+1,z+1/3

Appendix (C)

Table C1. Crystal data and structure refinement for Compound **(66)**.

Empirical formula	$C_{19}H_{24}O_6$	
Formula weight	348.38	
Temperature	293(2) K	
Wavelength	0.71073 Å	
Crystal system	Monoclinic	
Space group	P 2_1	
Unit cell dimensions	a = 6.7901(10) Å	a= 90º.
	b = 7.9490(12) Å	b= 93.444(2)º.
	c = 17.457(3) Å	g = 90º.
Volume	940.5(2) $Å^3$	
Z	2	
Density (calculated)	1.230 Mg/m^3	
Absorption coefficient	0.091 mm^{-1}	
F(000)	372	
Crystal size	0.44 x 0.20 x 0.16 mm^3	
Theta range for data collection	2.82 to 26.45º.	
Index ranges	-2<=h<=8, -9<=k<=9, -21<=l<=19	
Reflections collected	4309	
Independent reflections	2907 [R(int) = 0.0259]	
Completeness to theta = 25.00º	99.0 %	
Absorption correction	Semi-empirical from equivalents	
Max. and min. transmission	0.986 and 0.966	
Refinement method	Full-matrix least-squares on F^2	
Data / restraints / parameters	2907 / 1 / 231	
Goodness-of-fit on F^2	1.064	
Final R indices [I>2sigma(I)]	R1 = 0.0587, wR2 = 0.1601	

R indices (all data)	R1 = 0.0731, wR2 = 0.1771
Extinction coefficient	0.012(7)
Largest diff. peak and hole	0.485 and -0.424 e.Å^{-3}

Table C2. Atomic coordinates (x 10^4) and equivalent isotropic displacement parameters (Å^{2}x 10^3) for Compound **(66)**. U(eq) is defined as one third of the trace of the orthogonalized U^{ij} tensor.

	x	y	z	U(eq)
O(1)	7715(4)	2754(4)	3955(1)	73(1)
O(2)	11032(3)	3728(3)	1685(2)	64(1)
O(3)	13733(4)	2238(4)	1994(2)	86(1)
O(4)	7773(4)	8704(5)	981(2)	89(1)
O(5)	8048(8)	4505(6)	4942(2)	125(2)
O(6)	10540(10)	8971(16)	1504(4)	352(9)
C(1)	7171(5)	7615(6)	1611(2)	68(1)
C(2)	5491(6)	8534(6)	1985(3)	83(1)
C(3)	4661(6)	7527(7)	2644(3)	82(1)
C(4)	6292(6)	6758(6)	3157(2)	70(1)
C(5)	6493(5)	5099(6)	3165(2)	64(1)
C(6)	8252(5)	4114(5)	3436(2)	59(1)
C(7)	9096(5)	3213(5)	2755(2)	56(1)
C(8)	9349(5)	4413(5)	2072(2)	56(1)
C(9)	7671(5)	4557(5)	1497(2)	58(1)
C(10)	6682(5)	5942(6)	1275(2)	62(1)
C(11)	11132(6)	2506(5)	2881(2)	64(1)
C(12)	12155(5)	2748(5)	2169(2)	66(1)
C(13)	12067(9)	1815(8)	3479(3)	99(2)
C(14)	4990(6)	5846(7)	678(3)	87(1)
C(15)	7675(9)	7953(7)	3577(3)	101(2)
C(16)	7634(7)	3133(7)	4695(2)	81(1)

C(17)	6967(9)	1704(9)	5145(3)	103(2)
C(18)	9519(7)	9276(7)	1004(2)	81(1)
C(19)	9997(8)	10337(7)	356(3)	87(1)

Table C3. Bond lengths [Å] and angles [º] for Compound **(66)**.

O(1)-C(16)	1.330(5)	C(6)-H(6)	0.9800
O(1)-C(6)	1.471(5)	C(7)-C(11)	1.496(5)
O(2)-C(12)	1.351(4)	C(7)-C(8)	1.544(5)
O(2)-C(8)	1.467(4)	C(7)-H(7)	0.9800
O(3)-C(12)	1.202(5)	C(8)-C(9)	1.478(5)
O(4)-C(18)	1.268(5)	C(8)-H(8)	0.9800
O(4)-C(1)	1.477(5)	C(9)-C(10)	1.334(6)
O(5)-C(16)	1.200(7)	C(9)-H(9)	0.9300
O(6)-C(18)	1.110(6)	C(10)-C(14)	1.506(5)
C(1)-C(10)	1.483(6)	C(11)-C(13)	1.310(6)
C(1)-C(2)	1.533(6)	C(11)-C(12)	1.472(6)
C(1)-H(1)	0.9800	C(13)-H(13A)	0.9300
C(2)-C(3)	1.537(7)	C(13)-H(13B)	0.9300
C(2)-H(2A)	0.9700	C(14)-H(14A)	0.9600
C(2)-H(2B)	0.9700	C(14)-H(14B)	0.9600
C(3)-C(4)	1.510(6)	C(14)-H(14C)	0.9600
C(3)-H(3A)	0.9700	C(15)-H(15A)	0.9600
C(3)-H(3B)	0.9700	C(15)-H(15B)	0.9600
C(4)-C(5)	1.326(6)	C(15)-H(15C)	0.9600
C(4)-C(15)	1.496(6)	C(16)-C(17)	1.468(8)
C(5)-C(6)	1.482(6)	C(17)-H(17A)	0.9600
C(5)-H(5)	0.9300	C(17)-H(17B)	0.9600
C(6)-C(7)	1.529(5)	C(17)-H(17C)	0.9600

C(18)-C(19)	1.462(6)	C(6)-C(5)-H(5)	116.2
C(19)-H(19A)	0.9600	O(1)-C(6)-C(5)	111.1(3)
C(19)-H(19B)	0.9600	O(1)-C(6)-C(7)	104.7(3)
C(19)-H(19C)	0.9600	C(5)-C(6)-C(7)	109.3(3)
		O(1)-C(6)-H(6)	110.5
C(16)-O(1)-C(6)	117.2(4)	C(5)-C(6)-H(6)	110.5
C(12)-O(2)-C(8)	110.6(3)	C(7)-C(6)-H(6)	110.5
C(18)-O(4)-C(1)	119.1(3)	C(11)-C(7)-C(6)	116.6(3)
O(4)-C(1)-C(10)	107.3(3)	C(11)-C(7)-C(8)	101.6(3)
O(4)-C(1)-C(2)	106.5(3)	C(6)-C(7)-C(8)	112.0(3)
C(10)-C(1)-C(2)	116.2(4)	C(11)-C(7)-H(7)	108.7
O(4)-C(1)-H(1)	108.9	C(6)-C(7)-H(7)	108.7
C(10)-C(1)-H(1)	108.9	C(8)-C(7)-H(7)	108.7
C(2)-C(1)-H(1)	108.9	O(2)-C(8)-C(9)	107.8(3)
C(1)-C(2)-C(3)	112.7(4)	O(2)-C(8)-C(7)	104.6(3)
C(1)-C(2)-H(2A)	109.0	C(9)-C(8)-C(7)	117.1(3)
C(3)-C(2)-H(2A)	109.0	O(2)-C(8)-H(8)	109.0
C(1)-C(2)-H(2B)	109.0	C(9)-C(8)-H(8)	109.0
C(3)-C(2)-H(2B)	109.0	C(7)-C(8)-H(8)	109.0
H(2A)-C(2)-H(2B)	107.8	C(10)-C(9)-C(8)	127.9(4)
C(4)-C(3)-C(2)	111.4(3)	C(10)-C(9)-H(9)	116.0
C(4)-C(3)-H(3A)	109.3	C(8)-C(9)-H(9)	116.0
C(2)-C(3)-H(3A)	109.3	C(9)-C(10)-C(1)	121.9(3)
C(4)-C(3)-H(3B)	109.3	C(9)-C(10)-C(14)	120.6(4)
C(2)-C(3)-H(3B)	109.3	C(1)-C(10)-C(14)	117.5(4)
H(3A)-C(3)-H(3B)	108.0	C(13)-C(11)-C(12)	119.8(4)
C(5)-C(4)-C(15)	124.4(4)	C(13)-C(11)-C(7)	132.4(4)
C(5)-C(4)-C(3)	118.7(4)	C(12)-C(11)-C(7)	107.8(3)
C(15)-C(4)-C(3)	116.7(4)	O(3)-C(12)-O(2)	120.9(4)
C(4)-C(5)-C(6)	127.5(4)	O(3)-C(12)-C(11)	130.1(4)
C(4)-C(5)-H(5)	116.2	O(2)-C(12)-C(11)	109.0(3)

C(11)-C(13)-H(13A)	120.0	O(1)-C(16)-C(17)	112.1(5)
C(11)-C(13)-H(13B)	120.0	C(16)-C(17)-H(17A)	109.5
H(13A)-C(13)-H(13B)	120.0	C(16)-C(17)-H(17B)	109.5
C(10)-C(14)-H(14A)	109.5	H(17A)-C(17)-H(17B)	109.5
C(10)-C(14)-H(14B)	109.5	C(16)-C(17)-H(17C)	109.5
H(14A)-C(14)-H(14B)	109.5	H(17A)-C(17)-H(17C)	109.5
C(10)-C(14)-H(14C)	109.5	H(17B)-C(17)-H(17C)	109.5
H(14A)-C(14)-H(14C)	109.5	O(6)-C(18)-O(4)	119.0(5)
H(14B)-C(14)-H(14C)	109.5	O(6)-C(18)-C(19)	125.3(5)
C(4)-C(15)-H(15A)	109.5	O(4)-C(18)-C(19)	115.7(4)
C(4)-C(15)-H(15B)	109.5	C(18)-C(19)-H(19A)	109.5
H(15A)-C(15)-H(15B)	109.5	C(18)-C(19)-H(19B)	109.5
C(4)-C(15)-H(15C)	109.5	H(19A)-C(19)-H(19B)	109.5
H(15A)-C(15)-H(15C)	109.5	C(18)-C(19)-H(19C)	109.5
H(15B)-C(15)-H(15C)	109.5	H(19A)-C(19)-H(19C)	109.5
O(5)-C(16)-O(1)	122.2(5)	H(19B)-C(19)-H(19C)	109.5
O(5)-C(16)-C(17)	125.7(4)		

Table C4. Anisotropic displacement parameters ($Å^2 x\ 10^3$) for Compound **(66)**. The anisotropic displacement factor exponent takes the form:

$-2p^2[\ h^2a^{*2}U^{11} + ... + 2\ h\ k\ a^*\ b^*\ U^{12}\ ]$

	U^{11}	U^{22}	U^{33}	U^{23}	U^{13}	U^{12}
O(1)	99(2)	70(2)	51(1)	-1(1)	14(1)	-10(2)
O(2)	64(1)	62(2)	70(1)	5(1)	19(1)	11(1)
O(3)	72(2)	68(2)	118(2)	0(2)	19(2)	17(2)
O(4)	64(2)	101(2)	101(2)	48(2)	-8(1)	-12(2)
O(5)	192(4)	117(4)	66(2)	-29(2)	19(2)	-17(3)
O(6)	156(5)	640(20)	242(7)	308(11)	-111(5)	-224(9)
C(1)	55(2)	70(3)	79(2)	18(2)	7(2)	1(2)

C(2)	73(2)	62(3)	116(4)	10(3)	9(2)	17(2)
C(3)	78(2)	72(3)	98(3)	-4(3)	27(2)	15(2)
C(4)	77(2)	63(3)	73(2)	-7(2)	23(2)	4(2)
C(5)	65(2)	62(3)	65(2)	-11(2)	19(2)	-2(2)
C(6)	67(2)	55(2)	56(2)	-4(2)	9(2)	-11(2)
C(7)	64(2)	47(2)	56(2)	-2(2)	6(2)	-3(2)
C(8)	58(2)	50(2)	60(2)	0(2)	14(2)	3(2)
C(9)	64(2)	55(2)	55(2)	-3(2)	9(2)	-2(2)
C(10)	52(2)	72(3)	64(2)	7(2)	7(2)	-1(2)
C(11)	74(2)	52(2)	66(2)	0(2)	3(2)	5(2)
C(12)	67(2)	50(2)	80(2)	-1(2)	10(2)	5(2)
C(13)	107(4)	100(4)	90(3)	26(3)	4(3)	27(3)
C(14)	66(2)	105(4)	88(3)	13(3)	-10(2)	-4(2)
C(15)	127(4)	61(3)	116(4)	-25(3)	8(3)	-10(3)
C(16)	96(3)	97(4)	51(2)	-6(2)	12(2)	1(3)
C(17)	125(4)	121(5)	65(3)	18(3)	25(3)	-7(4)
C(18)	71(2)	104(4)	67(2)	22(2)	-9(2)	-19(2)
C(19)	101(3)	86(3)	76(3)	6(2)	17(2)	-14(3)

Table C5. Hydrogen coordinates (x 10^4) and isotropic displacement parameters (Å^2 x 10^3) for Compound **(66)**.

	x	y	z	U(eq)
H(1)	8286	7493	1990	81
H(2A)	4437	8754	1598	100
H(2B)	5973	9609	2181	100
H(3A)	3873	8264	2946	98
H(3B)	3809	6641	2433	98
H(5)	5404	4481	2978	76
H(6)	9248	4850	3690	71

H(7)	8196	2304	2587	67
H(8)	9690	5536	2270	67
H(9)	7253	3561	1260	69
H(13A)	13373	1479	3453	119
H(13B)	11425	1661	3929	119
H(14A)	3826	6307	884	131
H(14B)	4757	4693	537	131
H(14C)	5308	6478	234	131
H(15A)	6948	8904	3748	152
H(15B)	8652	8328	3240	152
H(15C)	8311	7394	4012	152
H(17A)	5628	1434	4984	154
H(17B)	7043	1996	5680	154
H(17C)	7795	749	5066	154
H(19A)	10227	9640	-79	131
H(19B)	11161	10981	493	131
H(19C)	8916	11085	229	131

Table C6. Torsion angles [º] for Compound **(66)**.

C(18)-O(4)-C(1)-C(10)	-116.8(4)	C(16)-O(1)-C(6)-C(7)	155.8(3)
C(18)-O(4)-C(1)-C(2)	118.1(5)	C(4)-C(5)-C(6)-O(1)	131.4(4)
O(4)-C(1)-C(2)-C(3)	178.5(4)	C(4)-C(5)-C(6)-C(7)	-113.6(4)
C(10)-C(1)-C(2)-C(3)	59.1(5)	O(1)-C(6)-C(7)-C(11)	-75.4(4)
C(1)-C(2)-C(3)-C(4)	43.8(6)	C(5)-C(6)-C(7)-C(11)	165.5(3)
C(2)-C(3)-C(4)-C(5)	-112.2(5)	O(1)-C(6)-C(7)-C(8)	168.2(3)
C(2)-C(3)-C(4)-C(15)	63.1(5)	C(5)-C(6)-C(7)-C(8)	49.1(4)
C(15)-C(4)-C(5)-C(6)	-13.7(7)	C(12)-O(2)-C(8)-C(9)	-146.8(3)
C(3)-C(4)-C(5)-C(6)	161.3(4)	C(12)-O(2)-C(8)-C(7)	-21.5(4)
C(16)-O(1)-C(6)-C(5)	-86.3(4)	C(11)-C(7)-C(8)-O(2)	24.8(3)

C(6)-C(7)-C(8)-O(2)	149.9(3)	C(6)-C(7)-C(11)-C(12)	-142.6(3)
C(11)-C(7)-C(8)-C(9)	144.0(3)	C(8)-C(7)-C(11)-C(12)	-20.5(4)
C(6)-C(7)-C(8)-C(9)	-90.8(4)	C(8)-O(2)-C(12)-O(3)	-170.6(4)
O(2)-C(8)-C(9)-C(10)	-120.1(4)	C(8)-O(2)-C(12)-C(11)	8.4(4)
C(7)-C(8)-C(9)-C(10)	122.4(4)	C(13)-C(11)-C(12)-O(3)	9.4(8)
C(8)-C(9)-C(10)-C(1)	-0.8(6)	C(7)-C(11)-C(12)-O(3)	-172.4(4)
C(8)-C(9)-C(10)-C(14)	-179.7(4)	C(13)-C(11)-C(12)-O(2)	-169.6(4)
O(4)-C(1)-C(10)-C(9)	118.4(4)	C(7)-C(11)-C(12)-O(2)	8.6(4)
C(2)-C(1)-C(10)-C(9)	-122.6(4)	C(6)-O(1)-C(16)-O(5)	-2.7(7)
O(4)-C(1)-C(10)-C(14)	-62.7(4)	C(6)-O(1)-C(16)-C(17)	176.5(4)
C(2)-C(1)-C(10)-C(14)	56.3(5)	C(1)-O(4)-C(18)-O(6)	-1.5(11)
C(6)-C(7)-C(11)-C(13)	35.3(7)	C(1)-O(4)-C(18)-C(19)	179.7(4)
C(8)-C(7)-C(11)-C(13)	157.4(5)		

Symmetry transformations used to generate equivalent atoms:

Appendix (D)

Table D1. Crystal data and structure refinement for Compound **(63)**.

Empirical formula	$C_{15}H_{20}O_4$	
Formula weight	264.31	
Temperature	293(2) K	
Wavelength	0.71073 Å	
Crystal system	Orthorhombic	
Space group	$P2_12_12_1$	
Unit cell dimensions	a = 8.6195(7) Å	= 90°.
	b = 10.6697(9) Å	= 90°.
	c = 15.3527(12) Å	= 90°.
Volume	1411.9(2) $Å^3$	
Z	4	
Density (calculated)	1.243 Mg/m^3	
Absorption coefficient	0.089 mm^{-1}	
F(000)	568	
Crystal size	0.40 x 0.14 x 0.12 mm^3	
Theta range for data collection	2.65 to 26.53°.	
Index ranges	-10<=h<=3, -12<=k<=13, -18<=l<=19	
Reflections collected	7767	
Independent reflections	2677 [R(int) = 0.0264]	
Completeness to theta = 25.00°	99.9 %	
Absorption correction	Semi-empirical from equivalents	
Max. and min. transmission	0.989 and 0.968	
Refinement method	Full-matrix least-squares on F^2	
Data / restraints / parameters	2677 / 0 / 252	
Goodness-of-fit on F^2	1.071	
Final R indices [I>2sigma(I)]	R1 = 0.0322, wR2 = 0.0811	
R indices (all data)	R1 = 0.0397, wR2 = 0.0886	
Absolute structure parameter	-0.4(10)	
Extinction coefficient	0	

Largest diff. peak and hole 0.107 and -0.127 e.Å^{-3}

Table D2. Atomic coordinates (x 10^4) and equivalent isotropic displacement parameters (Å^{2}x 10^3) for Compound **(63)**. U(eq) is defined as one third of the trace of the orthogonalized U^{ij} tensor.

	x	y	z	U(eq)
O(1)	12946(1)	5262(2)	6459(1)	68(1)
O(2)	9714(2)	4923(1)	4057(1)	61(1)
O(3)	11601(2)	4179(2)	3218(1)	81(1)
O(4)	5301(2)	6732(1)	5664(1)	65(1)
C(1)	6751(2)	6542(2)	6109(1)	52(1)
C(2)	6698(2)	7141(2)	7010(1)	61(1)
C(3)	8228(2)	7070(2)	7535(1)	62(1)
C(4)	9633(2)	7102(2)	6948(1)	54(1)
C(5)	10353(2)	6035(2)	6781(1)	49(1)
C(6)	11535(2)	5755(2)	6096(1)	50(1)
C(7)	10869(2)	4759(2)	5478(1)	46(1)
C(8)	9443(2)	5255(2)	4976(1)	46(1)
C(9)	7858(2)	4725(2)	5214(1)	51(1)
C(10)	7177(2)	5159(2)	6062(1)	49(1)
C(11)	11953(2)	4337(2)	4772(1)	52(1)
C(12)	11138(2)	4457(2)	3936(1)	57(1)
C(13)	13390(2)	3906(2)	4804(2)	72(1)
C(14)	6821(2)	4363(2)	6698(1)	63(1)
C(15)	10023(4)	8335(2)	6532(2)	76(1)

Table D3. Bond lengths [Å] and angles [°] for Compound **(63)**.

O(1)-C(6)	1.437(2)	C(1)-C(10)	1.523(2)
O(2)-C(12)	1.337(2)	C(1)-C(2)	1.525(3)
O(2)-C(8)	1.4734(18)	C(2)-C(3)	1.547(3)
O(3)-C(12)	1.209(2)	C(3)-C(4)	1.510(3)
O(4)-C(1)	1.439(2)	C(4)-C(5)	1.321(2)

C(4)-C(15)	1.500(3)	C(4)-C(5)-C(6)	128.94(16)
C(5)-C(6)	1.495(2)	O(1)-C(6)-C(5)	112.16(13)
C(6)-C(7)	1.536(2)	O(1)-C(6)-C(7)	107.62(15)
C(7)-C(11)	1.499(2)	C(5)-C(6)-C(7)	108.56(13)
C(7)-C(8)	1.544(2)	C(11)-C(7)-C(6)	114.90(14)
C(8)-C(9)	1.523(2)	C(11)-C(7)-C(8)	103.80(12)
C(9)-C(10)	1.501(2)	C(6)-C(7)-C(8)	111.62(13)
C(10)-C(14)	1.329(3)	O(2)-C(8)-C(9)	106.41(13)
C(11)-C(13)	1.322(3)	O(2)-C(8)-C(7)	105.61(12)
C(11)-C(12)	1.469(3)	C(9)-C(8)-C(7)	117.82(13)
		C(10)-C(9)-C(8)	116.42(14)
C(12)-O(2)-C(8)	111.58(13)	C(14)-C(10)-C(9)	122.01(17)
O(4)-C(1)-C(10)	108.87(15)	C(14)-C(10)-C(1)	121.96(17)
O(4)-C(1)-C(2)	110.20(14)	C(9)-C(10)-C(1)	115.68(15)
C(10)-C(1)-C(2)	117.12(16)	C(13)-C(11)-C(12)	120.71(18)
C(1)-C(2)-C(3)	115.20(15)	C(13)-C(11)-C(7)	131.41(18)
C(4)-C(3)-C(2)	111.85(14)	C(12)-C(11)-C(7)	107.88(14)
C(5)-C(4)-C(15)	124.63(18)	O(3)-C(12)-O(2)	121.43(17)
C(5)-C(4)-C(3)	118.21(17)	O(3)-C(12)-C(11)	128.07(18)
C(15)-C(4)-C(3)	116.93(18)	O(2)-C(12)-C(11)	110.49(14)

Symmetry transformations used to generate equivalent atoms:

Table D4. Anisotropic displacement parameters ($Å^2 x\ 10^3$) for Compound **(63)**. The anisotropic displacement factor exponent takes the form: $-2\ ^2[\ h^2 a^{*2} U^{11} + ... + 2\ h\ k\ a^*\ b^*\ U^{12}\ ]$

	U^{11}	U^{22}	U^{33}	U^{23}	U^{13}	U^{12}
O(1)	49(1)	109(1)	46(1)	-7(1)	-10(1)	7(1)
O(2)	68(1)	80(1)	34(1)	-1(1)	-5(1)	5(1)
O(3)	94(1)	106(1)	44(1)	-11(1)	17(1)	0(1)
O(4)	59(1)	75(1)	62(1)	7(1)	-10(1)	13(1)
C(1)	48(1)	58(1)	50(1)	4(1)	-2(1)	2(1)
C(2)	61(1)	67(1)	55(1)	-4(1)	5(1)	9(1)

C(3)	68(1)	76(1)	43(1)	-10(1)	2(1)	4(1)
C(4)	57(1)	67(1)	37(1)	-9(1)	-4(1)	-5(1)
C(5)	49(1)	66(1)	33(1)	3(1)	-4(1)	-3(1)
C(6)	46(1)	66(1)	37(1)	2(1)	-3(1)	-5(1)
C(7)	47(1)	53(1)	37(1)	5(1)	-1(1)	-2(1)
C(8)	52(1)	52(1)	33(1)	0(1)	-4(1)	0(1)
C(9)	49(1)	53(1)	52(1)	-3(1)	-7(1)	-3(1)
C(10)	41(1)	56(1)	51(1)	2(1)	-5(1)	-2(1)
C(11)	55(1)	55(1)	47(1)	-2(1)	4(1)	-2(1)
C(12)	66(1)	64(1)	42(1)	1(1)	6(1)	-7(1)
C(13)	62(1)	80(1)	75(1)	-16(1)	6(1)	9(1)
C(14)	62(1)	62(1)	66(1)	11(1)	4(1)	-4(1)
C(15)	97(2)	57(1)	73(1)	-14(1)	11(1)	-15(1)

Table D5. Hydrogen coordinates (x 10^4) and isotropic displacement parameters (Å^{2}x 10^3) for Compound **(63)**.

	x	y	z	U(eq)
H(1O)	12970(30)	5470(20)	7004(17)	75(6)
H(4O)	4580(40)	6260(30)	5946(18)	111(10)
H(1)	7510(20)	7000(18)	5768(12)	54(5)
H(2A)	6460(30)	8000(20)	6911(16)	86(7)
H(2B)	5850(30)	6750(20)	7335(15)	78(6)
H(3A)	8290(20)	6300(20)	7879(13)	69(6)
H(3B)	8290(30)	7810(20)	7942(17)	89(7)
H(5)	10060(20)	5267(19)	7113(13)	65(5)
H(6)	11740(20)	6508(18)	5750(12)	51(4)
H(7)	10540(20)	4031(19)	5807(12)	63(5)
H(8)	9431(18)	6214(16)	5018(10)	47(4)
H(9A)	7990(20)	3856(19)	5220(12)	55(5)
H(9B)	7130(20)	4962(16)	4722(12)	53(4)
H(13A)	13910(30)	3780(20)	5366(17)	84(7)
H(13B)	13960(30)	3720(20)	4187(17)	94(7)
H(14A)	6990(30)	3460(20)	6626(15)	76(6)

H(14B)	6330(20)	4640(20)	7260(14)	68(6)
H(15A)	9210(40)	8880(30)	6540(20)	131(12)
H(15B)	10840(50)	8730(40)	6850(30)	172(15)
H(15C)	10490(40)	8320(30)	6010(30)	144(13)

Table D6. Torsion angles [°] for Compound **(63)**.

O(4)-C(1)-C(2)-C(3)	-176.50(17)	O(2)-C(8)-C(9)-C(10)	-168.14(14)
C(10)-C(1)-C(2)-C(3)	58.3(2)	C(7)-C(8)-C(9)-C(10)	73.65(19)
C(1)-C(2)-C(3)-C(4)	31.6(2)	C(8)-C(9)-C(10)-C(14)	-120.41(18)
C(2)-C(3)-C(4)-C(5)	-101.7(2)	C(8)-C(9)-C(10)-C(1)	66.20(19)
C(2)-C(3)-C(4)-C(15)	73.0(2)	O(4)-C(1)-C(10)-C(14)	-94.8(2)
C(15)-C(4)-C(5)-C(6)	-8.2(3)	C(2)-C(1)-C(10)-C(14)	31.0(2)
C(3)-C(4)-C(5)-C(6)	166.05(15)	O(4)-C(1)-C(10)-C(9)	78.62(17)
C(4)-C(5)-C(6)-O(1)	123.79(19)	C(2)-C(1)-C(10)-C(9)	-155.57(15)
C(4)-C(5)-C(6)-C(7)	-117.44(19)	C(6)-C(7)-C(11)-C(13)	52.8(3)
O(1)-C(6)-C(7)-C(11)	-55.93(18)	C(8)-C(7)-C(11)-C(13)	175.0(2)
C(5)-C(6)-C(7)-C(11)	-177.53(14)	C(6)-C(7)-C(11)-C(12)	-127.78(15)
O(1)-C(6)-C(7)-C(8)	-173.76(12)	C(8)-C(7)-C(11)-C(12)	-5.62(18)
C(5)-C(6)-C(7)-C(8)	64.64(17)	C(8)-O(2)-C(12)-O(3)	-176.84(17)
C(12)-O(2)-C(8)-C(9)	-133.57(15)	C(8)-O(2)-C(12)-C(11)	4.1(2)
C(12)-O(2)-C(8)-C(7)	-7.59(18)	C(13)-C(11)-C(12)-O(3)	1.8(3)
C(11)-C(7)-C(8)-O(2)	7.74(17)	C(7)-C(11)-C(12)-O(3)	-177.72(19)
C(6)-C(7)-C(8)-O(2)	132.06(13)	C(13)-C(11)-C(12)-O(2)	-179.26(18)
C(11)-C(7)-C(8)-C(9)	126.37(15)	C(7)-C(11)-C(12)-O(2)	1.24(19)
C(6)-C(7)-C(8)-C(9)	-109.31(16)		

Table D7. Hydrogen bonds for Compound **(63)** [Å and °].

D-H...A	d(D-H)	d(H...A)	d(D...A)	<(DHA)
O(1)-H(1O)...O(3)#1	0.87(3)	1.94(3)	2.7935(19)	170(2)
O(4)-H(4O)...O(1)#2	0.92(3)	1.93(3)	2.841(2)	175(3)

Symmetry transformations used to generate equivalent atoms:

#1 -x+5/2,-y+1,z+1/2 #2 x-1,y,z